Electronic Supplementary Material (ESI) for Organic Chemistry Frontiers.

Enantioselective Au(I)-Catalyzed Tandem Reactions between 2-Alkynyl Enones and Naphthols by the TCDC Strategy.

Yunliang Yu, [a] Nazarii Sabat,[a,‡] Meriem Daghmoum,[a,‡] Zhenhao Zhang,[a,b] Pascal Retailleau,[a] Gilles Frison, [b,c] ,*Angela Marinetti,[a,*] and Xavier Guinchard[a,*]

[a] Université Paris-Saclay, CNRS, Institut de Chimie des Substances Naturelles, UPR2301, 91198 Gif-sur-Yvette, France.
[b] LCM, CNRS, Ecole Polytechnique, Institut Polytechnique de Paris, 91128 Palaiseau, France.
[c] Sorbonne Université, CNRS, Laboratoire de Chimie Théorique, 75005 Paris, France.

[‡] Equal contribution to this work.

gilles.frison@cnrs.fr
angela.marinetti@cnrs.fr
xavier.guinchard@cnrs.fr

Contents

1. General methods.

Unless otherwise noted, all of the reactions were performed under argon atomosphere, the solvents were distilled under argon, and the separations were carried out under flash-chromatographic conditions on silica gel (Redi Sep prepacked column, 230-400 mesh) with use of a CombiFlash Companion. Reagent-grade chemicals were obtained from diverse commercial suppliers (Sigma-Aldrich, Acros Organics, TCI, Fluorochem and Alfa-Aesar) and were used as received. *n*-BuLi was used as commercially available solutions and titrated before use. ^{1}H (300 and 500 MHz), ^{31}P (120 MHz and 202 MHz), ^{19}F (282 MHz) and ^{13}C (75 and 125 MHz) NMR spectra were recorded on Bruker Advance spectrometers. The chemical shifts (δ) are reported in part per million (ppm) and coupling values (*J*) are given in hertz (Hz). Multiplicities are abbreviated as follows: s (singlet), d (doublet), t (triplet), q (quadruplet), bs (broad singlet) dd (doublet of doublet), dt (doublet of triplet), m (multiplet). Infrared spectra (IR) were recorded on a Perkin-Elmer FT-IR system using diamond window Dura SamplIR II and the data are reported in reciprocal centimeters (cm^{-1}). Optical rotations were measured on an Anton Paar MCP 300 polarimeter at 589 nm. $[\alpha]_D$ is expressed in deg. $cm^3 \cdot g^{-1} \cdot dm^{-1}$ and *c* is expressed in g/100 cm^3. High resolution mass spectra (HRMS) were recorded using a Micromass LCT Premier XE instrument (Waters) and were determined by electrospray ionization (ESI) with a TOF analyzer.

2. Synthesis of gold(I) complexes 3a and 3b

The two complexes **3a** and **3b** were prepared according to our previous studies.[1]

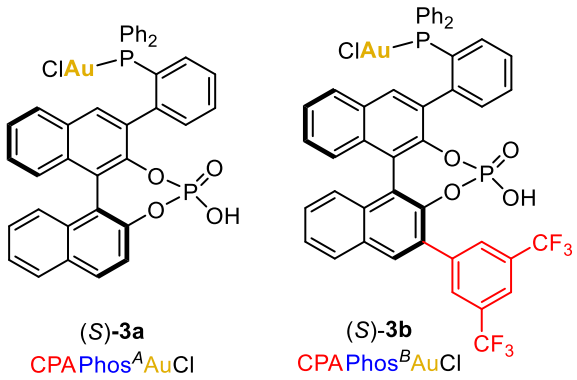

3. Synthesis of 2-alkynyl enones 1

2-Alkynyl enones **1** are known and were prepared as reported in our previous studies.[1]

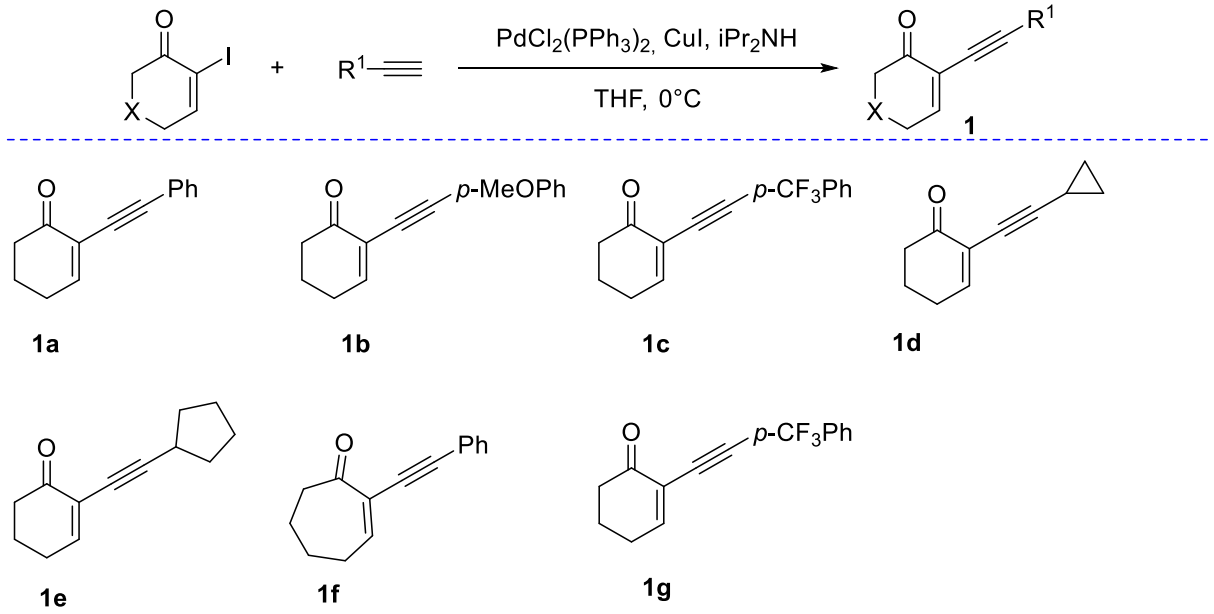

Scheme S1. Synthesis of 2-alkynyl enones 1

General Protocol : A solution of 2-iodo-enone (10 mmol, 1.0 equiv.) in THF (40 mL) was treated

[1] (a) Zhang, Z.; Smal, V.; Retailleau, P.; Voituriez, A.; Frison, G.; Marinetti, A.; Guinchard, X., Tethered Counterion-Directed Catalysis: Merging the Chiral Ion-Pairing and Bifunctional Ligand Strategies in Enantioselective Gold(I) Catalysis. *J. Am. Chem. Soc.* **2020,** *142*, 3797. (b) Zhang, Z.; Sabat, N.; Frison, G.; Marinetti, A.; Guinchard, X., Enantioselective Au(I)-Catalyzed Multicomponent Annulation via Tethered Counterion-Directed Catalysis (TCDC). *ACS Catal.* **2022**, *12*, 4046.

with $PdCl_2(PPh_3)_2$ (350 mg, 0.5 mmol, 5 mol %) and CuI (190 mg, 1 mmol, 10 mol %) and cooled down to 0 °C under an Ar atmosphere and in the dark. After 10 min of stirring, acetylene (20 mmol, 2.0 equiv.) and diisopropyl amine (4.24 mL, 3.0 g, 30 mmol) were added, and the resulting yellow to dark brown solution was stirred at 0 °C for 3 hours. The reaction mixture was diluted with ethyl acetate and washed with saturated aqueous NH_4Cl. The mixture was subsequently extracted with ethyl acetate and dried over $MgSO_4$, filtered and concentrated under vacuum. The crude product was purified by flash column chromatography to yield 2-alkynyl enones **1**.

4. Naphthols 3

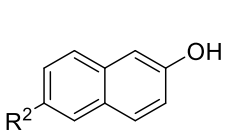

3a: R^1= H
3b: R^1= CN
3c: R^1= Br

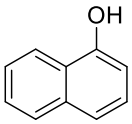

3'a

α- and β-naphthols used in this study are commercially available.

5. Optimization of the catalytic systems

5.1. Reactions using 2-naphthol 3a

Table S1: Optimization of the reaction

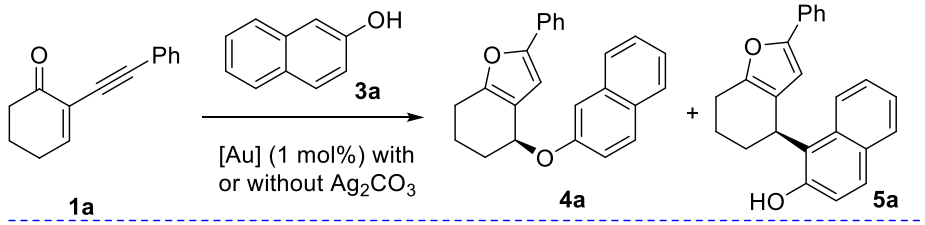

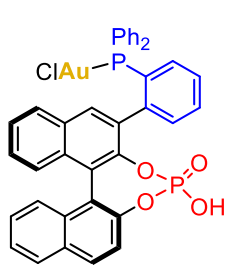

CPAPhos^{A}AuCl
(*S*)-2a

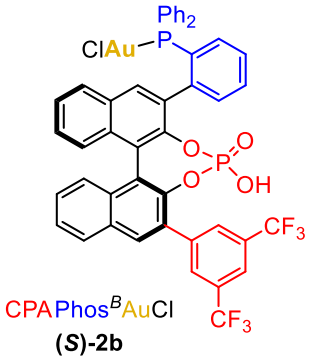

CPAPhos^{B}AuCl
(*S*)-2b

entry	[Au]	**1a/3a** ratio	solvent	T °C	t	Ratio **4a/5a**	**4a** ee (%)	**5a** ee (%)
1	(*S*)-**2a**	1/1	DCM	rt	30 min	43/57	60 (-)	70 (-)
2	(*S*)-**2a**	1/1	DCM	rt	2 min	63/37	82 (-)	92 (-)
3	(*S*)-**2a**	1/1	DCM	rt	~80 sec	60/40	**85** (-)	94 (-)
4	(*S*)-**2a**	1/1	Toluene	rt	2-30 min	~63/37	80 (-)	92 (-)
5 [b]	(*S*)-**2a**	1.5/1	THF	rt	22 h	72/28	42 (+)	66 (-)
6 [b]	(*S*)-**2a**	1.5/1	dioxane	rt	3 h	67/33	1 (+)	94 (-)
7 [b]	(*S*)-**2b**	1/1	DCM	rt	~60 s	50/50	33 (-)	91 (-)
8 [b]	(*S*)-**2b**	1/1	DCM	10	5 min	35/65	46 (-)	**92** (-)
9	(*S*)-**2b**	1/1	Toluene	rt	4 min	75/25	27 (-)	84 (-)
10 [b]	(*S*)-**2b**	1.5/1	THF	rt	16 h	86/14	64 (+)	ND
11 [b]	(*S*)-**2b**	1.5/1	dioxane	rt	16 h	75/25	77 (+)	90 (-)
12 [b]	(*S*)-**2b**	1.5/1	dioxane	15	16 h	78/22	82 (+)	ND
13 [b]	(*S*)-**2b**	1/1	Et_2O	15	1.5 h	70/30	85 (+)	90 (-)
14 [b]	(*S*)-**2b**	1/1	MTBE	15	1.5 h	83/17	**87** (+)	92 (-)
15 [b,c]	(*S*)-**2b**	1/1	MTBE	15	1.5 h	>95/5	85 (+)	ND
16 [b]	(*S*)-**2b**	1/1	$^{i}Pr_2O$	15	1.5 h	66/34	47 (+)	93 (-)
17 [b]	(*S*)-**2b**	1/1	CPME	15	1.5 h	74/26	76 (+)	89 (-)

Reaction conditions: [a] [Au] 1 mol%, **3a** (0.1 mmol, 1 eq), solvent (1 mL), under Ar. Product ratios were measured by ^{1}H NMR. [b] These reactions were run in the presence of molecular sieve since water can behave as a competitive nucleophile. [c] with Ag_2CO_3. MTBE stands for methyl *tert*-butyl ether. CPME stands for cyclopentyl methyl ether. ND stands for not determined.

5.2. Control experiments

Figure S1

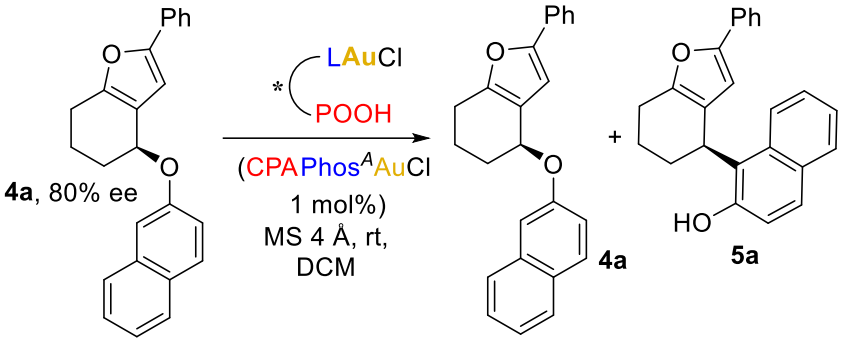

Reaction conditions: **4a** (0.2 mmol), CPAPhos^{A}AuCl (*S*)-**2a** (1 mol%), solvent (2 mL), MS 4 Å (50 mg), at rt, under argon, ^{1}H NMR yield, enantiomeric excesses were measured by chiral HPLC.

Time	% **4a**	% **5a**	%ee **4a**	%ee **5a**
0	100	0	80	
15 min	87	13	63	53
30 min	85	15	68	48
45 min	72	28	40	49
60 min	67	33	35	43

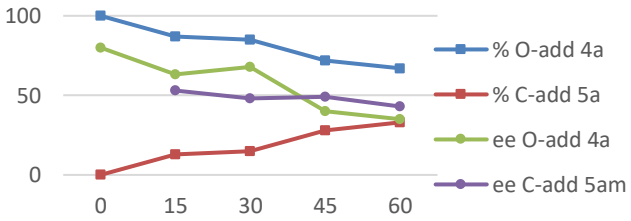

Figure S2

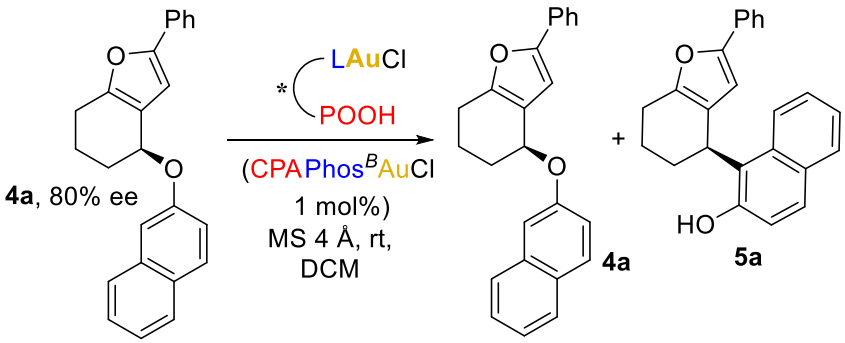

Reaction conditions: **4a** (0.2 mmol), CPAPhos^{B}AuCl (*S*)-**2b** (1 mol%), solvent (2 mL), MS 4 Å (50 mg), at rt, under argon, ^{1}H NMR yield, enantiomeric excesses were measured by chiral HPLC.

Time	% **4a**	% **5a**	%ee **4a**	%ee **5a**
0	100	0	80	
15 min	87	13	62	51
30 min	68	32	49	44
45 min	60	40	32	38
60 min	47	53	22	34

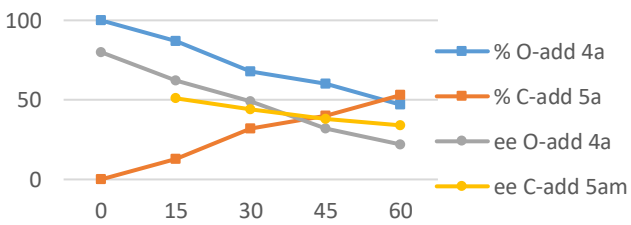

6. Scope of the reaction

6.1. General procedures

General procedure 1 for the reaction of 2-alkynyl enones **1** with naphthols

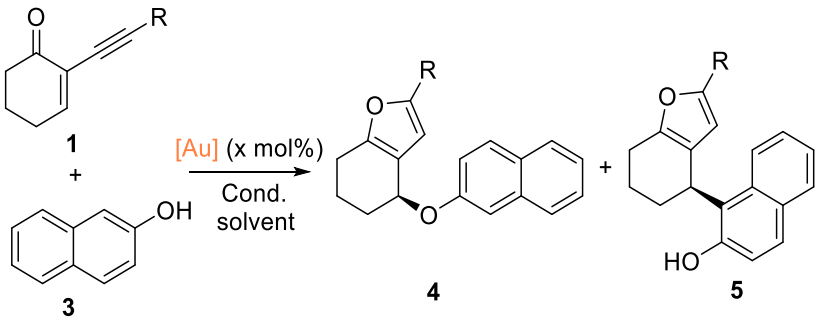

An oven-dried flask was charged with anhydrous solvent (1 mL), Au(I) catalyst **2** (x mol%) [If adding Ag_2CO_3 (x/2 mol%), stirring with Au(I) catalyst for 15 min at rt before adding starting materials], 2-alkynyl enones **1** (1-2 equiv), unsubstituted naphthols **3** (0.1 mmol, 1 equiv) and molecular sieves 4 Å (25 mg) were added. Then, the reaction was kept stirring at the required temperature under argon, and the reaction conversion was followed by TLC. The crude mixture was quenched by drops of aqueous NaOH (2 M), the organic layer was directly transferred into silica gel column chromatography (0% to 10% EtOAc/ petroleum ether) or purified by preparative TLC (10% EtOAc/ petroleum ether) to afford compounds **4** and/or **5**.

General procedure 2 for the synthesis of oxidized products **6**

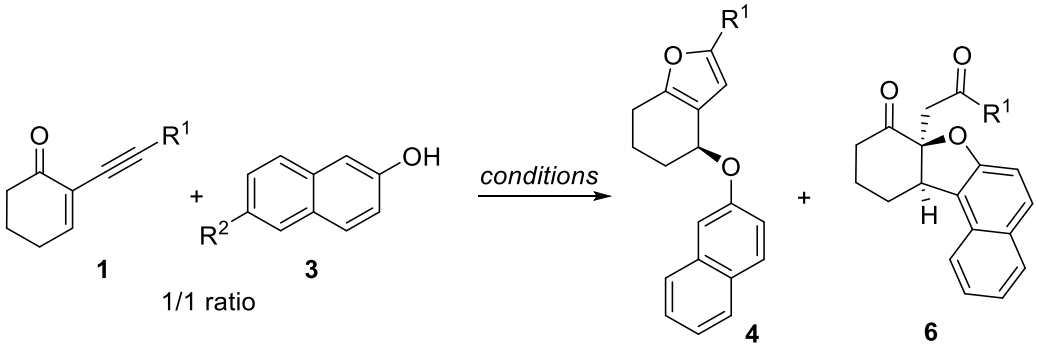

An oven-dried flask was charged with anhydrous DCM (2 mL), (*S*)-**2b** (1 mol%) [If adding Ag_2CO_3 (x/2 mol%), stirring with Au(I) catalyst for 15 min at rt before adding starting materials], 2-alkynyl enones **1** (0.2 mmol, 1 equiv), naphthols **3** (0.2 mmol, 1 equiv) and molecular sieves 4 Å (50 mg) were added. Then, the reaction was kept stirring at 10 °C under argon, and the reaction conversion was followed by TLC. The crude mixture was quenched by drops of aqueous NaOH (2 M). The solvent was then removed under vacuum. The residue was dissolved in DCE (2 mL) and added AgTFA (20 mol%). The mixture was then stirred at 40 °C for 36 h under air. After all residue completing, the crude mixture was directly transferred into silica gel column chromatography (0% to 10% EtOAc/ petroleum ether) or purified by preparative TLC (10% EtOAc/ petroleum ether) to afford compounds **6**.

6.2. Full scope of the enantioselective reactions (Results highlighted in yellow are those reported in the paper)

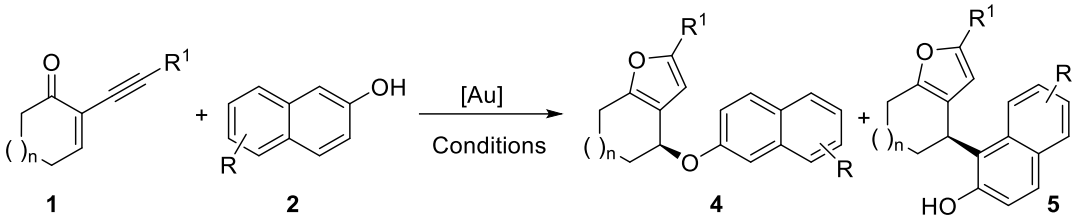

1 2 4 5

entry		R^1	n	cond.	yield (%)[b]	ee (%)[c]	yield (%)[b]	ee (%)[c]
					4a		**5a**	
1	**1a**	Ph	1	①	51	85 (-)	34	94
2	**1a**	Ph	1	③	28	58 (-)	60	93
3	**1a**	Ph	1	②[d]	> 90	85 (+)	trace	-
					4c		**S5c**	
4	**1c**	*p*-$CF_3C_6H_4$	1	①[f]	49	64 (-)	0	-
5	**1c**	*p*-$CF_3C_6H_4$	1	③[f]	56	50 (-)	0	-
6	**1c**	*p*-$CF_3C_6H_4$	1	②	47	4 (+)	0	-
					S4b		**5b**	
7	**1d**	*c*-Pr	1	①	16	45 (-)	16	89
8	**1d**	*c*-Pr	1	③	16	25 (-)	77	80
9	**1d**	*c*-Pr	1	③[d]	16	27 (-)	80	93
10	**1d**	*c*-Pr	1	②[h]	9	25 (-)	85	92
11	**1d**	*c*-Pr	1	②[d]	6	27 (-)	64	96
					S4c		**5c**	
12	**1e**	*c*-Pent	1	①	traces	-	0	-
13	**1e**	*c*-Pent	1	③	29[e]	20	42	70
14	**1e**	*c*-Pent	1	C	27[e]	11	68	99
					4f		-	
15	**1f**	Ph	2	①	72	85 (+)	0	-
16	**1f**	Ph	2	③	61	68 (+)	0	-
17	**1f**	Ph	2	②	53	69 (+)	0	-
					4b		-	
18	**1b**	*p*-$MeOC_6H_4$	1	①	28	75 (+)	nd	
19	**1b**	*p*-$MeOC_6H_4$	1	②	22	6 (-)	nd	
					4d		-	
20	**1a**	Ph	1	①	80	85 (+)	0	
					4e		-	
21	**1a**	Ph	1	①	66	79 (+)	0	
22	**1a**	Ph	1	②	51	56 (-)	0	

Conditions ①: **1** (1.5 equiv), **2m** (0.3 mmol), CPAPhos^{A}AuCl (*S*)-**3a** (1 mol%), DCM, MS 4 Å, rt, about 80 s;

Conditions ②: **1** (1.5 equiv)**, 2m** (0.3 mmol), CPAPhos^{B}AuCl (*S*)-**3b** (1 mol%), MTBE, MS 4 Å, 15 °C, 3 h;

Conditions ③: **1** (1 equiv)**, 2m** (0.3 mmol), CPAPhos^{B}AuCl (*S*)-**3b** (1 mol%), DCM, MS 4 Å, 10 °C, 5 min;

[a] Reactions were performed under Ar. [b] Isolated yields. [c] Enantiomeric excesses were measured by chiral HPLC. [d] Reactions performed in the presence of Ag_2CO_3 (0.5 mol%). [e] ^{1}H NMR yields. [f] Reaction time 1 h. [h] Reaction time 30 min.

6.3. Experimental data

6.3.1. *O*-Addition products 4

(*S*)-4-(naphthalen-2-yloxy)-2-phenyl-4,5,6,7-tetrahydrobenzofuran (4a). Obtained using **general procedure 1** from **1a** (37 mg, 0.2 mmol), **3a** (29 mg, 0.2 mmol) and catalyst **2a** (1.6 mg, 0.002 mmol, 1 mol%) in DCM, at room temperature, using 80 s reaction time, yielding **4a** (35 mg, 0.1 mmol, 51% yield) as a white solid. ^{1}H NMR (500 MHz, $CDCl_3$) δ 7.80 – 7.74 (m, 3H), 7.60 (d, *J* = 7.5 Hz, 2H), 7.45 (t, *J* = 7.0 Hz, 1H), 7.37 – 7.31 (m, 4H), 7.24 – 7.19 (m, 2H), 6.62 (s, 1H), 5.51 (t, *J* = 4.1 Hz, 1H), 2.86 – 2.80 (m, 1H), 2.73 – 2.66 (m, 1H), 2.22 – 2.13 (m, 2H), 2.07 – 2.00 (m, 1H), 1.95 – 1.89 (m, 1H). ^{13}C NMR (125 MHz, $CDCl_3$) δ 156.1, 153.6, 152.9, 134.8, 131.2, 129.8, 129.3, 128.8, 127.9, 127.2, 127.0, 126.6, 123.9, 123.7, 120.1, 119.7, 109.0, 105.2, 70.0, 28.8, 23.4, 19.4. HRMS calcd for $C_{24}H_{21}O_2$ $[M+H]^+$: 341.1536, found: 341.1531; $[\alpha]_D$ = -93.8 (*c* 1.00, $CHCl_3$); HPLC Analysis: 85% ee [©Chiralpak IA, 25 °C, 5% *i*PrOH/*n*-heptane, 1 mL/min, 264 nm, retention times: 5.3 min (minor) and 6.0 min (major)].

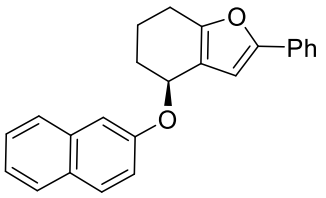

Its enantiomer **(*R*)-4-(naphthalen-2-yloxy)-2-phenyl-4,5,6,7-tetrahydrobenzofuran (4a)** was obtained using **general procedure 1** from **1a** (37 mg, 0.2 mmol), **3a** (29 mg, 0.2 mmol) and catalyst **2b** (2.1 mg, 0.002 mmol, 1 mol%) in MTBE, at 15 °C, using 1.5 h reaction time, yielding **4a** (56 mg, 0.17 mmol, 83% yield) as a white solid. $[\alpha]_D$ = +129.0 (*c* 0.69, $CHCl_3$); HPLC Analysis: 87% ee [©Chiralpak IA, 25 °C, 5% *i*PrOH/*n*-heptane, 1 mL/min, 264 nm, retention times: 5.4 min (major) and 6.2 min (minor)].

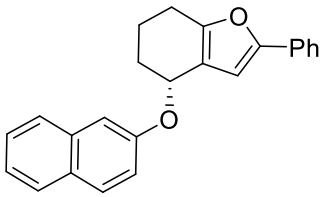

(*S*)-2-(4-methoxyphenyl)-4-(naphthalen-2-yloxy)-4,5,6,7 tetrahydrobenzofuran (4b). Obtained using **general procedure 1** from **1b** (67 mg, 0.3 mmol), **3a** (28 mg, 0.2 mmol) and catalyst **2a** (1.6 mg, 0.002 mmol, 1 mol%) in DCM, at room temperature, using 5 min reaction time, yielding **4b** Colourless oil, 21 mg, 28% yield. ^{1}H NMR (500 MHz, $CDCl_3$) δ 7.81-7.75 (m, 3H), 7.54 (d, *J* = 8.7 Hz, 2H), 7.49-7.44 (m, 1H), 7.39-7.35 (m, 1H), 7.21 (dd, *J* = 9.0 and 2.6 Hz, 1H), 6.89 (d, *J* = 9 Hz, 2H), 6.50 (s, 1H), 5.52 (t, *J* = 3.8 Hz, 1H), 3.82 (s, 3H), 2.88 – 2.78 (m, 1H), 2.74 – 2.64 (m, 1H), 2.24 – 2.11 (m, 2H), 2.08 – 1.88 (m, 2H). ^{13}C NMR (300 MHz, $CDCl_3$) δ 159.0, 156.1, 152.9, 152,9, 134.7, 129.7, 127.8, 126.9, 126.5, 125.2, 125.1, 124.3, 123.9, 120.0, 119.5, 114.2, 109.0, 103.5, 70.0, 55.45, 28.8, 23.3, 19.4 . HRMS calcd for $C_{25}H_{21}O_3$ $[M-H]^+$: 369.1491, found: 369.1475; $[\alpha]_D$ = -32.2 (*c* 1.00, $CHCl_3$); HPLC Analysis: 75% ee [©Chiralpak IA, 25 °C, 5% iPrOH/n-heptane, 1 mL/min, 260 nm, retention times: 7.7 min (minor) and 8.8 min (major)].

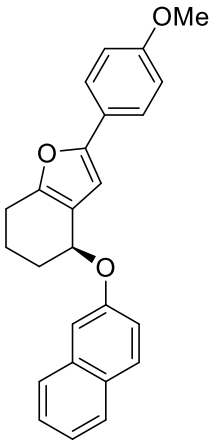

(*S*)-4-(naphthalen-2-yloxy)-2-(4-(trifluoromethyl)phenyl)-4,5,6,7 tetrahydrobenzofuran (4c) Obtained using **general procedure 1** from **1c** (26 mg, 0.1 mmol), **3a** (14 mg, 0.1 mmol) and catalyst **2a** (0.8 mg, 0.001 mmol, 1 mol%) in DCM, at room temperature, using 80 s reaction time, yielding **4c** (23 mg, 0.06 mmol, 56% yield) as a colourless oil. ^{1}H NMR (500 MHz, $CDCl_3$) δ 7.79 – 7.74 (m, 3H), 7.87 (d, *J* = 8.6 Hz, 2H), 7.56 (d, *J* = 8.6 Hz, 2H), 7.46 – 7.43 (m, 1H), 7.36 – 7.33 (m, 2H), 7.20 (dd, *J* = 8.8 and 2.4 Hz, 1H), 6.73 (s, 1H), 5.51 (t, *J* = 4.2 Hz, 1H), 2.86 – 2.80 (m, 1H), 2.73 – 2.67 (m, 1H), 2.21 – 2.13 (m, 2H), 2.07 – 2.01 (m, 1H), 1.96 – 1.90 (m, 1H). ^{13}C NMR (125 MHz, $CDCl_3$) δ 156.0, 154.8, 151.4, 134.7, 134.2, 129.9, 129.4, 127.9, 126.9, 126.7, 125.8, 125.8, 124.0, 123.6, 120.1, 119.9, 109.0, 107.2, 69.7, 28.8, 23.4, 19.3. ^{19}F NMR (282 MHz, $CDCl_3$): δ = -62.5. HRMS calcd for $C_{25}H_{18}F_3O_2$ $[M-H]^+$: 407.1259, found: 407.1244; $[\alpha]_D$ = +20.6 (*c* 1.00, $CHCl_3$); HPLC Analysis: 64% ee [©Chiralpak IA, 25 °C, 5% *i*PrOH/*n*-heptane, 1 mL/min, 227 nm, retention times: 8.7 min (major) and 6.8 min (minor)].

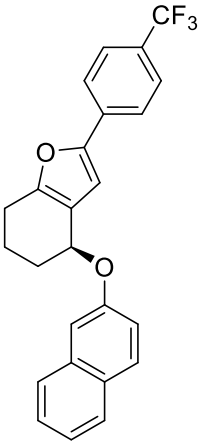

(*S*)-6-((2-phenyl-4,5,6,7-tetrahydrobenzofuran-4-yl)oxy)-2-naphthonitrile (4d). Obtained using **general procedure 1** from **1a** (29 mg, 0.15mmol)**, 3b** (17 mg, 0.1mmol) and catalyst **2a** (0.8 mg, 0.001 mmol, 1 mol%) in DCM at room temperature, using 120 s reaction time, yielding **4d** (29 mg, 0.079 mmol, 79% yield) as a white solid. ^{1}H NMR (500 MHz, $CDCl_3$) δ 8.151 (s, 1H), 7.82-7.79 (t, *J*= 8.5Hz, 2H), 7.60-7.57 (m, 3H), 7.35-7.29 (m, 4H), 7.24-1.20 (t, *J*=7.6 Hz, 1H), 6.59 (s, 1H), 5.57-5.55 (t, *J*= 4.3 Hz, 1H), 2.85-2.81 (m, 1H), 2.74-2.69 (m, 1H), 2.20-2.14 (m, 2H), 2.09-2.06 (m, 1H), 1.97-1.92 (m, 1H). ^{13}C NMR (500 MHz, $CDCl_3$) δ 158.8, 154.0, 153.2, 136.7, 134.1, 131.1, 130.6, 129.0, 128.1, 127.6, 127.4, 123.9, 121.9, 119.9, 119.2, 108.7, 107.2, 105.0, 70.3, 28.9, 23.5, 19.4. HRMS calcd for $C_{25}H_{19}NO_2$ $[M+H]^+$:366.1489, found: 366.1490; $[\alpha]_D$ = -38.40 (*c* 1.00, $CHCl_3$); HPLC Analysis: 84% ee [©Chiralpak IB, 25 °C, 20% iPrOH/n-heptane, 1 mL/min, 285 nm, retention times: 6.4 min (major) and 8.5 min (minor)].

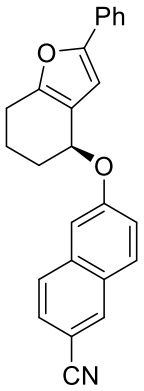

(*S*)-4-((6-bromonaphthalen-2-yl)oxy)-2-phenyl-4,5,6,7-tetrahydrobenzofuran (4e). Obtained using **general procedure 1** from **1a** (29mg, 0.15mmol)**, 3c** (17 mg, 0.1mmol) and catalyst **2a** (0.8 mg, 0.001 mmol, 1 mol%) in DCM at room temperature, using 120 s reaction time, yielding **4e** (29 mg, 0.079 mmol, 79% yield) as a yellow solid.^{1}H NMR (500 MHz, $CDCl_3$) δ 7.91 (s, 1H), 7.68-7.64 (d, *J*= 9.2 Hz, 1H), 7.60-7.57 (m, 3H), 7.50-7.48 (dd, *J*= 8.5 Hz and 1.9 Hz, 1H), 7.39-7.30 (t, *J*= 7.9 Hz, 1H), 7.27 (s, 1H), 7.21-7.18 (m, 1H), 6.58 (s, 1H), 5.48-5.47 (t, *J*= 4.3 Hz, 1H), 2.83-2.81 (m, 1H), 2.7-2.6 (m, 1H), 2.17-2.10 (m, 2H), 2.04-1.98 (m, 1H), 1.92-1.88 (m, 1H). ^{13}C NMR (500 MHz, $CDCl_3$) δ 156.3, 153.5, 152.8, 133.1, 130.9, 130.2, 129.7, 128.9, 128.9, 128.8, 128.6, 128.4, 127.1, 123.6, 120.9, 119.3, 117.2, 108.7, 104.9, 69.8, 28.6, 23.2, 19.2. HRMS calcd for $C_{24}H_{19}BrO_2$ $[M+H]^+$: 419.0641, found: 319.0644; $[\alpha]_D$ =-97.6(*c* 0.8, $CHCl_3$); HPLC Analysis: 79% ee [©Chiralpak IB, 25 °C, 20% iPrOH/n-heptane, 1 mL/min, 312 nm, retention times: 4.5 min (major) and 5.6 min (minor)].

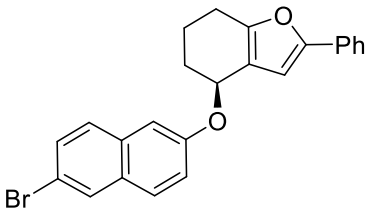

Its enantiomer **(*R*)-4-((6-bromonaphthalen-2-yl)oxy)-2-phenyl-4,5,6,7-tetrahydrobenzofuran (4e)** was obtained using **general procedure 1** from **1a** (29mg, 0.15mmol)**, 3c** (17 mg, 0.1mmol) and catalyst **2b** (0.8 mg, 0.001 mmol, 1 mol%) in DCM at room temperature, using 120 s reaction time, yielding **4e** (29 mg, 0.079 mmol, 79% yield) as a yellow solid. $[\alpha]_D$ = +77.5 (*c* 1.1, $CHCl_3$); HPLC Analysis: 64% ee [©Chiralpak IB, 25 °C, 20% iPrOH/n-heptane, 1 mL/min, 229 nm, retention times: 4.5 min (minor) and 5.6 min (major)].

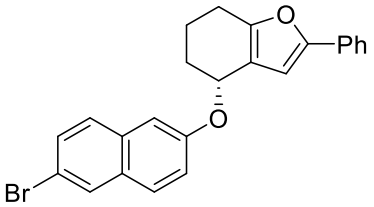

(*S*)-4-(naphthalen-2-yloxy)-2-phenyl-5,6,7,8-tetrahydro-4*H*-cyclohepta[*b*]furan (4f). Obtained using **general procedure 1** from **1f** (32 mg, 0.1 mmol), **3a** (14 mg, 0.1 mmol) and catalyst **2a** (0.8 mg, 0.001 mmol, 1 mol%) in DCM, at room temperature, using 80 s reaction time, yielding **4f** (26 mg, 0.07 mmol, 73% yield) as a colourless oil. ^{1}H NMR (500 MHz, $CDCl_3$) δ 7.71 (d, *J* = 8.5 Hz, 2H), 7.66 (d, *J* = 8.0 Hz, 1H), 7.51 (d, *J* = 7.5 Hz, 2H), 7.37 (t, *J* = 7.5 Hz, 1H), 7.30 – 7.24 (m, 3H), 7.22 – 7.16 (m, 2H), 7.13 (t, *J* = 7.4 Hz, 1H), 6.55 (s, 1H), 5.35 (d, *J* = 7.0 Hz, 1H), 3.00 – 2.94 (m, 1H), 2.89 – 2.80 (m, 1H), 2.18 – 2.05 (m, 3H), 1.83 – 1.72 (m, 3H). ^{13}C NMR (125 MHz, $CDCl_3$) δ 156.2, 153.4, 150.7, 134.8, 131.1, 129.7, 129.3, 128.8, 127.9, 127.0, 127.0, 126.5, 123.9, 123.8, 123.6, 120.0, 109.4, 107.4, 73.8, 33.8, 29.0, 26.5, 25.0. HRMS calcd for $C_{25}H_{23}O_2$ $[M+H]^+$: 355.1693, found: 355.1697; $[\alpha]_D$ = -175.8 (*c* 1.00, $CHCl_3$); HPLC Analysis: 85% ee [©Chiralpak IF, 25 °C, 2% *i*PrOH/*n*-heptane, 1 mL/min, 338 nm, retention times: 5.7 min (minor) and 6.2 min (major)].

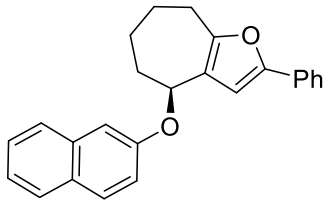

(*S*)-4-(naphthalen-1-yloxy)-2-phenyl-4,5,6,7-tetrahydrobenzofuran (4a'). [2] Obtained using **general procedure 1** from **1a** (59 mg, 0.3 mmol), **3a'** (43 mg, 0.3 mmol) and catalyst **2a** (2.5 mg, 0.003 mmol, 1 mol%) in DCM, at room temperature, using 80 s reaction time, yielding **4a'** (37 mg, 0.1 mmol, 36% yield) as a yellow oil for which characterization data match those of the literature.[2] ^{1}H NMR (500 MHz, $CDCl_3$) δ 8.28 (d, *J* = 8.0 Hz, 1H), 7.80 (d, *J* = 8.0 Hz, 1H), 7.61 (d, *J* = 8.0 Hz, 2H), 7.49 – 7.41 (m, 4H), 7.34 (t, *J* = 7.8 Hz, 2H), 7.21 (t, *J* = 7.4 Hz, 1H), 7.06 (d, *J* = 7.0 Hz, 1H), 6.64 (s, 1H), 5.56 (t, *J* = 4.2 Hz, 1H), 2.89 – 2.82 (m, 1H), 2.74 – 2.67 (m, 1H), 2.27 – 2.19 (m, 2H), 2.10 – 2.03 (m, 1H), 1.98 – 1.90 (m, 1H). ^{13}C NMR (125 MHz, $CDCl_3$) δ 154.2, 153.5, 152.7, 135.0, 131.2, 128.8, 127.6, 127.2, 126.8, 126.6, 126.0, 125.4, 123.7, 122.7, 120.6, 120.0, 106.9, 105.4, 70.4, 29.2, 23.5, 19.6. HRMS calcd for $C_{24}H_{21}O_2$ $[M+H]^+$: 341.1536, found: 341.1537; $[\alpha]_D$ = +96.8 (*c* 1.00, $CHCl_3$); HPLC Analysis: 88% ee [©Chiralpak IA, 25 °C, 5% *i*PrOH/*n*-heptane, 1 mL/min, 212 nm, retention times: 4.5 min (minor) and 5.0 min (major)].

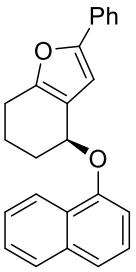

[2] Martí, À.; Montesinos-Magraner, M.; Echavarren, A. M.; Franchino, A., H-Bonded Counterion-Directed Catalysis: Enantioselective Gold(I)-Catalyzed Addition to 2-Alkynyl Enones as a Case Study. *Eur. J. Org. Chem.* **2022,** *2022*, e202200518.

Its enantiomer **(*R*)-4-(naphthalen-1-yloxy)-2-phenyl-4,5,6,7-tetrahydrobenzofuran (4a')** was obtained using **general procedure 1** from **1a** (59 mg, 0.3 mmol), **3a'** (43 mg, 0.3 mmol) and catalyst **2b** (3.1 mg, 0.003 mmol, 1 mol%) in MTBE, at 15 °C, using 3 h reaction time, yielding **4a'** (56 mg, 0.16 mmol, 55% yield) as a yellow oil. Yellow oil, 55.9 mg, 55% yield in MTBE. $[\alpha]_D$ = -56.9 (*c* 1.00, $CHCl_3$); HPLC Analysis: 50% ee [©Chiralpak IA, 25 °C, 5% *i*PrOH/*n*-heptane, 1 mL/min, 212 nm, retention times: 4.5 min (major) and 5.0 min (minor)].

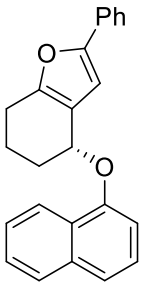

6.3.2. *C*-Addition products 5

(*S*)-1-(2-phenyl-4,5,6,7-tetrahydrobenzofuran-4-yl)naphthalen-2-ol (5a). [3] Obtained using **general procedure 1** from **1a** (37 mg, 0.2 mmol), **3a** (29 mg, 0.2 mmol) and catalyst **2b** (2.1 mg, 0.002 mmol, 1 mol%) in DCM, at 10 °C, using 5 min reaction time, yielding **5a** (41 mg, 0.1 mmol, 60% yield) as a white solid for which characterization data match that of the literature.[3] ^{1}H NMR (500 MHz, $CDCl_3$) δ 8.07 (d, *J* = 9.0 Hz, 1H), 7.82 (d, *J* = 7.5 Hz, 1H), 7.70 (d, *J* = 8.5 Hz, 1H), 7.58 (d, *J* = 7.5 Hz, 2H), 7.52 (t, *J* = 7.2 Hz, 1H), 7.37 (t, *J* = 7.4 Hz, 1H), 7.33 (t, *J* = 7.7 Hz, 2H), 7.22 (t, *J* = 7.4 Hz, 1H), 7.08 (d, *J* = 9.0 Hz, 1H), 6.41 (s, 1H), 5.69 (s, 1H), 4.82 – 4.85 (m, 1H), 2.88 – 2.86 (m, 2H), 2.24 – 2.17 (m, 2H), 2.03 – 1.91 (m, 2H). ^{13}C NMR (125 MHz, $CDCl_3$) δ 154.0, 153.1, 152.4, 133.1, 130.8, 129.7, 129.1, 129.0, 128.8, 127.6, 126.9, 123.8, 123.3, 122.0, 120.3, 119.9, 119.7, 105.0, 32.6, 29.7, 23.5, 23.2. HRMS calcd for $C_{24}H_{21}O_2$ $[M+H]^+$: 341.1536, found: 341.1540; $[\alpha]_D$ = -124.3 (*c* 1.00, $CHCl_3$); HPLC Analysis: 93% ee [©Chiralpak IA, 25 °C, 5% *i*PrOH/*n*-heptane, 1 mL/min, 318 nm, retention times: 9.7 min (minor) and 10.7 min (major)].

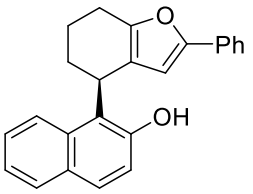

(*S*)-1-(2-cyclopropyl-4,5,6,7-tetrahydrobenzofuran-4-yl)naphthalen-2-ol (5b). Obtained using **general procedure 1** from **1d** (32 mg, 0.2 mmol), **3a** (29 mg, 0.2 mmol), catalyst **2b** (2.1 mg, 0.002 mmol, 1 mol%) and Ag_2CO_3 (0.3 mg, 0.001 mmol, 0.5 mol%) in DCM, at 10 °C, using 5 min reaction time, yielding **5b** (49 mg, 0.1 mmol, 80% yield) as a colourless oil. ^{1}H NMR (500 MHz, $CDCl_3$) δ 8.02 (d, *J* = 9.0 Hz, 1H), 7.79 (d, *J* = 8.0 Hz, 1H), 7.67 (d, *J* = 9.0 Hz, 1H), 7.49 (t, *J* = 7.7 Hz, 1H), 7.34 (t, *J* = 7.4 Hz, 1H), 7.06 (d, *J* = 8.5 Hz, 1H), 5.81 (s, 1H), 5.72 (s, 1H), 4.72 (t, *J* = 7.3 Hz, 1H), 2.72 (s, 2H), 2.18 – 2.11 (m, 2H), 1.91 – 1.79 (m, 3H), 0.85 – 0.80 (m, 2H), 0.74 – 0.70 (m, 2H). ^{13}C NMR (125 MHz, $CDCl_3$) δ 157.8, 153.2, 150.5, 133.1, 129.6, 129.1, 128.9, 126.7, 123.1, 122.0, 119.9, 119.8, 118.5, 103.6, 32.5, 29.8, 23.3, 23.1, 9.1, 7.0, 6.8. HRMS calcd for $C_{21}H_{21}O_2$ $[M+H]^+$: 305.1536, found: 305.1539; $[\alpha]_D$ = -25.1 (*c* 1.00, $CHCl_3$); HPLC Analysis: 93% ee [©Chiralpak IA, 25 °C, 5% *i*PrOH/*n*-heptane, 1 mL/min, 241 nm, retention times: 6.6 min (minor) and 7.2 min (major)].

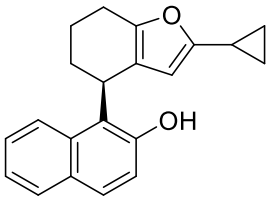

[3] Li, Z.; Peng, J.; He, C.; Xu, J.; Ren, H., Silver(I)-Mediated Cascade Reaction of 2-(1-Alkynyl)-2-alken-1-ones with 2-Naphthols. *Org. Lett.* **2020,** *22*, 5768-5772.

(*S*)-1-(2-cyclopentyl-4,5,6,7-tetrahydrobenzofuran-4-yl)naphthalen-2-ol (5c). 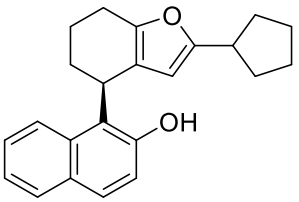 Obtained using **general procedure 1** from **1e** (38 mg, 0.2 mmol), **3a** (29 mg, 0.2 mmol) and catalyst **2b** (2.1 mg, 0.002 mmol, 1 mol%) in MTBE, at 15 °C, using 3 h reaction time, yielding **5c** (45 mg, 0.14 mmol, 68% yield) as a colourless oil. ^{1}H NMR (500 MHz, $CDCl_3$) δ 8.02 (d, *J* = 8.5 Hz, 1H), 7.79 (d, *J* = 8.0 Hz, 1H), 7.67 (d, *J* = 9.0 Hz, 1H), 7.48 (t, *J* = 8.3 Hz, 1H), 7.34 (t, *J* = 7.2 Hz, 1H), 7.05 (d, J = 8.5 Hz, 1H), 5.85 (s, 1H), 5.75 (s, 1H), 4.74 (t, *J* = 6.8 Hz, 1H), 3.05 – 2.98 (m, 1H), 2.75 – 2.72 (m, 2H), 2.18 – 2.11 (m, 2H), 1.96 – 1.88 (m, 4H), 1.70 – 1.58 (m, 6H). ^{13}C NMR (125 MHz, $CDCl_3$) δ 160.4, 153.2, 150.8, 133.1, 129.6, 129.1, 128.8, 126.7, 123.1, 122.0, 119.9, 119.9, 118.1, 103.5, 39.0, 32.6, 32.0, 29.9, 25.4, 23.4, 23.2. HRMS calcd for $C_{23}H_{25}O_2$ $[M+H]^+$: 333.1849, found: 333.1850; $[\alpha]_D$ = -24.3 (*c* 1.00, $CHCl_3$); HPLC Analysis: 99% ee [©Chiralpak IA, 25 °C, 2% *i*PrOH/*n*-heptane, 1 mL/min, 280 nm, retention times: 7.4 min (minor) and 8.1 min (major)].

(*R*)-2-(2-phenyl-4,5,6,7-tetrahydrobenzofuran-4-yl)naphthalen-1-ol (5a'). 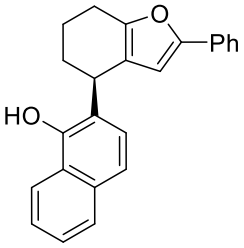 Obtained using **general procedure 1** from **1a** (59 mg, 0.3 mmol), **3a'** (43 mg, 0.3 mmol) and catalyst **2b** (3.1 mg, 0.003 mmol, 1 mol%) in DCM, at 10 °C, using 5 min reaction time, yielding **5a'** (62 mg, 0.18 mmol, 61% yield) as a colourless oil. ^{1}H NMR (500 MHz, $CDCl_3$) δ 8.15 – 8.10 (m, 1H), 7.80 – 7.75 (m, 1H), 7.58 (d, *J* = 7.5 Hz, 2H), 7.48 – 7.43 (m, 2H), 7.41 (d, *J* = 8.0 Hz, 1H), 7.32 (t, *J* = 7.8 Hz, 2H), 7.24 (d, *J* = 8.5 Hz, 1H), 7.20 (t, *J* = 7.4 Hz, 1H), 6.38 (s, 1H), 5.53 (s, 1H), 4.14 (t, *J* = 7.0 Hz, 1H), 2.83 (s, 2H), 2.22 – 2.09 (m, 2H), 1.95 – 1.85 (m, 2H). ^{13}C NMR (125 MHz, $CDCl_3$) δ 153.4, 152.3, 149.3, 133.8, 131.0, 128.8, 128.2, 127.7, 127.3, 126.0, 125.5, 125.4, 123.7, 123.0, 121.6, 120.7, 120.4, 105.3, 37.6, 31.3, 23.5, 22.7. HRMS calcd for $C_{24}H_{21}O_2$ $[M+H]^+$: 341.1536, found: 341.1540; $[\alpha]_D$ = +63.8 (*c* 1.00, $CHCl_3$); HPLC Analysis: 98% ee [©Chiralpak IA, 25 °C, 5% *i*PrOH/*n*-heptane, 1 mL/min, 280 nm, retention times: 13.4 min (major) and 16.3 min (minor)].

6.3.3. Oxidation products 6

(*7aS,11aR*)-7a-(2-oxo-2-phenylethyl)-9,10,11,11a-tetrahydronaphtho[2,1-*b*]benzofuran-8(7*aH*)-one (6a). 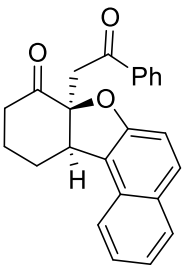 Obtained using **general procedure 2** from **1a** (59 mg, 0.3 mmol), **3a** (43 mg, 0.3 mmol) and catalyst **2b** (3.1 mg, 0.003 mmol, 1 mol%) in DCM, at 10 °C, for 5 min at step 1. It was then heated in DCE, at 40 °C for 31 h, yielding **6a** (48 mg, 0.14 mmol, 45% yield) as a white solid for which characterization data match that of the literature.[3] ^{1}H NMR (500 MHz, $CDCl_3$) δ 7.87 (d, *J* = 7.5 Hz, 2H), 7.83 (d, *J* = 8.0 Hz, 1H), 7.72 (d, *J* = 8.5 Hz, 1H), 7.66 (d, *J* = 8.0 Hz, 1H), 7.53 (t, *J* = 7.4 Hz, 1H), 7.46 (t, *J* = 7.5 Hz, 1H), 7.40 (t, *J* = 7.7 Hz, 2H), 7.32 (t, *J* = 7.5 Hz, 1H), 7.14 (d, *J* = 9.0 Hz, 1H), 4.14 (t, *J* = 6.3 Hz, 1H), 4.06 (d, *J* = 17.5 Hz, 1H), 3.49 (d, *J* = 17.5 Hz, 1H), 2.77 – 2.62 (m, 2H), 2.44 – 2.37 (m, 1H), 2.13 – 2.04 (m, 1H), 1.91 – 1.81 (m, 2H). ^{13}C NMR (125 MHz, $CDCl_3$) δ 205.0, 198.8, 155.1, 136.5, 133.8, 130.5, 130.3, 130.1, 129.3, 128.8, 128.2, 127.2, 123.6, 122.5, 122.3, 112.6, 89.2, 47.7, 45.3, 38.3, 28.7, 19.7. HRMS calcd for $C_{24}H_{21}O_3$ $[M+H]^+$: 357.1485, found: 357.1487; $[\alpha]_D$ =

+142.1 (*c* 1.00, $CHCl_3$); HPLC Analysis: 93% ee [©Chiralpak IA, 25 °C, 5% *i*PrOH/*n*-heptane, 1 mL/min, 251 nm, retention times: 7.7 min (minor) and 8.9 min (major)].

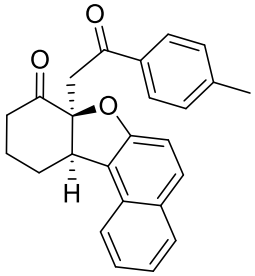

(*7aS,11aR*)-7a-(2-oxo-2-(*p*-tolyl)ethyl)-9,10,11,11a-tetrahydronaphtho[2,1-*b*]benzofuran-8(7*aH*)-one (6b). Obtained using **general procedure 2** from **1g** (42 mg, 0.2 mmol), **3a** (29 mg, 0.2 mmol) and catalyst **2b** (2.1 mg, 0.002 mmol, 1 mol%) in DCM, at 10 °C, for 30 min at step 1. It was then heated in DCE, at 40 °C for 48 h, yielding **6b** (35 mg, 0.1 mmol, 52% yield) as a colourless oil. ^{1}H NMR (500 MHz, $CDCl_3$) δ 7.83 (d, *J* = 8.0 Hz, 1H), 7.77 (d, *J* = 7.5 Hz, 2H), 7.72 (d, *J* = 8.5 Hz, 1H), 7.66 (d, *J* = 8.0 Hz, 1H), 7.45 (t, *J* = 7.6 Hz, 1H), 7.32 (t, *J* = 7.2 Hz, 1H), 7.19 (d, *J* = 8.0 Hz, 2H), 7.14 (d, *J* = 9.0 Hz, 1H), 4.13 (t, *J* = 6.3 Hz, 1H), 4.04 (d, *J* = 17.5 Hz, 1H), 3.47 (d, *J* = 17.5 Hz, 1H), 2.77 – 2.61 (m, 2H), 2.45 – 2.38 (m, 1H), 2.36 (s, 3H), 2.14 – 2.06 (m, 1H), 1.89 – 1.82 (m, 2H). ^{13}C NMR (125 MHz, $CDCl_3$) δ 205.0, 198.4, 155.1, 144.7, 134.1, 130.5, 130.3, 130.0, 129.5, 129.4, 129.3, 128.4, 127.2, 123.5, 122.5, 112.6, 89.2, 47.7, 45.3, 38.4, 28.7, 21.9, 19.8. HRMS calcd for $C_{25}H_{23}O_3$ $[M+H]^+$: 371.1642, found: 371.1645; $[\alpha]_D$ = +118.6 (*c* 1.00, $CHCl_3$); HPLC Analysis: 86% ee [©Chiralpak IA, 25 °C, 10% *i*PrOH/*n*-heptane, 1 mL/min, 246 nm, retention times: 12.5 min (minor) and 15.1 min (major)].

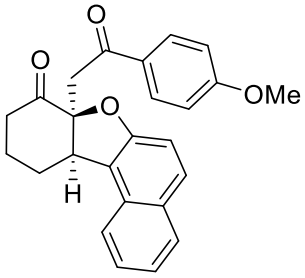

(*7aS,11aR*)-7a-(2-(4-methoxyphenyl)-2-oxoethyl)-9,10,11,11a tetrahydronaphtho[2,1-*b*]benzofuran-8(7*aH*)-one (6c). Obtained using **general procedure 2** from **1b** (28 mg, 0.125 mmol), **3a** (18 mg, 0.125 mmol) and catalyst **2b** (1 mg, 0.0012 mmol, 1 mol%) in DCM, at 10 °C, for 5 min at step 1. It was then heated in DCE, at 40 °C for 24 h, yielding **6c** (27 mg, 0.07 mmol, 56% yield) as a colourless oil for which characterization data match that of the literature.[3] ^{1}H NMR (500 MHz, $CDCl_3$) δ 7.83 (t, *J* = 8.6 Hz, 3H), 7.71 (d, *J* = 8.6 Hz, 1H), 7.66 (d, *J* = 8.6 Hz, 1H), 7.45 (t, *J* = 7.5 Hz, 1H), 7.32 (t, *J* = 7.5 Hz, 1H), 7.13 (d, *J* = 8.6 Hz, 1H), 6.86 (d, *J* = 8.6 Hz, 2H), 4.12 (t, *J* = 6.4 Hz, 1H), 4.01 (d, *J* = 17.5 Hz, 1H), 3.82 (s, 3H), 3.46 (d, *J* = 17.5 Hz, 1H), 2.76 – 2.70 (m, 1H), 2.67 – 2.60 (m, 1H), 2.44 – 2.39 (m, 1H), 2.14 – 2.06 (m, 1H), 1.88 – 1.80 (m, 2H). ^{13}C NMR (125 MHz, $CDCl_3$) δ 205.1, 197.2, 164.1, 155.1, 130.6, 130.5, 130.3, 130.0, 129.7, 129.2, 127.1, 123.5, 122.5, 122.4, 114.0, 112.6, 89.2, 55.7, 47.7, 45.2, 38.4, 28.7, 19.8. HRMS calcd for $C_{25}H_{23}O_4$ $[M+H]^+$: 387.1596, found: 387.1591; $[\alpha]_D$ = -27.9 (*c* 1.00, $CHCl_3$); HPLC Analysis: 91% ee [©Chiralpak IA, 25 °C, 20% *i*PrOH/*n*-heptane, 1 mL/min, 234 nm, retention times: 13.4 min (minor) and 16.4 min (major)].

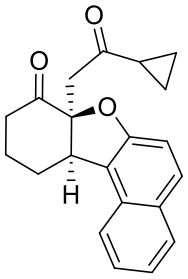

(*7aS,11aR*)-7a-(2-cyclopropyl-2-oxoethyl)-9,10,11,11a-tetrahydronaphtho[2,1-*b*]benzofuran-8(7*aH*)-one (6d). Obtained using **general procedure 2** from **1d** (32 mg, 0.2 mmol), **3a** (29 mg, 0.2 mmol), catalyst **2b** (2.1 mg, 0.002 mmol, 1 mol%) and Ag_2CO_3 (0.3 mg, 0.001 mmol, 0.5 mol%) in DCE, at 10 °C, for 30 min at step 1. It was then heated in DCE, at 40 °C for 48 h, yielding **6d** (40 mg, 0.13 mmol, 66% yield) as a yellow oil for which characterization data match that of the literature.[3] ^{1}H NMR (500 MHz, $CDCl_3$) δ 7.83 (d, *J* = 8.0 Hz, 1H), 7.71 (d, *J* = 9.0 Hz, 1H), 7.67 (d, *J* = 8.5 Hz, 1H), 7.47 (t, *J* = 7.1 Hz, 1H), 7.33 (t, *J* = 7.1 Hz, 1H), 7.11 (d, *J* = 8.5 Hz, 1H), 4.03 (t, *J* = 6.2

Hz, 1H), 3.60 (d, *J* = 17.5 Hz, 1H), 3.05 (d, *J* = 17.5 Hz, 1H), 2.60 (t, *J* = 6.7 Hz, 2H), 2.31 – 2.24 (m, 1H), 1.99 – 1.73 (m, 4H), 1.05 – 0.94 (m, 2H), 0.92 – 0.86 (m, 1H), 0.84 – 0.78 (m, 1H). ^{13}C NMR (125 MHz, $CDCl_3$) δ 209.4, 205.2, 155.2, 130.5, 130.3, 130.0, 129.3, 127.2, 123.5, 122.5, 122.1, 112.6, 88.8, 49.2, 47.7, 38.2, 28.5, 21.3, 19.6, 11.4, 11.2. HRMS calcd for $C_{21}H_{21}O_3$ $[M+H]^+$: 321.1485, found: 321.1489; $[\alpha]_D$ = +213.4 (c 1.00, $CHCl_3$); HPLC Analysis: 87% ee [©Chiralpak IA, 25 °C, 10% iPrOH/n-heptane, 1 mL/min, 236 nm, retention times: 6.3 min (minor) and 12.3 min (major)].

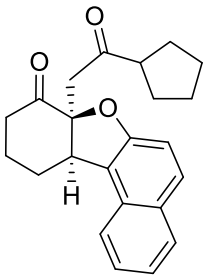

(*7aS,11aR*)-7a-(2-cyclopentyl-2-oxoethyl)-9,10,11,11a-tetrahydronaphtho[2,1-*b*]benzofuran-8(7*aH*)-one (6e). Obtained using **general procedure 2** from **1e** (38 mg, 0.2 mmol), **3a** (29 mg, 0.2 mmol) and catalyst **2b** (2.1 mg, 0.002 mmol, 1 mol%) in MTBE, at 15 °C, for 6 h at step 1. It was then heated in DCE, at 40 °C for 40 h, yielding **6e** (38 mg, 0.11 mmol, 55% yield) as a colourless oil. ^{1}H NMR (500 MHz, $CDCl_3$) δ 7.83 (d, *J* = 8.0 Hz, 1H), 7.71 (d, *J* = 9.0 Hz, 1H), 7.67 (d, *J* = 8.5 Hz, 1H), 7.47 (t, *J* = 7.6 Hz, 1H), 7.33 (t, *J* = 7.5 Hz, 1H), 7.10 (d, *J* = 9.0 Hz, 1H), 4.06 (t, *J* = 6.1 Hz, 1H), 3.52 (d, *J* = 18.0 Hz, 1H), 2.91 (d, *J* = 17.5 Hz, 1H), 2.83 (p, *J* = 8.0 Hz, 1H), 2.61 (t, *J* = 6.7 Hz, 2H), 2.34 – 2.27 (m, 1H), 2.00 – 1.92 (m, 1H), 1.87 – 1.51 (m, 10H). ^{13}C NMR (125 MHz, $CDCl_3$) δ 212.3, 205.3, 155.2, 130.5, 130.3, 130.0, 129.3, 127.2, 123.5, 122.5, 122.1, 112.5, 89.0, 51.8, 47.9, 47.6, 38.2, 29.1, 28.8, 28.5, 28.5, 26.2, 19.6. HRMS calcd for $C_{23}H_{25}O_3$ $[M+H]^+$: 349.1798, found: 349.1800; $[\alpha]_D$ = +206.7 (c 1.00, $CHCl_3$); HPLC Analysis: 98% ee [©Chiralpak IA, 25 °C, 2% iPrOH/n-heptane, 1 mL/min, 245 nm, retention times: 8.9 min (minor) and 12.6 min (major)].

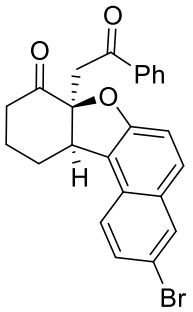

(*7aS,11aR*)-3-bromo-7a-(2-oxo-2-phenylethyl)-9,10,11,11a-tetrahydronaphtho[2,1-*b*]benzofuran-8(7*aH*)-one (6f). Obtained using **general procedure 2** from **1a** (59 mg, 0.3 mmol), **3c** (67 mg, 0.3 mmol) and catalyst **2b** (3 mg, 0.003 mmol, 1 mol%) in DCM, at 10 °C, for 1.5 h at step 1. It was then heated in DCE, at 40 °C for 24 h, yielding **6f** (42 mg, 0.1 mmol, 32% yield) as a white solid for which characterization data match that of the literature.[3] ^{1}H NMR (500 MHz, $CDCl_3$) δ 7.97 (s, 1H), 7.87 (d, *J* = 7.3 Hz, 2H), 7.62 (d, *J* = 8.8 Hz, 1H), 7.55 – 7.49 (m, 3H), 7.40 (t, *J* = 7.8 Hz, 2H), 7.14 (d, *J* = 8.8 Hz, 1H), 4.11 (t, *J* = 6.2 Hz, 1H), 4.06 (d, *J* = 17.7 Hz, 1H), 3.47 (d, *J* = 17.7 Hz, 1H), 2.80 – 2.59 (m, 2H), 2.45 – 2.33 (m, 1H), 2.14 – 2.04 (m, 1H), 1.88 – 1.77 (m, 2H). ^{13}C NMR (125 MHz, $CDCl_3$) δ 204.6, 198.6, 155.4, 136.4, 133.9, 131.4, 131.2, 130.5, 129.2, 129.0, 128.8, 128.3, 124.2, 122.7, 117.1, 113.7, 89.3, 47.6, 45.3, 38.2, 28.7, 19.7. HRMS calcd for $C_{24}H_{20}BrO_3$ $[M+H]^+$: 435.0590, found: 435.0589; $[\alpha]_D$ = +122.5 (*c* 1.00, $CHCl_3$); HPLC Analysis: 85% ee [©Chiralpak IA, 25 °C, 20% *i*PrOH/*n*-heptane, 1 mL/min, 283 nm, retention times: 11.7 min (minor) and 12.8 min (major)].

(*7aS,11aR*)-8-oxo-7a-(2-oxo-2-phenylethyl)-7a,8,9,10,11,11a-hexahydronaphtho[2,1-*b*]benzofuran-3-carbonitrile (6g). Obtained using **general procedure 2** from **1a** (39 mg, 0.2 mmol), **3b** (34 mg, 0.2 mmol) and catalyst **2b** (2.1 mg, 0.002 mmol, 1 mol%) in DCM, at 10 °C, for 25 min at step 1. It was then heated in DCE, at 40 °C for 48 h, yielding **6g** (10 mg, 0.03 mmol, 13% yield) as a white solid for which characterization data match that of the literature.[3] ^{1}H NMR (500 MHz, $CDCl_3$) δ 8.19 (s, 1H), 7.87 (d, *J* = 7.5 Hz, 2H), 7.78 (d, *J* = 8.5 Hz, 1H), 7.71 (d, *J* = 8.5 Hz, 1H), 7.59 - 7.52 (m, 2H), 7.41 (t, *J* = 7.8 Hz, 2H), 7.24 (d, *J* = 9.0 Hz, 1H), 4.14 (t, *J* = 6.2 Hz, 1H), 4.09 (d, *J* = 17.5 Hz, 1H), 3.46 (d, *J* = 17.5 Hz, 1H), 2.78 – 2.61 (m, 2H), 2.45 – 2.38 (m, 1H), 2.15 – 2.08 (m, 1H), 1.85 – 1.78 (m, 2H). ^{13}C NMR (125 MHz, $CDCl_3$) δ 204.1, 198.4, 157.7, 136.3, 135.4, 134.0, 132.1, 131.0, 129.1, 128.9, 128.3, 127.8, 123.7, 123.1, 119.6, 114.5, 106.9, 89.8, 47.4, 45.3, 38.2, 28.7, 19.6. HRMS calcd for $C_{25}H_{20}NO_3$ $[M+H]^+$: 382.1438, found: 382.1440; $[\alpha]_D$ = +176.3 (*c* 1.00, $CHCl_3$); HPLC Analysis: 85% ee [©Chiralpak IA, 25 °C, 20% *i*PrOH/*n*-heptane, 1 mL/min, 242 nm, retention times: 16.6 min (minor) and 19.6 min (major)].

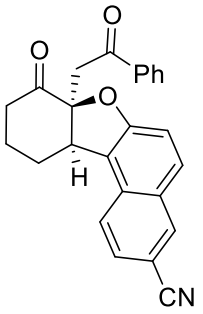

7. X-ray Crystallography

X-ray Diffraction. Crystals suitable to Single Crystal X-ray Diffraction analyses were grown in saturated solution after slow evaporation of ethyl acetate. Shortlisted samples cleaned and isolated in Paratone® oil were transferred upon an appropriate nylon loop to Rigaku diffractometers for irradiation under air ambient conditions. Since the three organic compounds are expected to be enantiomorphous pure, Cu(*Kα*) radiation (*λ* = 1.54187Å) delivered by a MM007 HF rotating-anode generator through Osmic CMF confocal optics was favored for measurements on a large Rapid II curved Image Plate when possible. *CrystalClear* 2.0 [1] software was employed to record complete set of Bijvoet pairs in the 0.8Å sphere of resolution permitted by the machine configuration and to process the data applying the multiscan absorption correction as implemented in Abscor.[4] In the case of **6g**, the analysis was nevertheless performed at the Mo(*Kα*) using a RIGAKU XtaLabPro diffractometer equipped with a microfocus sealed tube generator coupled to a double-bounce confocal Max-Flux® multilayer optic and a HPAD PILATUS3R 200K detector. *CrysAlisPro 1.171.41.122a*[5] was employed for the data strategy collection to record data with high redundancy and complete Bijvoet pairs and, for the data treatment applying an empirical absorption correction using spherical harmonics, implemented in SCALE3 ABSPACK scaling algorithm, combined with numerical absorption correction based on gaussian integration over a multifaceted crystal model. The three structures were readily solved by intrinsic phasing methods (*SHELXT* program),[6] then refined by full-matrix least-squares methods on F^2 using *SHELX-L*,[7] in the Sohnke orthorhombic space group $P\,2_1\,2_1\,2_1$ (n°19) for all of them. Thermal parameters for all non-hydrogen atoms were refined anisotropically. Afterwards, hydrogen atoms were mainly located in the difference Fourier maps but were refined using a riding model with U_{iso} set to $1.2U_{eq}$(C). In the **6g** structure, the remote fused cyclohexanone moiety appears disordered around the C7-C8 bond, these atoms were split over two distinct sites with refined occupancy factor of 0.67(1):0.33(1) and with distance soft restraints application (SADI sd 0.01). Crystal data, data collection and structure refinement details are summarized in Table S2. Absolute configuration for the three structures given that these compounds were enantiopure was investigated and for the data collected at the copper wavelength, the Flack[8] parameter accompanied by small standard deviation was reliable enough to assign the correct configuration. This was no longer the case for the third compound thus we explored the Bayesian statistical approach promoted by Hooft et al.[9] to convince ourselves that we characterized the *7aS,11aR* enantiomer of **6g** (see Table S3 output by Platon).[10]

CCDC 2180388-2180390 (for **(*R*)-4a**, **(*S*)-4a** and **6g** respectively) contain the supplementary crystallographic data for this paper. These data can be obtained free of charge from the Cambridge Crystallographic Data Centre via www.ccdc.cam.ac.uk/data_request/cif.

[4] Rigaku. (**2009**) CrystalClear-SM Expert 2.0 r4 Rigaku Corporation, Tokyo, Japan.
[5] Schneider, T. R.; Sheldrick, G. M., *Acta Crystallogr.* **2002**, *D58*, 1772.
[6] Sheldrick, G. M., *Acta Crystallogr.* **2015**, *C71*, 3.
[7] Sheldrick, G. M., *Acta Crystallogr.,* **2015**, *A71*, 3.
[8] Parsons, S.; Flack, H. D.; Wagner, T., *Acta Cryst.* **2013**, *B69*, 249.
[9] Hooft, R. W. W.; Straver, L. H.; Spek, A. L., *J. Appl. Cryst.* **2008**, *41*, 96.
[10] Spek, A. L., *Acta Cryst.* **2009**, *D65*, 148.

Table S2.Crystal data and structure refinement for the three enantiopure compounds

Identification code		**(*R*)-4a**	**(*S*)-4a**	**6g**
		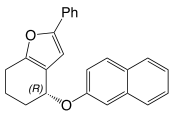	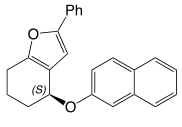	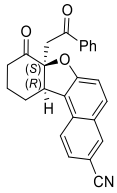
Empirical formula		$C_{24}H_{20}O_2$	$C_{24}H_{20}O_2$	$C_{25}H_{19}NO_3$
Formula weight		340.40	340.40	381.41
Temperature	(K)	293(2)	293(2)	293(2)
Diffractometer	Rigaku®	Rotating anode mm007HF Spider + CMF optics		µ-source mm003 XtaLabPro
Wavelength	(Å)	1.54187	1.54187	0.71073
Crystal system, Space group		Orthorhombic, $P\ 2_12_12_1$	Orthorhombic, $P\ 2_12_12_1$	Orthorhombic, $P\ 2_12_12_1$
Unit cell dimensions	(Å)	5.4569(3) 10.2136(4) 32.074(2)	5.4563(3) 10.2121(6) 32.052(2)	8.1453(3) 13.5230(5). 17.9736(7)
Volume	($Å^3$)	1787.62(18)	1785.94(19)	1979.77(13)
Z, Calculated density	(Mg/m^3)	4, 1.265	4, 1.266	4, 1.280
Absorption coefficient	(mm^{-1})	0.622	0.622	0.084
F(000)		720	720	800
Crystal size	(mm)	0.50 x 0.24 x 0.13	0.55 x 0.22 x 0.18	0.25 x 0.18 x 0.15
θ range for data collection	(°)	2.755 to 68.244	7.024 to 72.108	2.721 to 27.097
Limiting indices		$-6 \le h \le 5$, $-10 \le k \le 12$, $-38 \le l \le 38$	$-6 \le h \le 6$, $-10 \le k \le 12$, $-39 \le l \le 39$	$-10 \le h \le 10$, $-17 \le k \le 16$, $-22 \le l \le 23$
Reflections collected / unique Rint		16889 / 3270 0.0436	36229 / 3502 0.1106	37692 / 4367 0.0322
Completeness to θ_{max}	(%)	99.7	99.7	99.9

Absorption correction		Semi-empirical from equivalents		
				& Gaussian
Max. and min. transmission		1.000 and 0.802	1.000 and 0.764	1.000 and 0.374
Refinement method		Full-matrix least-squares on F^2		
Data / restraints / parameters		3265 / 0 / 235	3500 / 0 / 236	4367 / 15 / 282
Goodness-of-fit on F^2		1.114	1.111	1.035
Final R indices [I>2σ(I)]	R1, wR2	0.0304, 0.0638	0.0407, 0.0882	0.0322, 0.0862
R indices (all data)	R1, wR2	0.0502, 0.0827	0.0506, 0.1038	0.0367, 0.0891
Absolute structure parameter		-0.04(11)	-0.09(13)	-0.1(3)
Extinction coefficient		-	0.0163(11)	0.016(2)
Largest diff. peak and hole	e.Å^{-3}	0.106 and -0.119	0.143 and -0.141	0.144 and -0.098
CSD deposit number		2180388	2180389	2180390

Table S3 Bijvoet pair analyses for absolute structure determination as performed within PLATON

Identification code		**(*R*)-4a**	**(*S*)-4a**	**6g**
Empirical formula		C_{24} H_{20} O_2	C_{24} H_{20} O_2	C_{25} H_{19} N O_3
Wavelength	(Å)	1.54187	1.54187	0.71073
FriedIf		25	25	5.3
Observables		1092	1052	1572
FriedIf x Flack (su)		2.7	3.2	1.6
Theta max		68.2	72.1	27.09
Coverage		100	99	100
Bijvoet pairs		1329	1427	1874
Flack ('one-in-hole')		-0.04(11)	-0.09(13)	-0.1(3)
Parsons parameter		-0.04(15)	-0.16(8)	-0.1(3)
Parsons pairs		786	999	1569
Hooft parameter		-0.06(9)	-0.09(18)	-0.1(3)
P2(true)		1.0000	1.0000	1.0000
P3(true)		1.0000	0.9960	0.9050
P3(false)		$0.3.10^{-28}$	$0.7.10^{-8}$	0.0004

Figure S3. ORTEP views of the asymmetric unit of (*R*)-4a, (*S*)-4a, 6g. Ellipsoids are represented with 50% of probability. Only the major conformer of 6g is shown for sake of clarity.

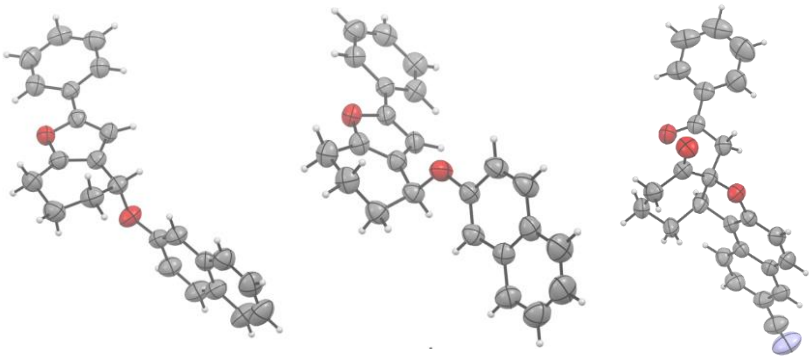

(-)-(*R*)-**4a**
CCDC 2180388

(+)-(*S*)-**4a**
CCDC 2180389

6g
CCDC 2180390

8. NMR spectra

^{1}H NMR ($CDCl_3$, 500 MHz) (**4a**)

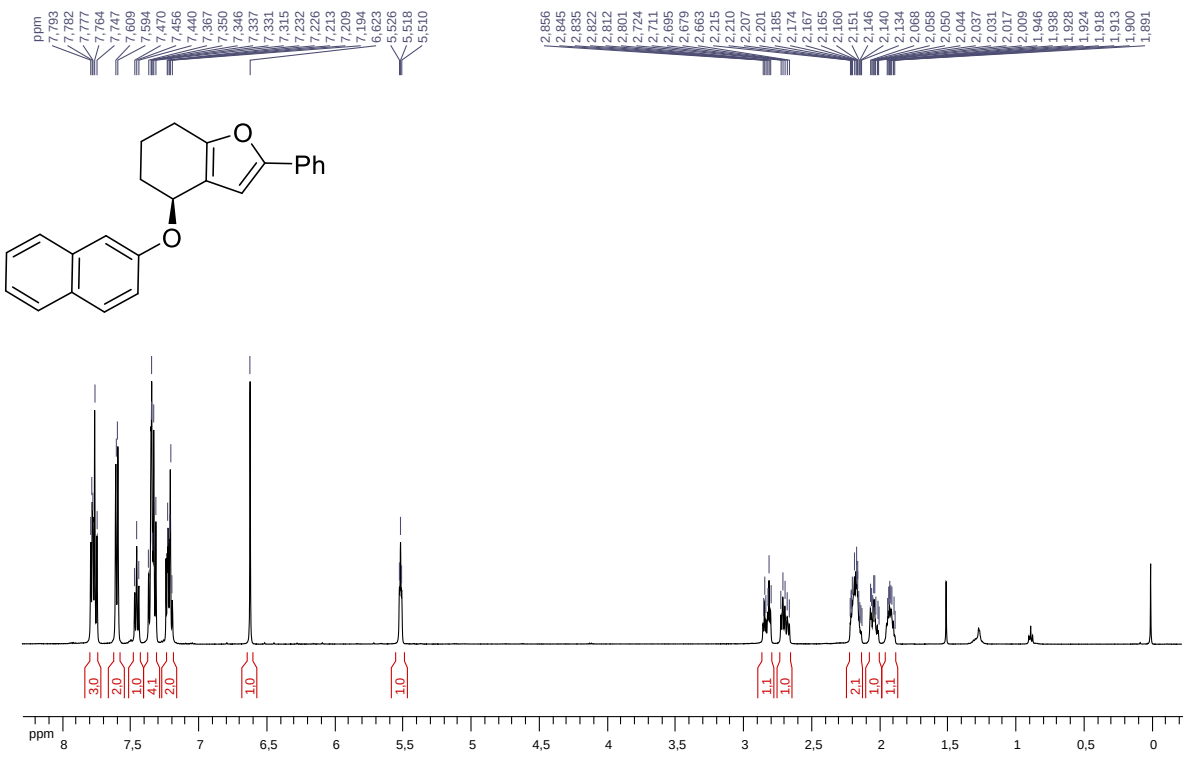

^{13}C NMR ($CDCl_3$, 125 MHz) (**4a**)

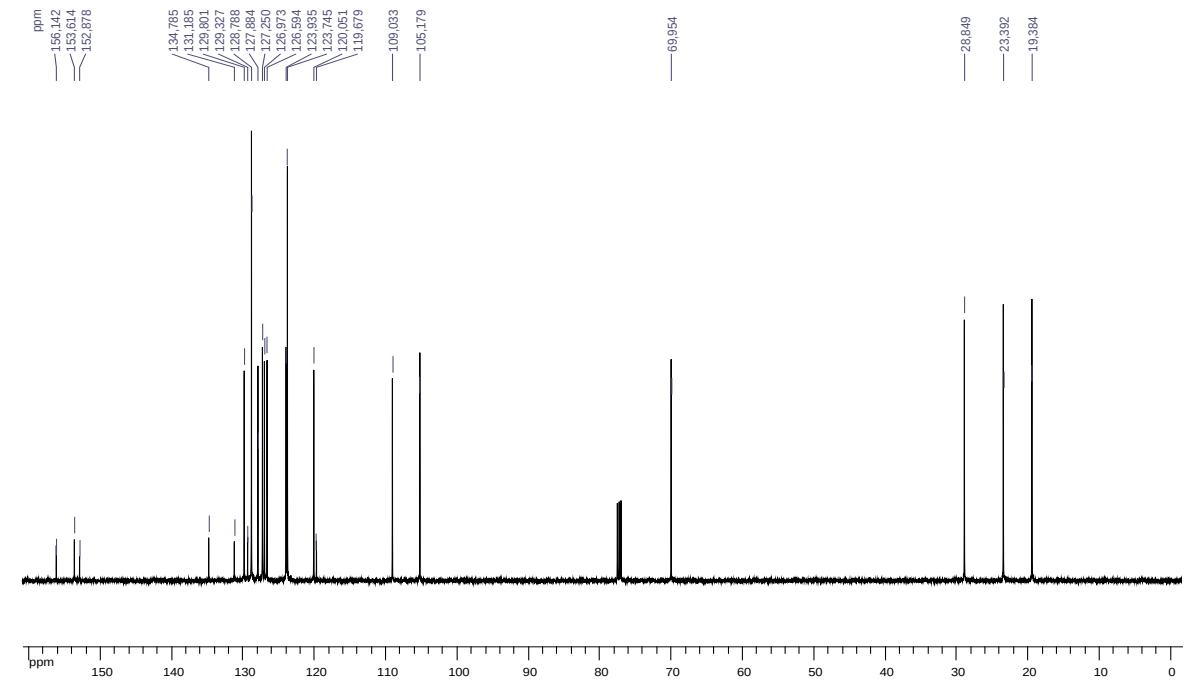

^{1}H NMR ($CDCl_3$, 500 MHz) (**4b**)

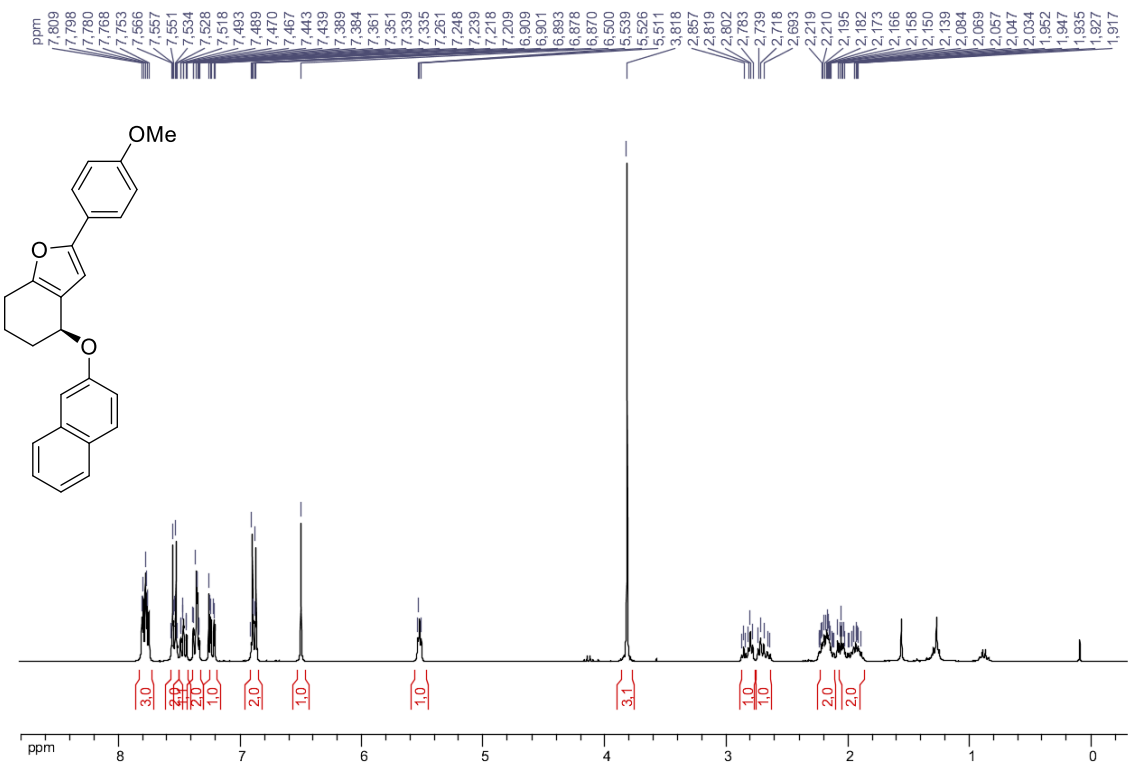

^{13}C NMR ($CDCl_3$, 300 MHz) (**4b**)

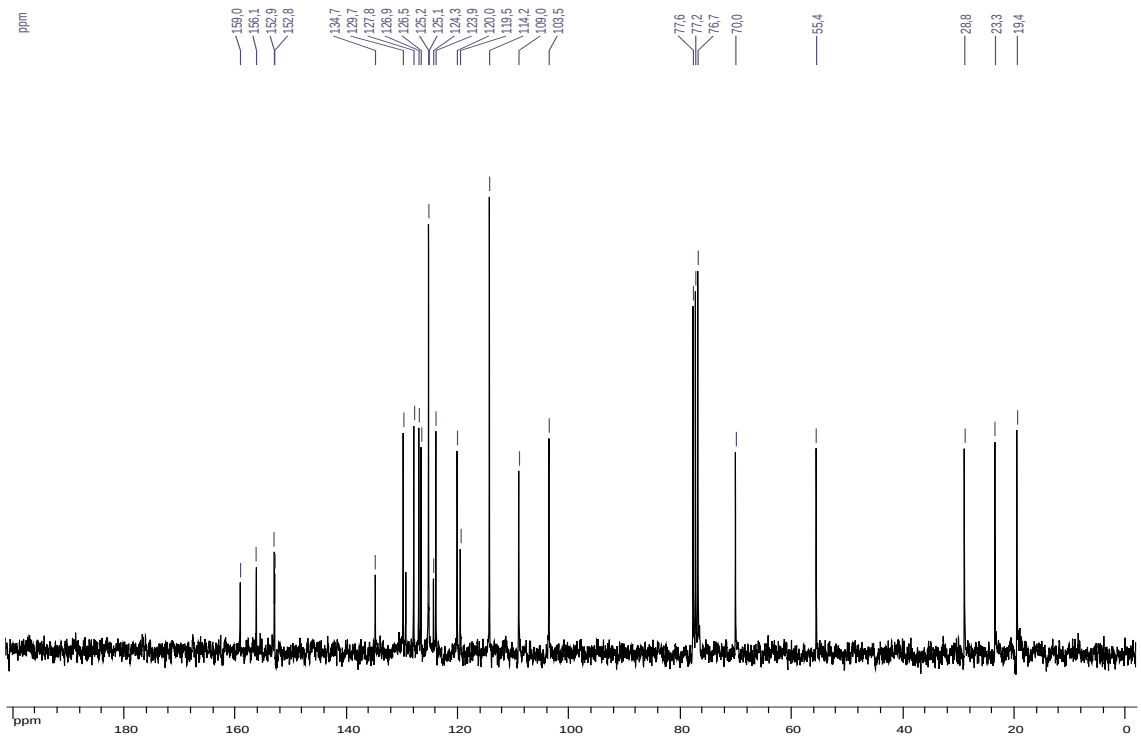

^{1}H NMR ($CDCl_3$, 500 MHz) (**4c**)

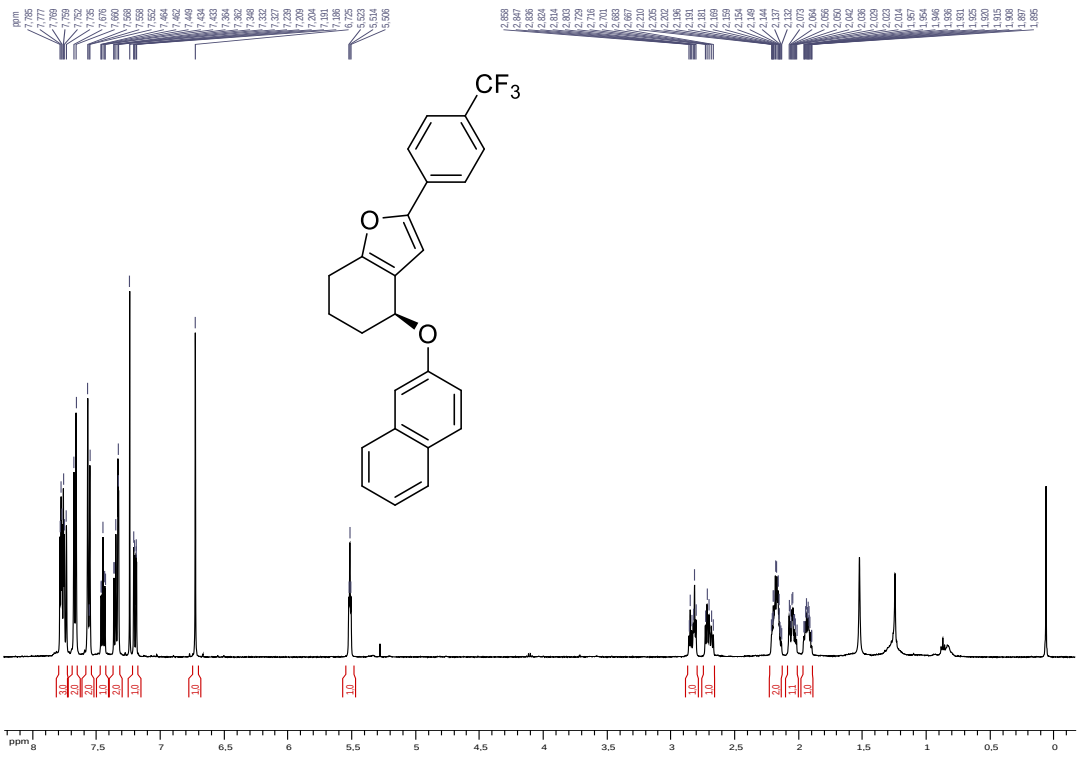

^{13}C NMR ($CDCl_3$, 125 MHz) (**4c**)

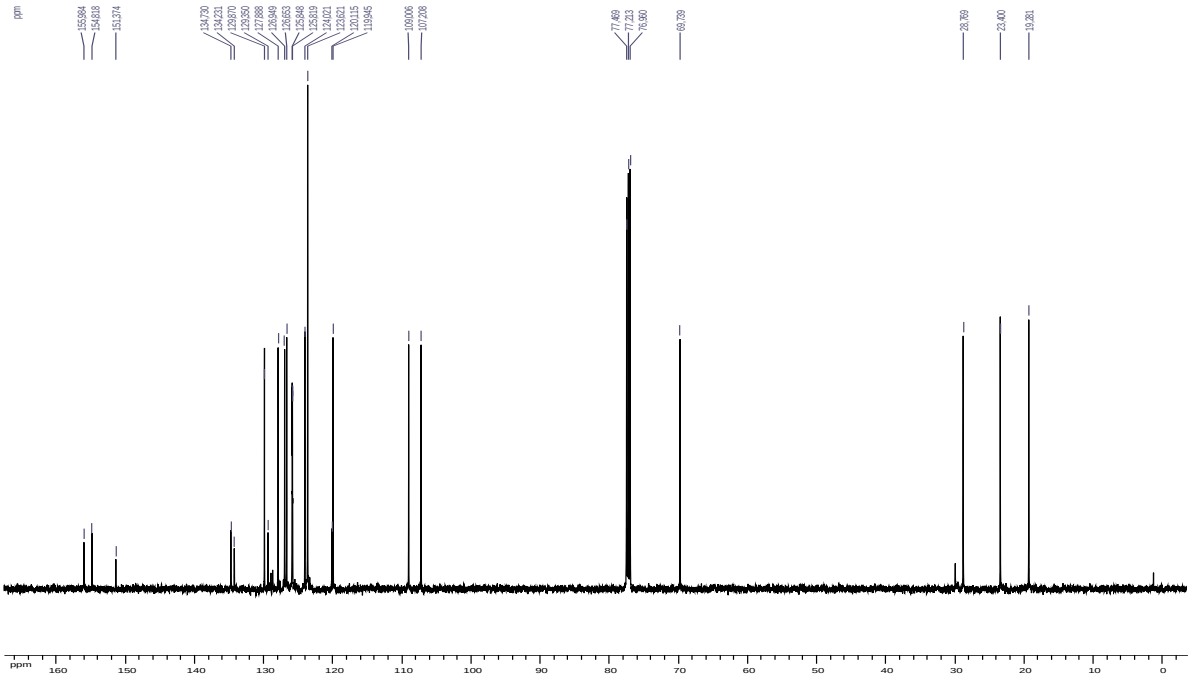

^{19}F NMR ($CDCl_3$, 282 MHz) (**4c**)

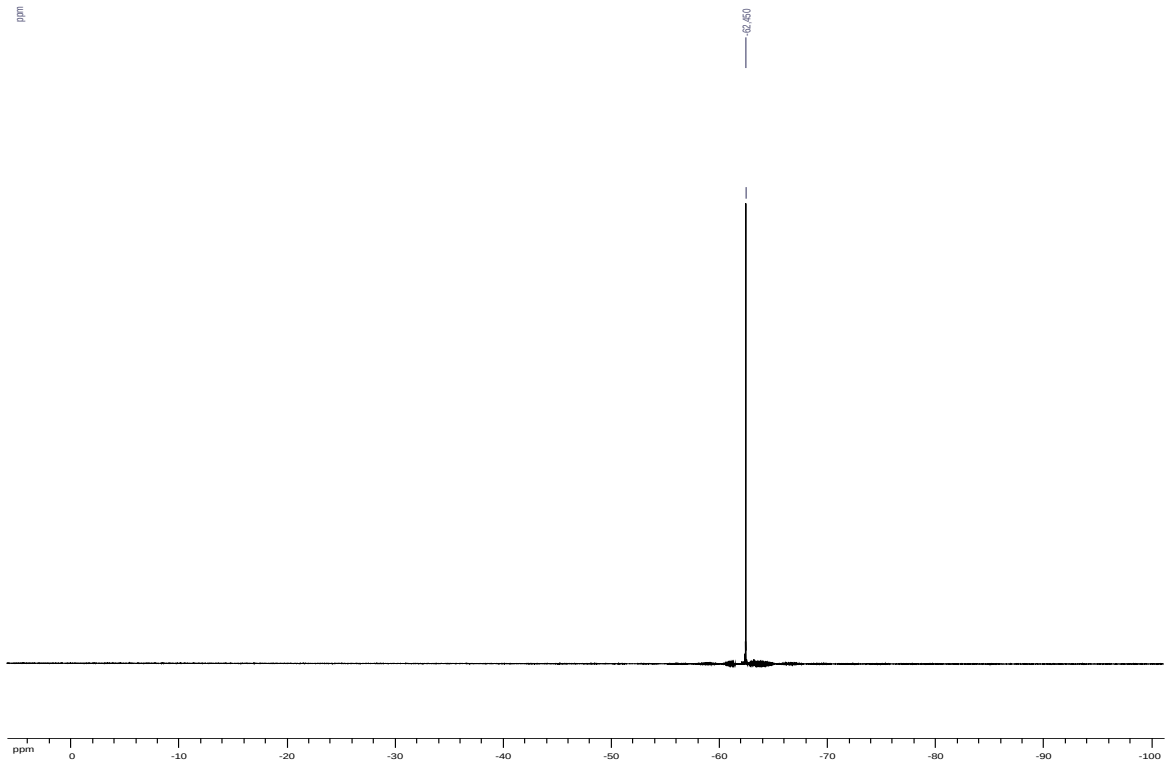

^{1}H NMR ($CDCl_3$, 500 MHz) (**4d**)

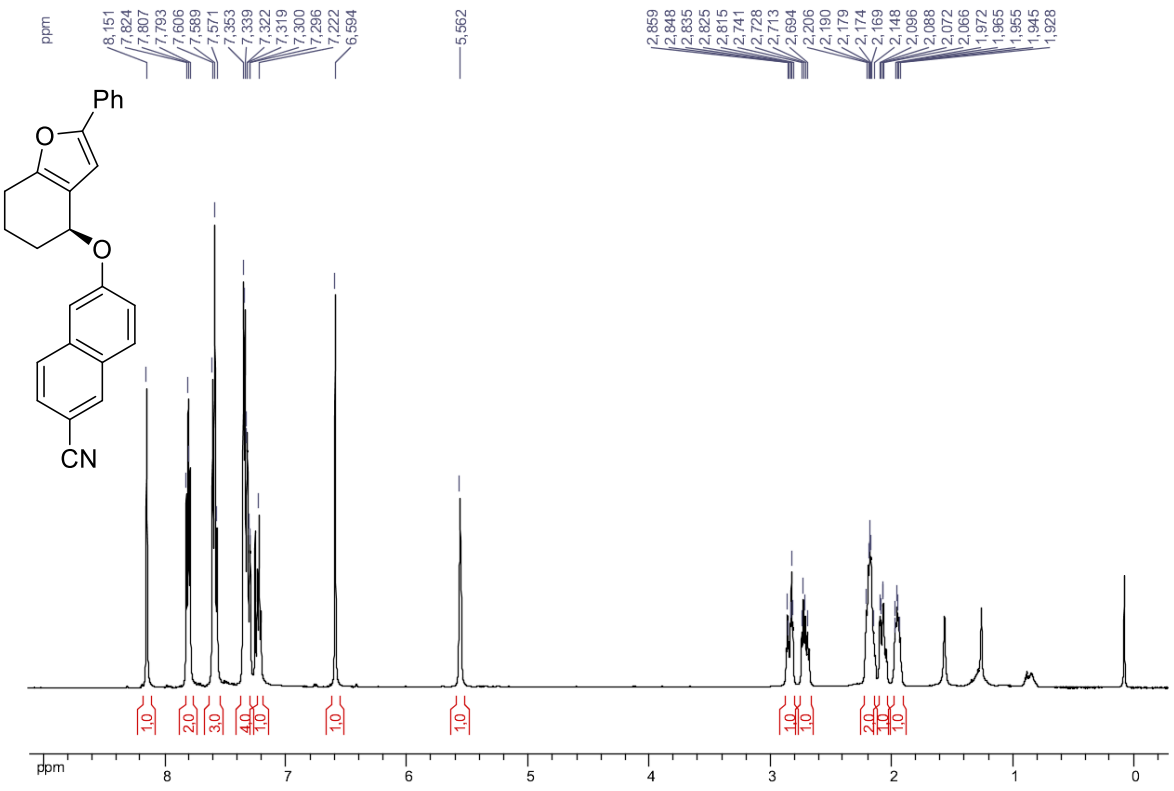

^{13}C NMR ($CDCl_3$, 125 MHz) (**4d**)

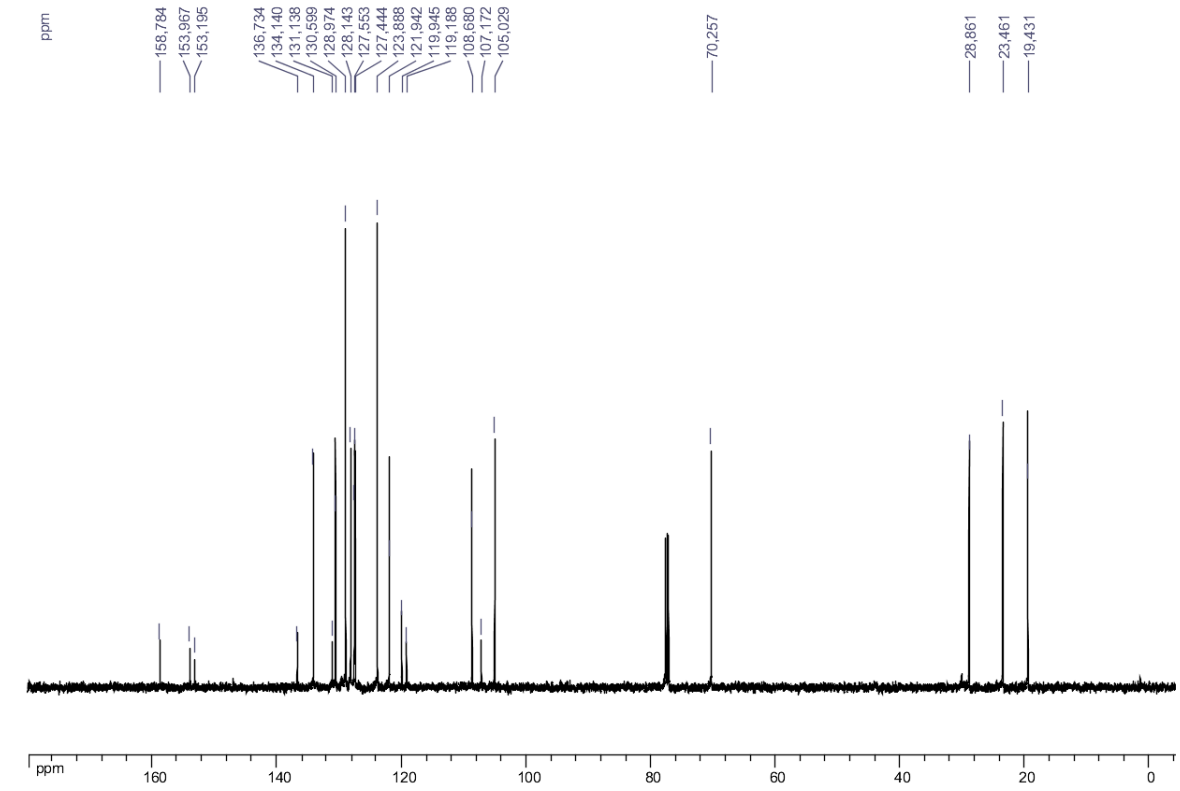

^{1}H NMR ($CDCl_3$, 500 MHz) (**4e**)

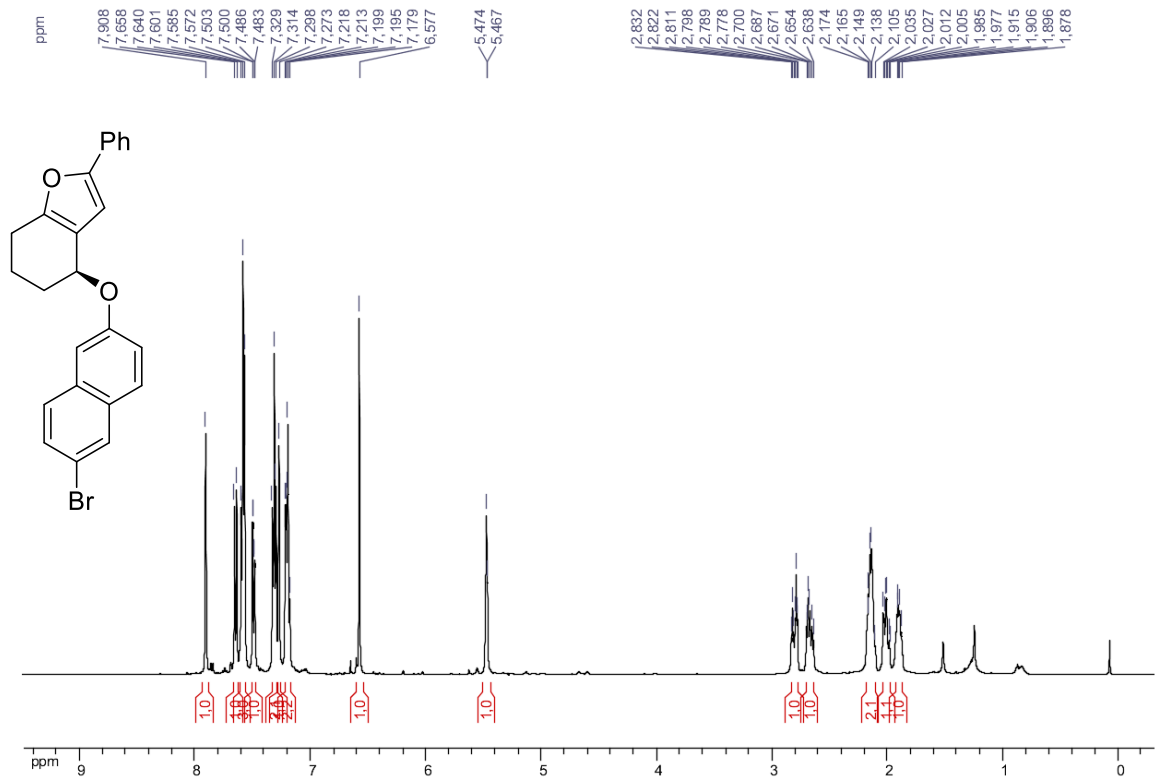

^{13}C NMR ($CDCl_3$, 125 MHz) (**4e**)

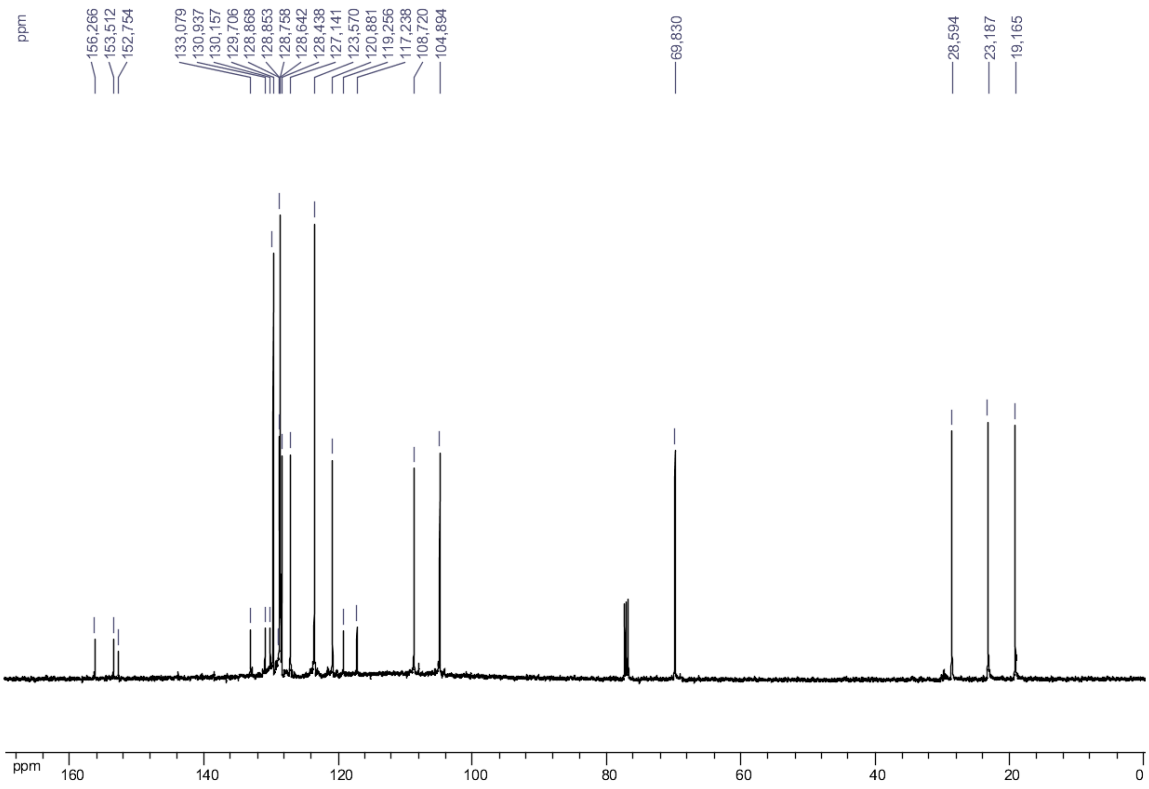

^{1}H NMR ($CDCl_3$, 500 MHz) (**4f**)

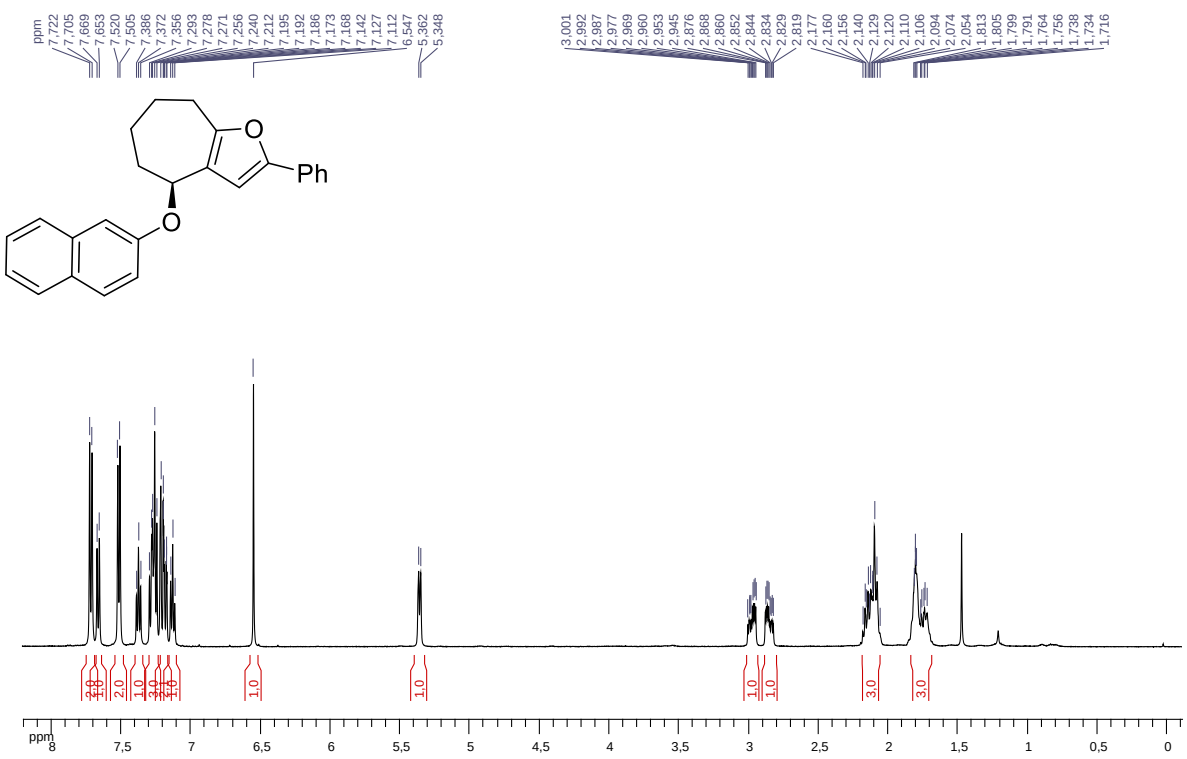

^{13}C NMR ($CDCl_3$, 125 MHz) (**4f**)

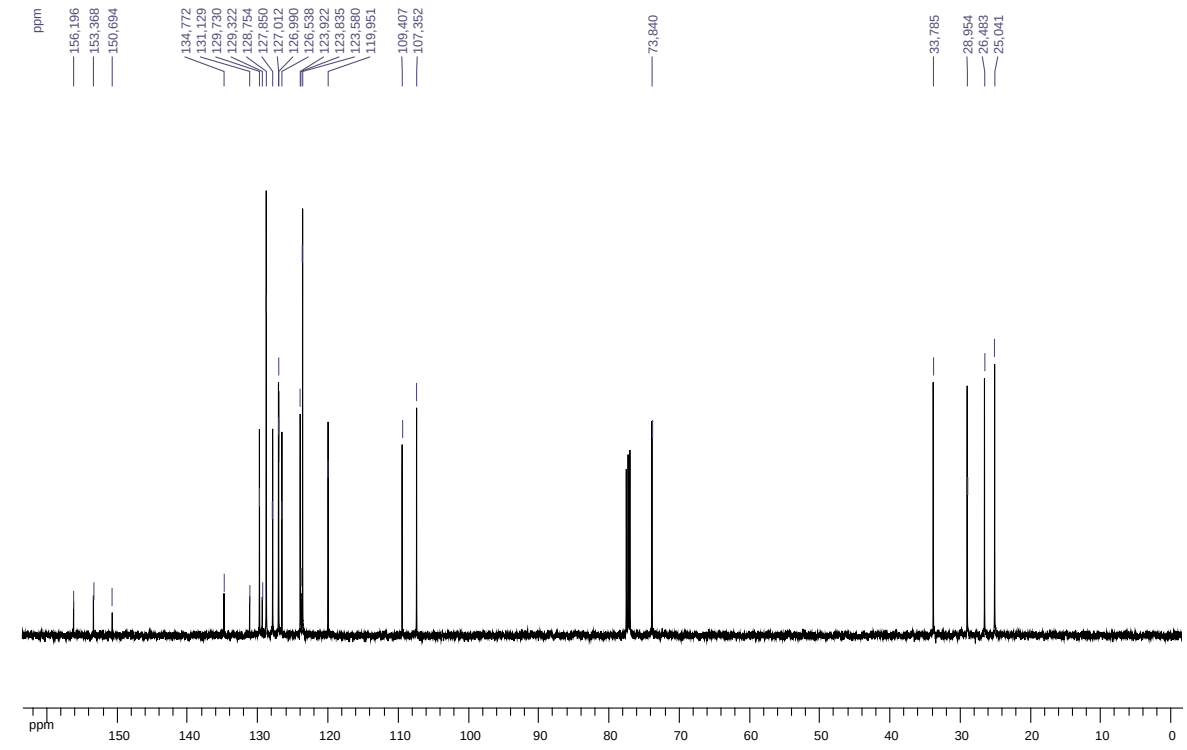

^{1}H NMR ($CDCl_3$, 500 MHz) (**4a'**)

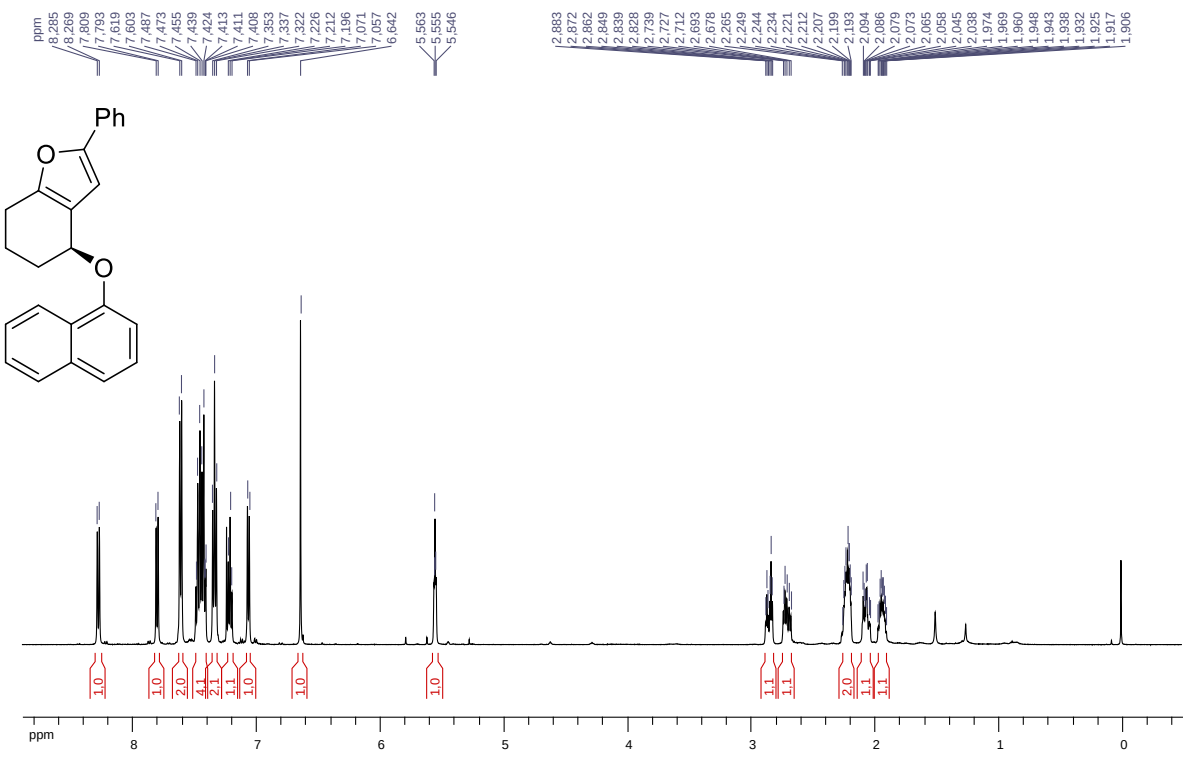

^{13}C NMR ($CDCl_3$, 125 MHz) (**4a'**)

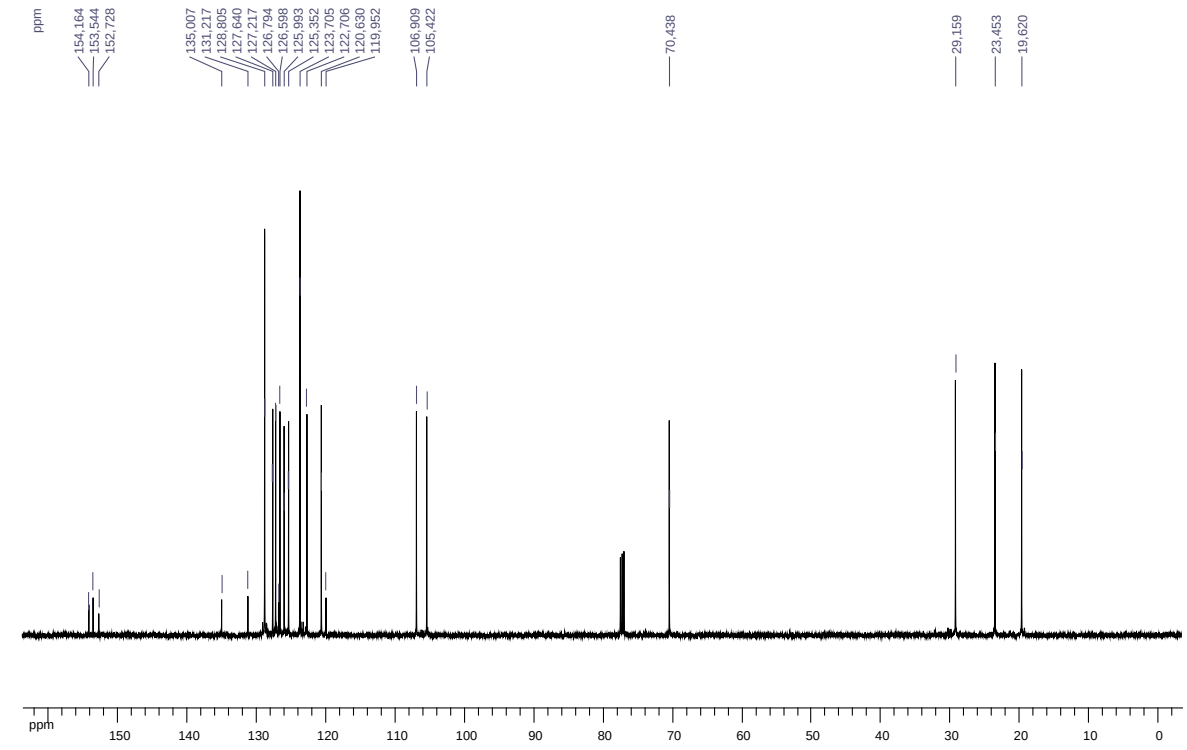

^{1}H NMR ($CDCl_3$, 500 MHz) (**5a**)

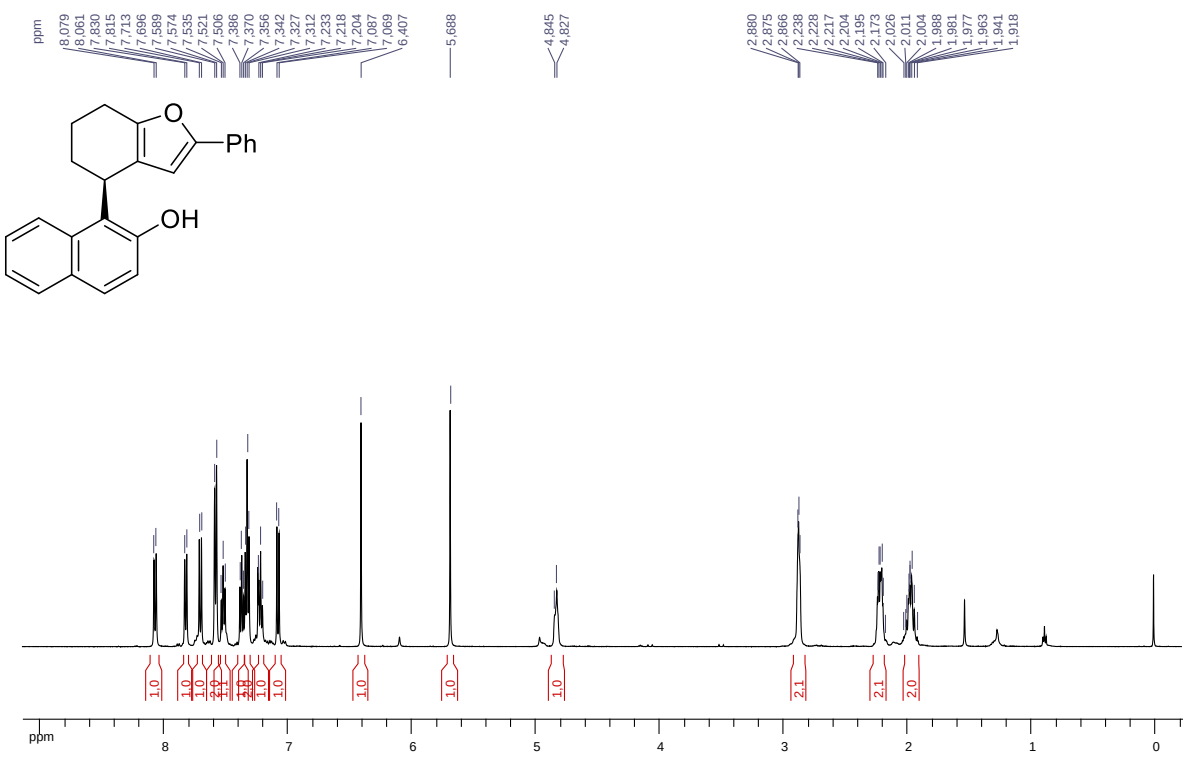

^{13}C NMR ($CDCl_3$, 125 MHz) (**5a**)

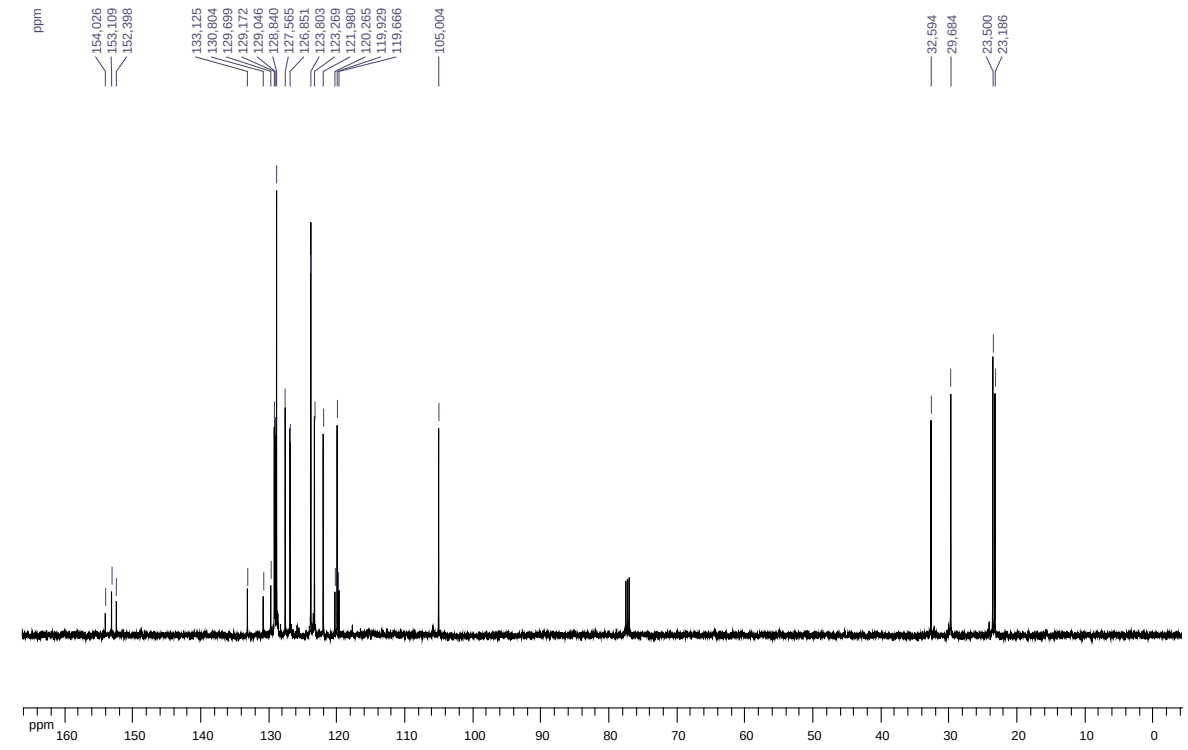

^{1}H NMR ($CDCl_3$, 500 MHz) (**5b**)

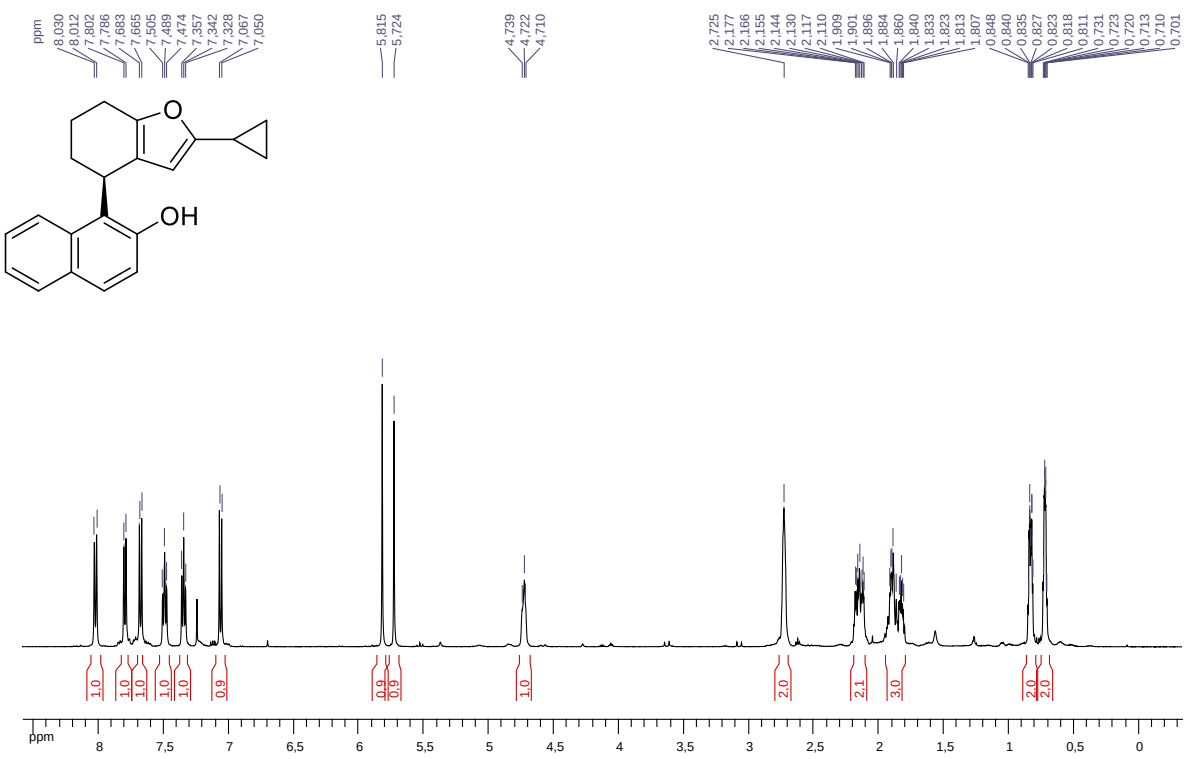

^{13}C NMR ($CDCl_3$, 125 MHz) (**5b**)

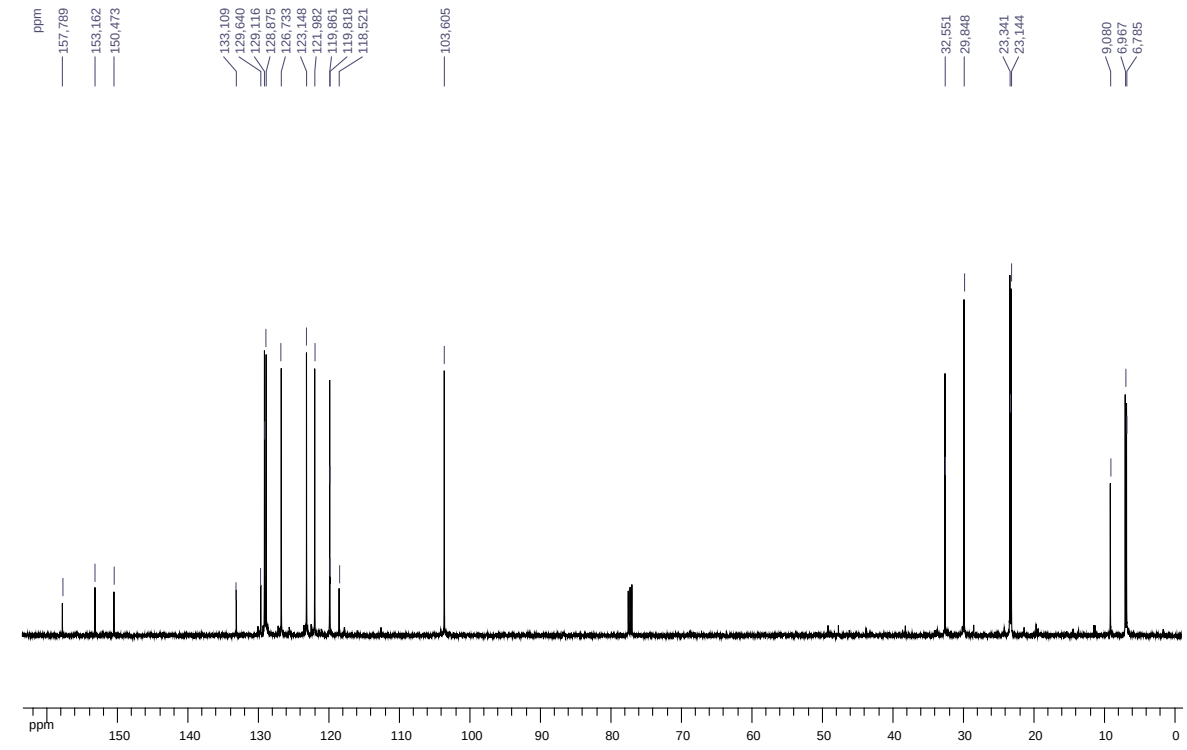

^{1}H NMR ($CDCl_3$, 500 MHz) (**5c**)

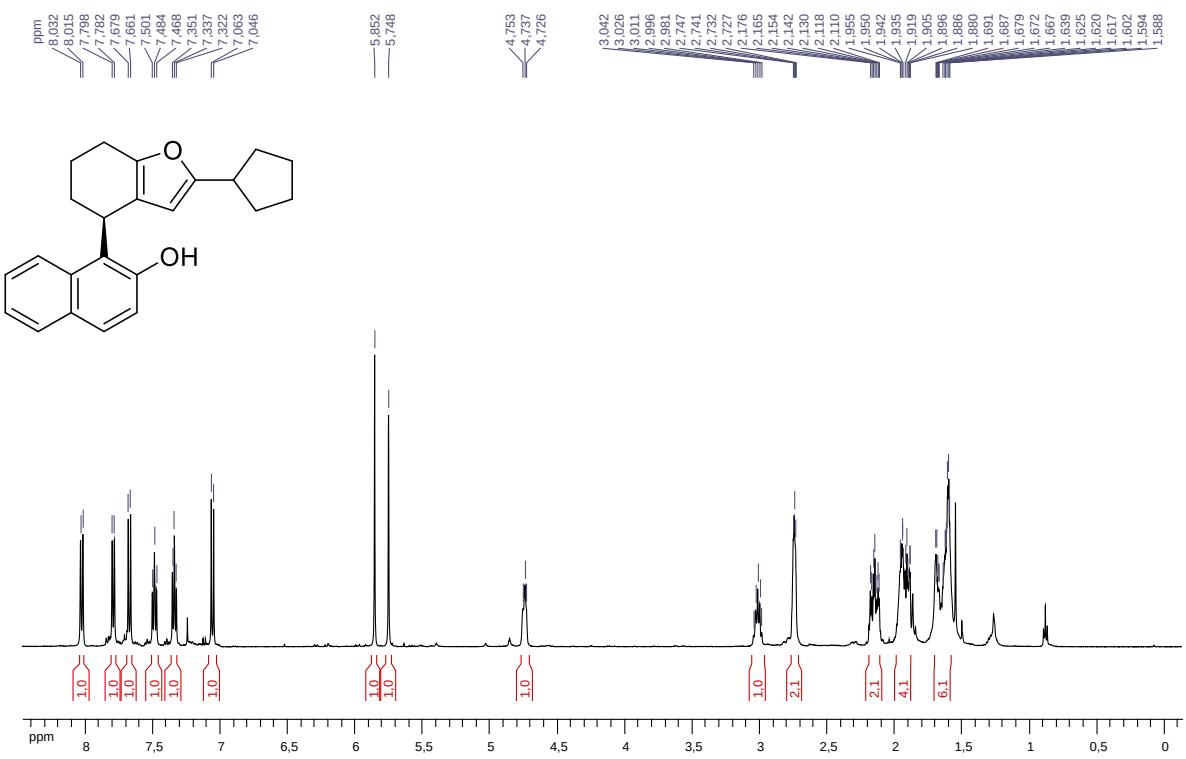

^{13}C NMR ($CDCl_3$, 125 MHz) (**5c**)

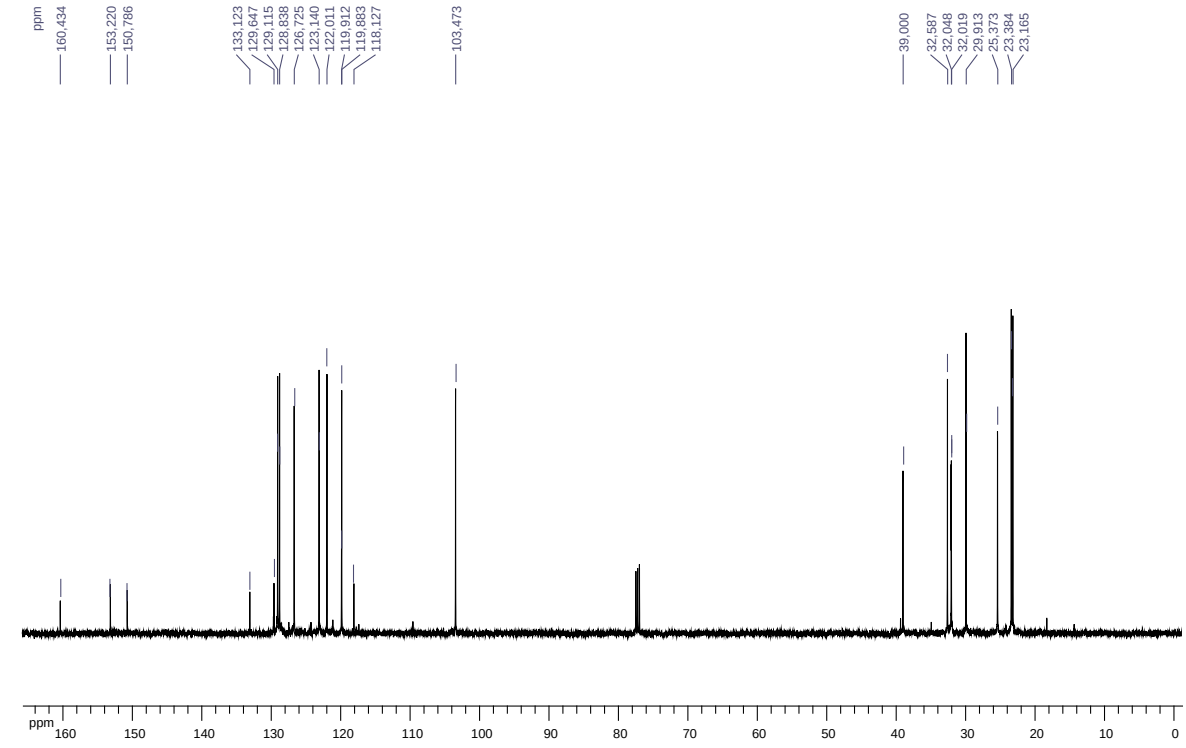

^{1}H NMR ($CDCl_3$, 500 MHz) (**5a'**)

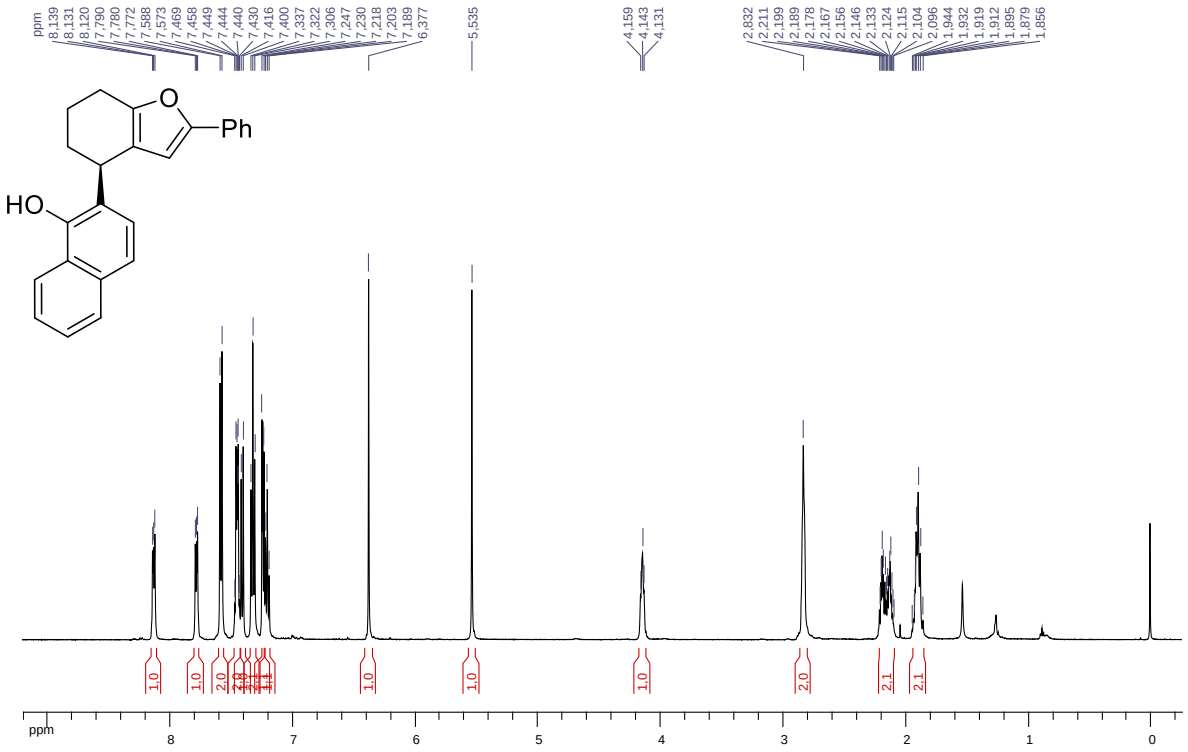

^{13}C NMR ($CDCl_3$, 125 MHz) (**5a'**)

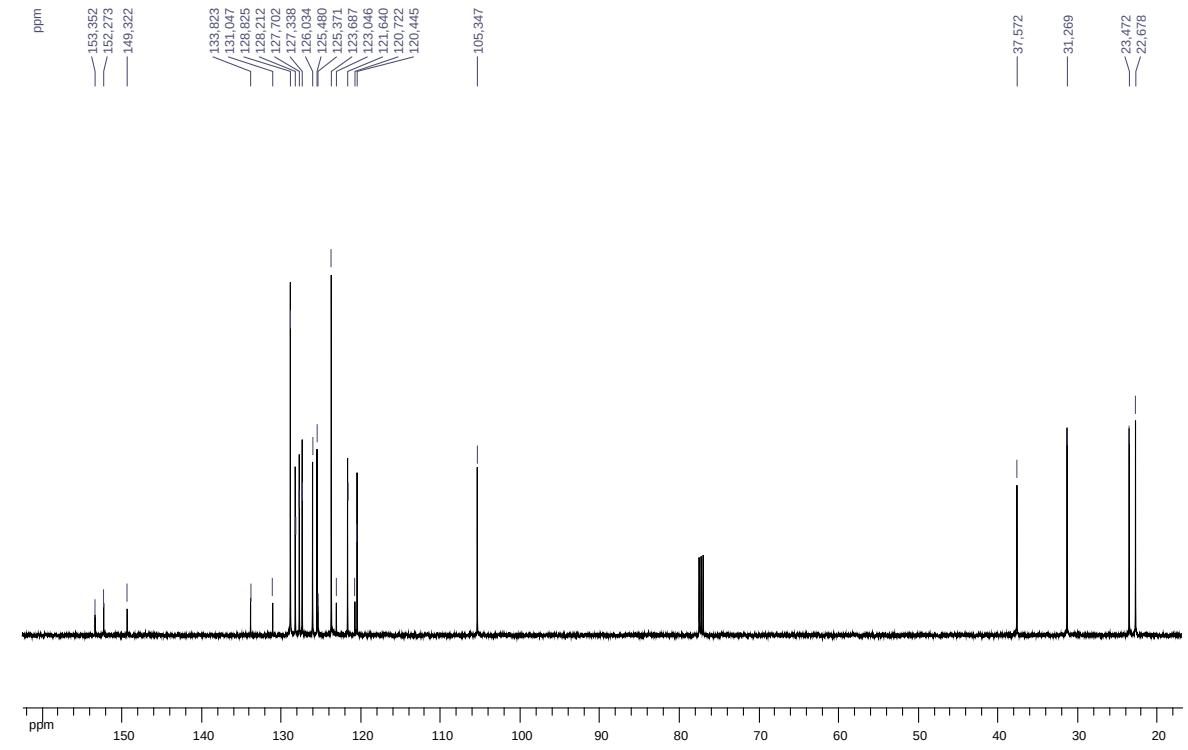

^{1}H NMR ($CDCl_3$, 500 MHz) (**6a**)

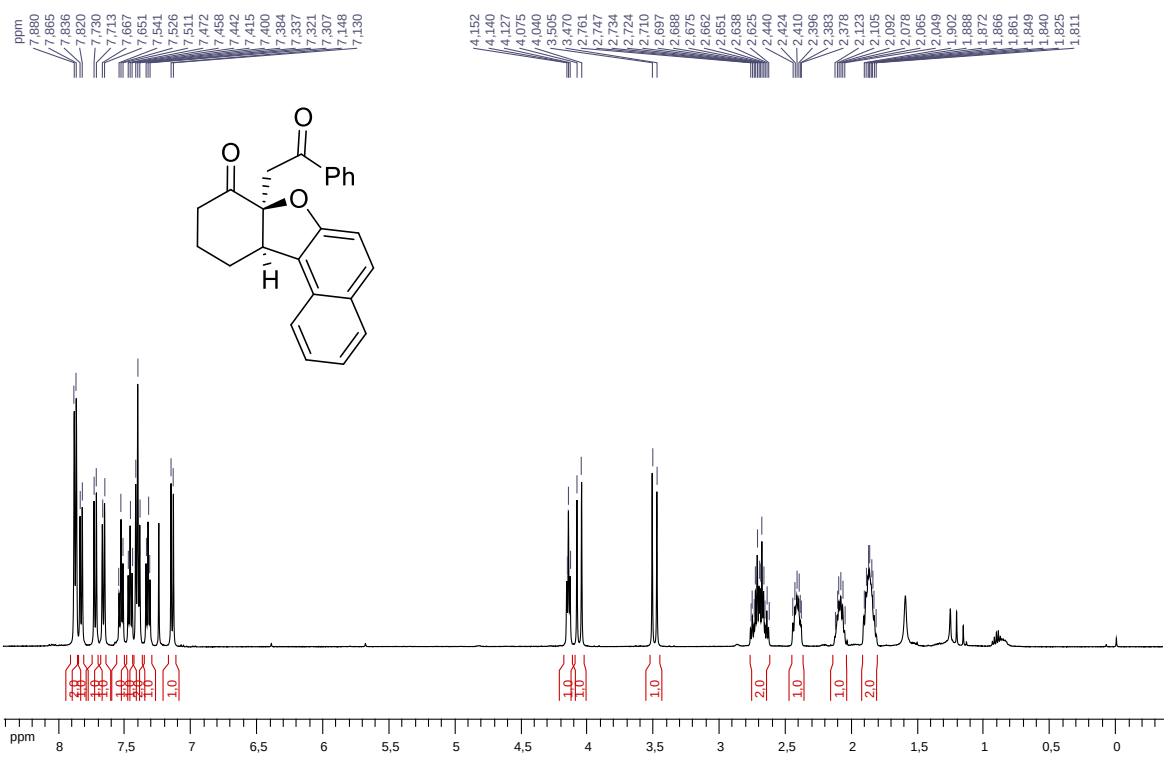

^{13}C NMR ($CDCl_3$, 125 MHz) (**6a**)

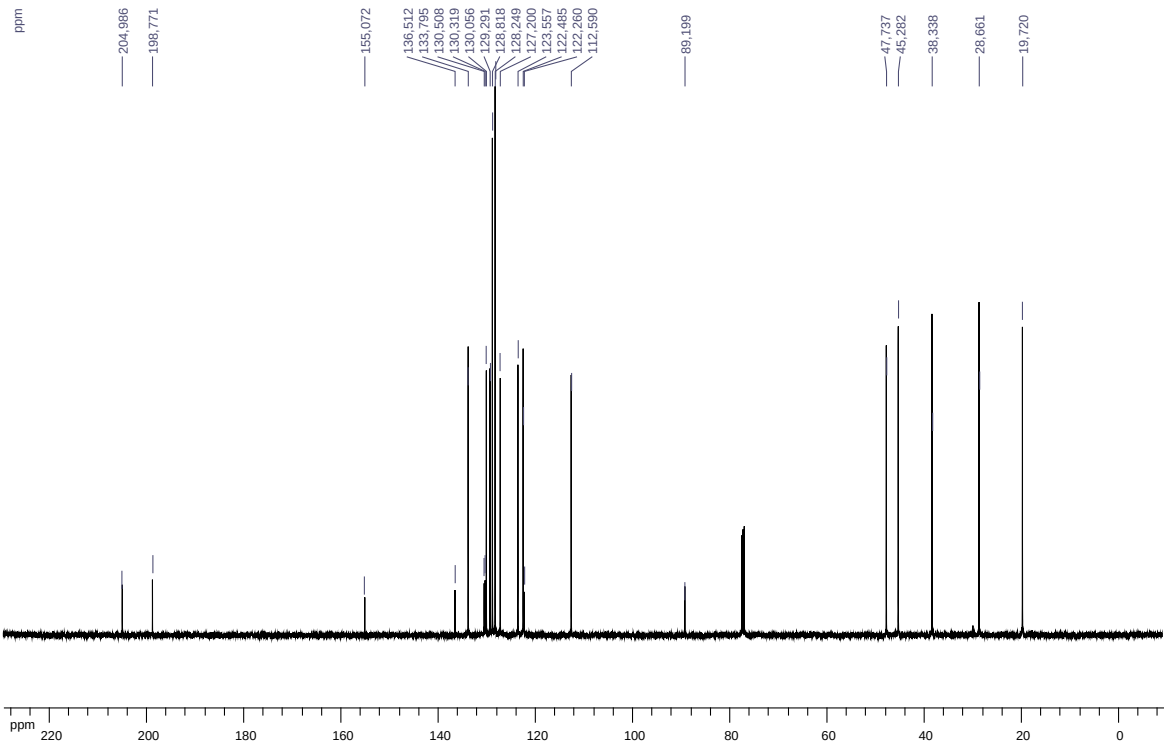

^{1}H NMR ($CDCl_3$, 500 MHz) (**6b**)

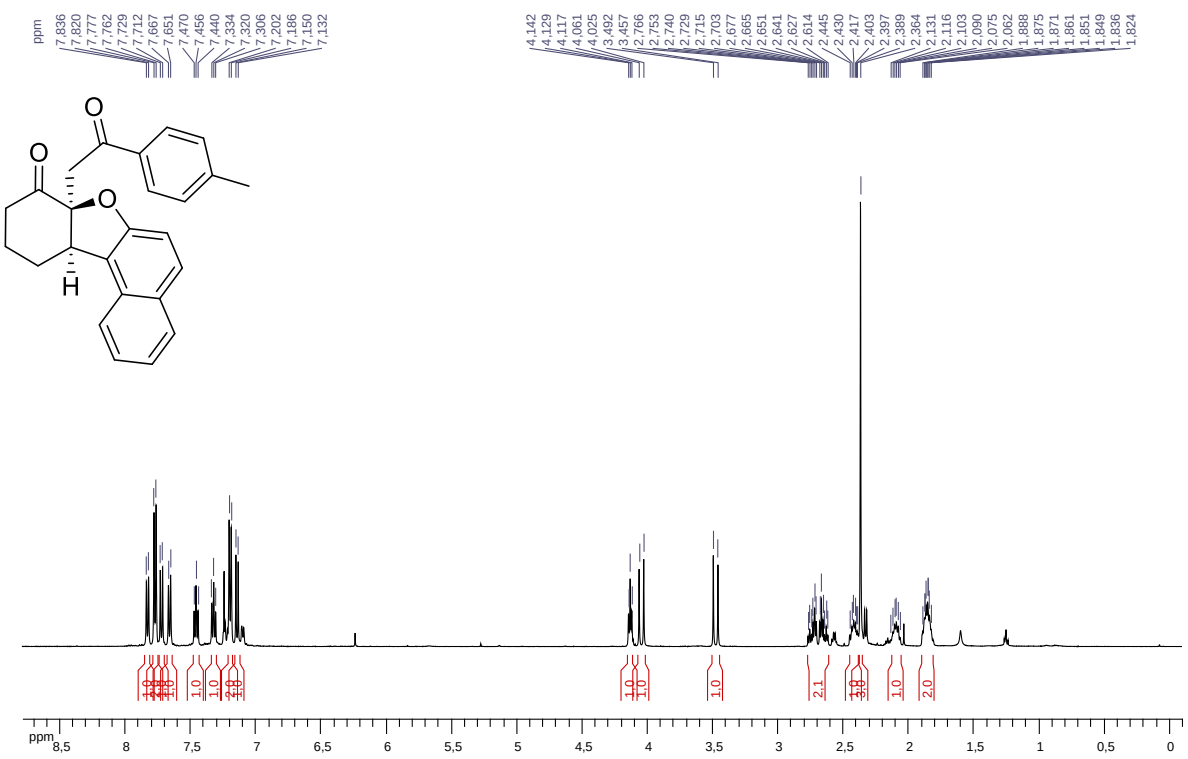

^{13}C NMR ($CDCl_3$, 125 MHz) (**6b**)

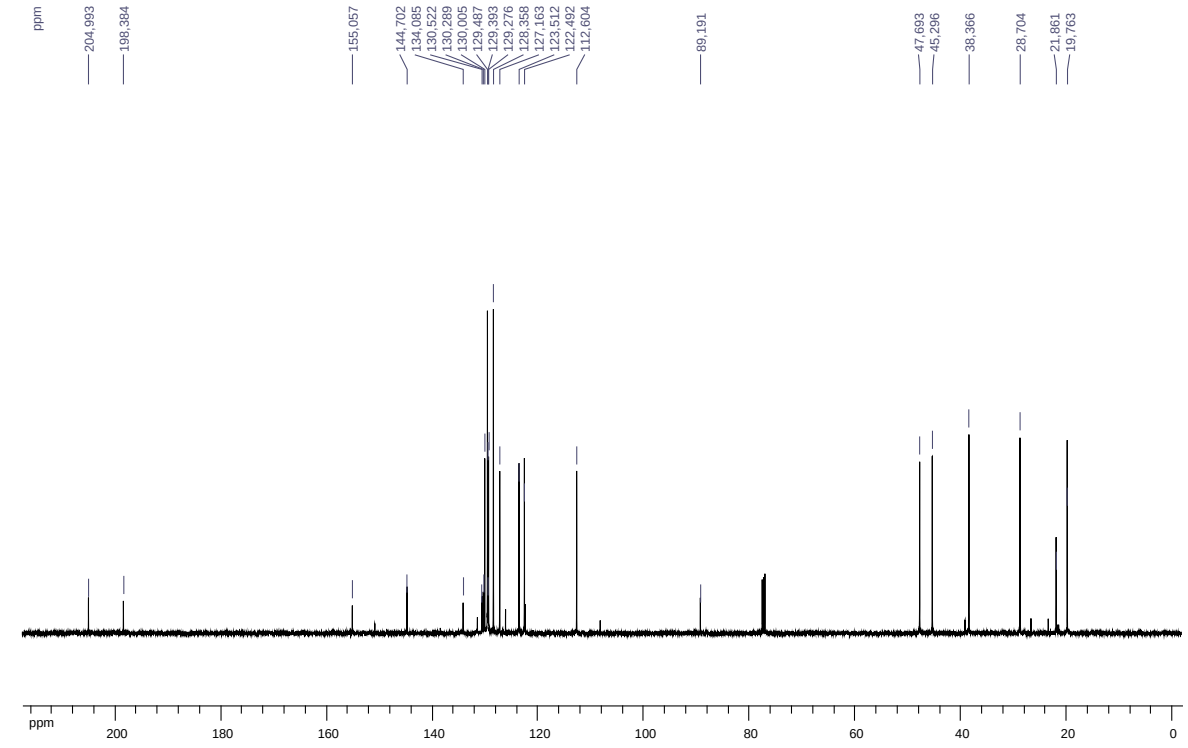

^{1}H NMR ($CDCl_3$, 500 MHz) (**6c**)

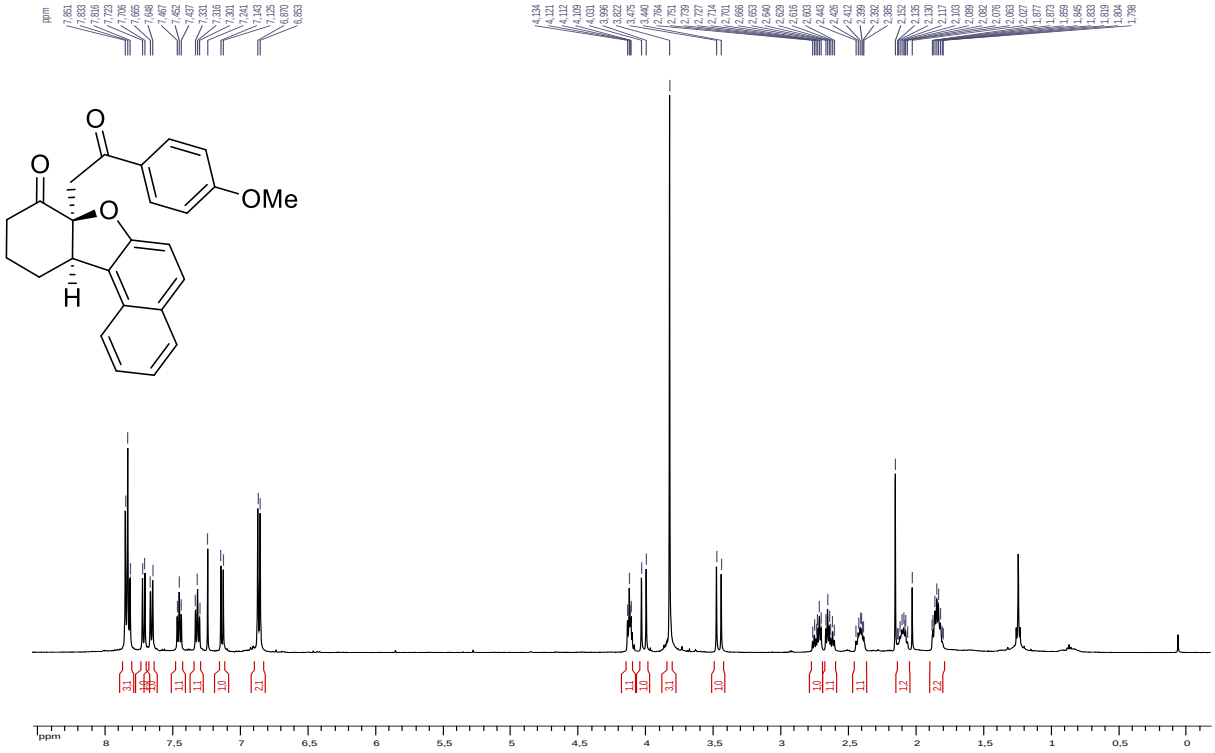

^{13}C NMR ($CDCl_3$, 125 MHz) (**6c**)

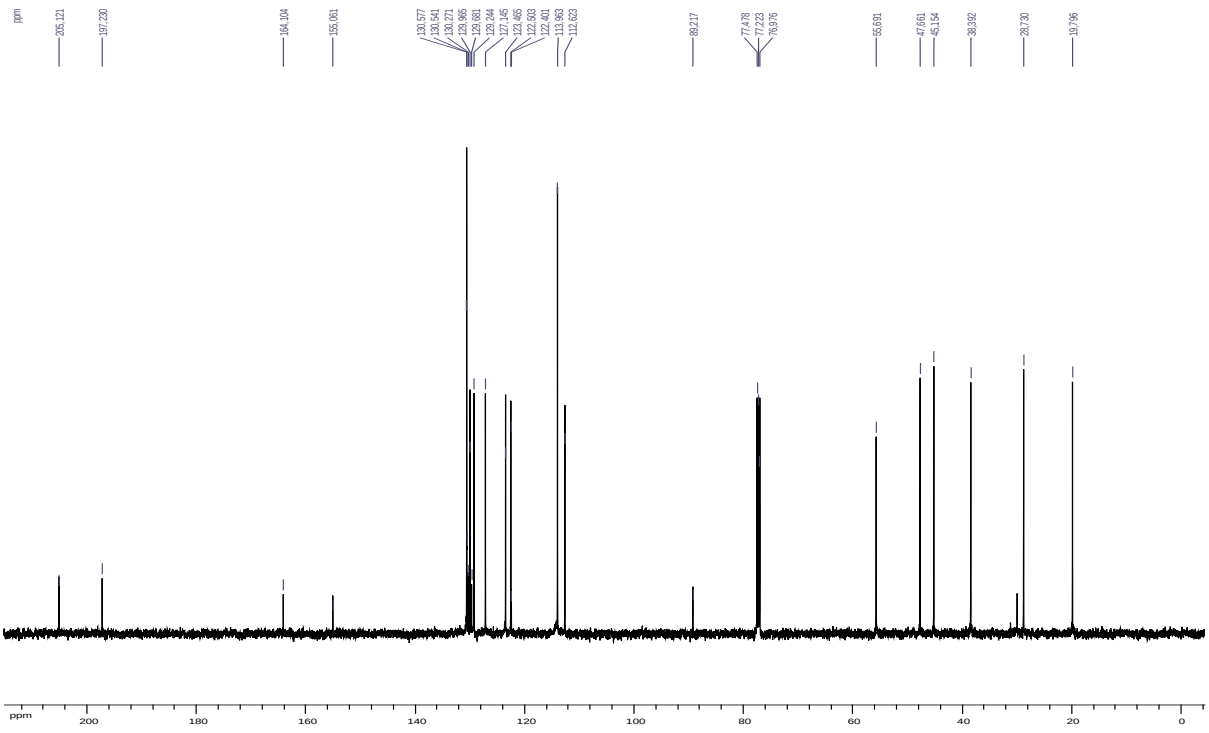

^{1}H NMR ($CDCl_3$, 500 MHz) (**6d**)

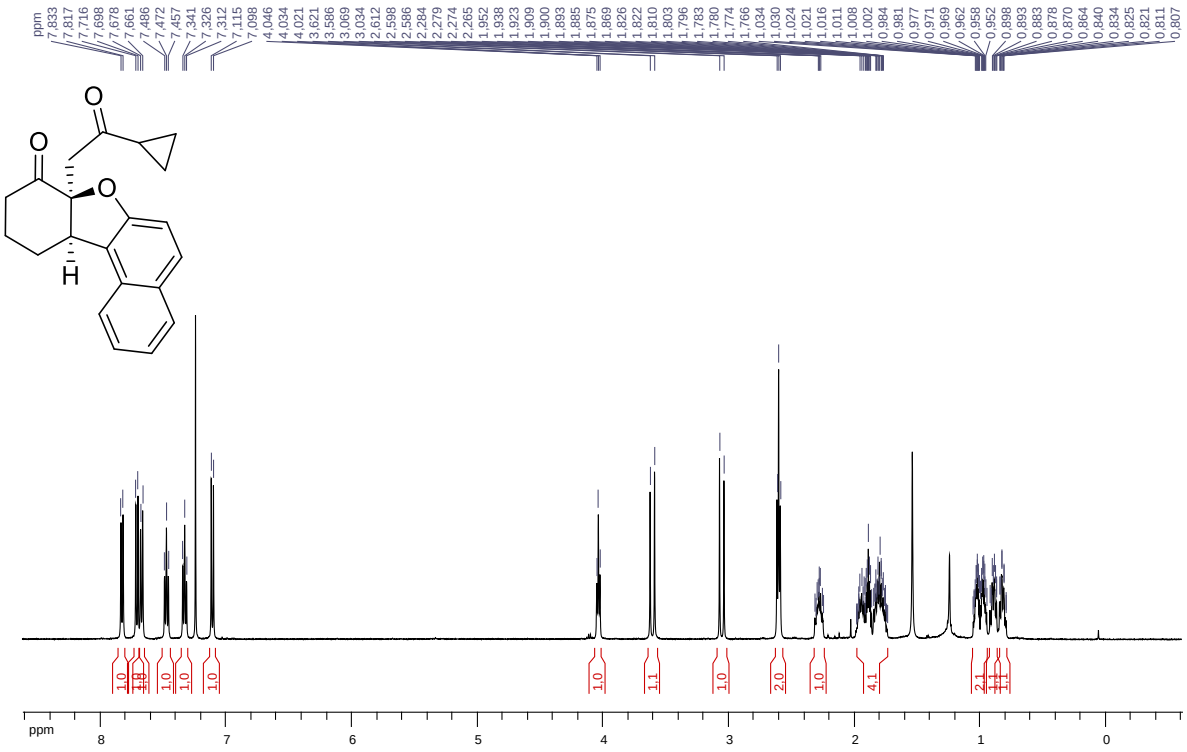

^{13}C NMR ($CDCl_3$, 125 MHz) (**6d**)

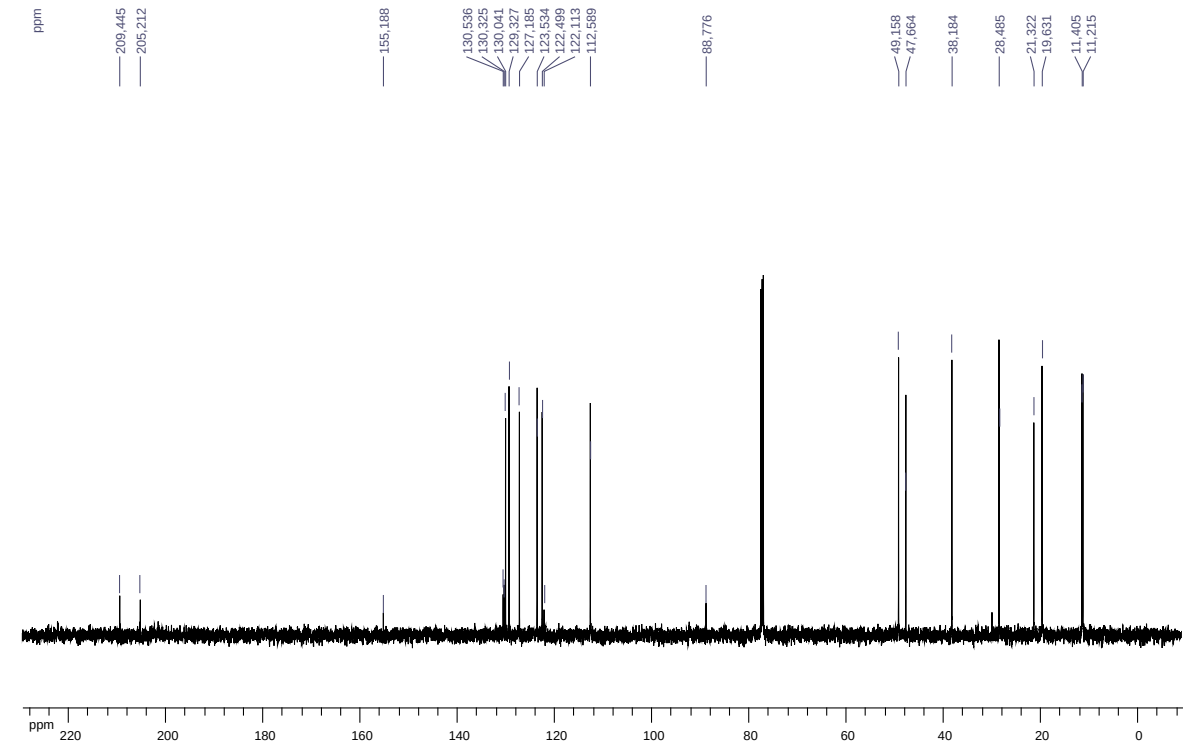

^{1}H NMR ($CDCl_3$, 500 MHz) (**6e**)

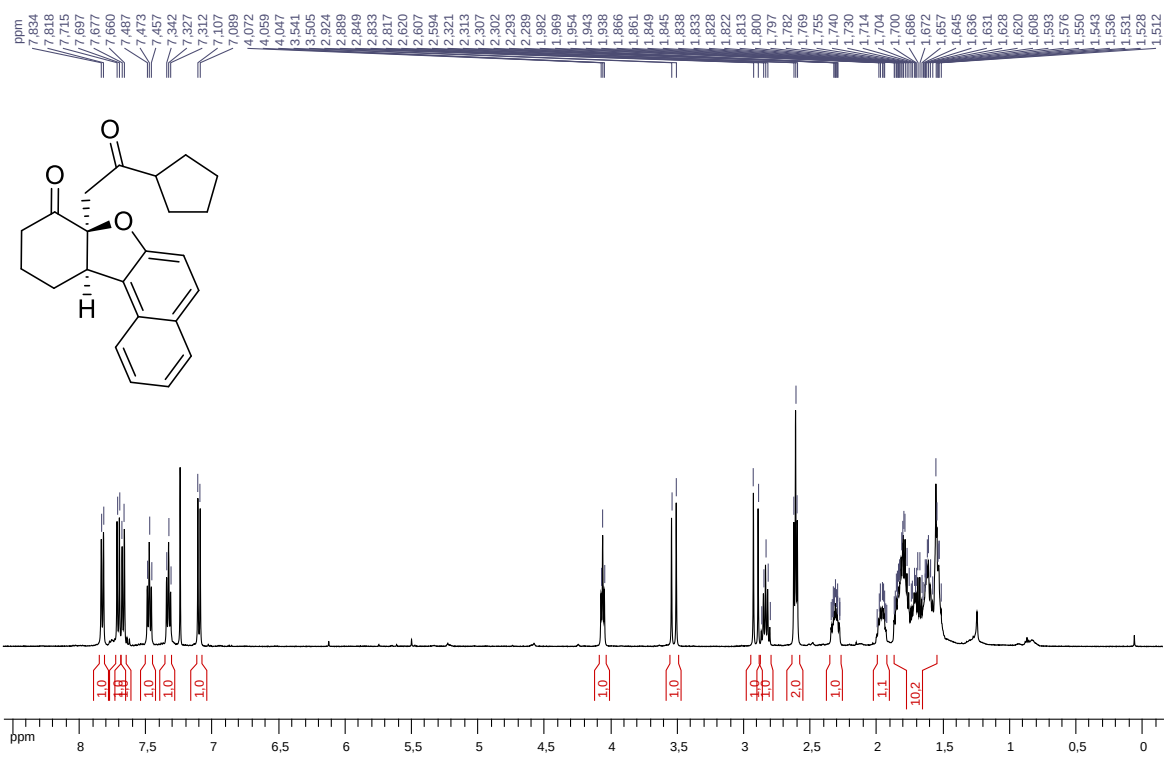

^{13}C NMR ($CDCl_3$, 125 MHz) (**6e**)

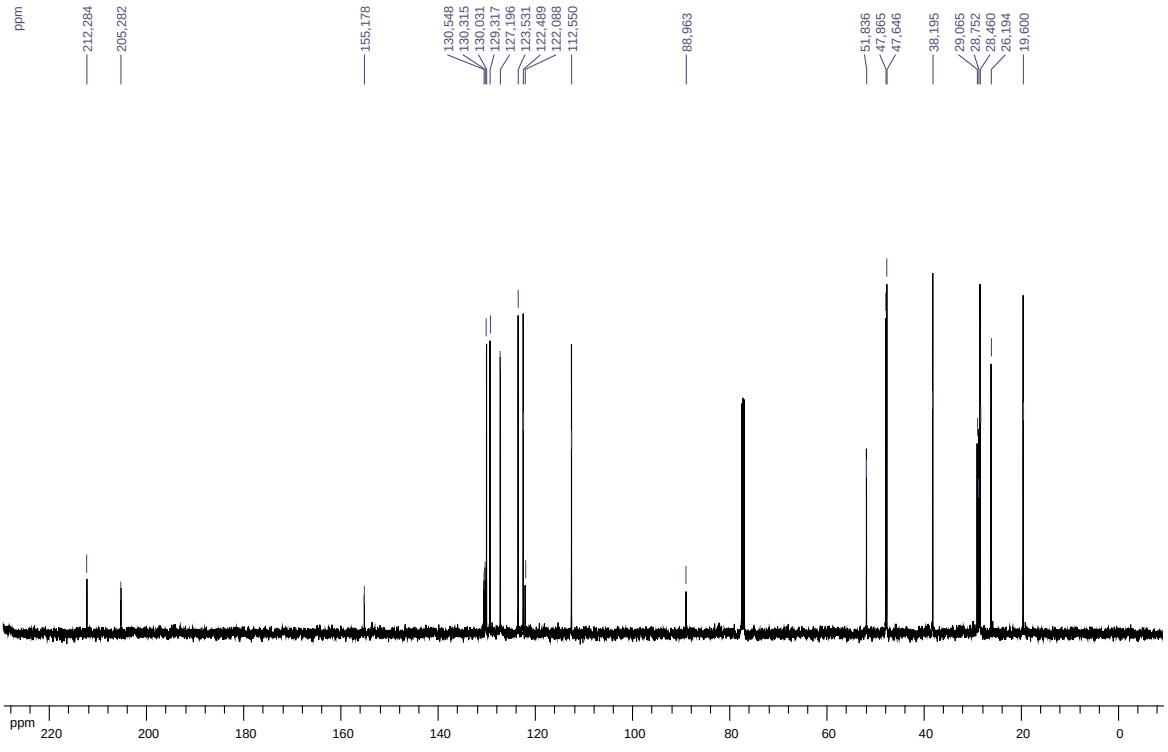

^{1}H NMR ($CDCl_3$, 500 MHz) (**6g**)

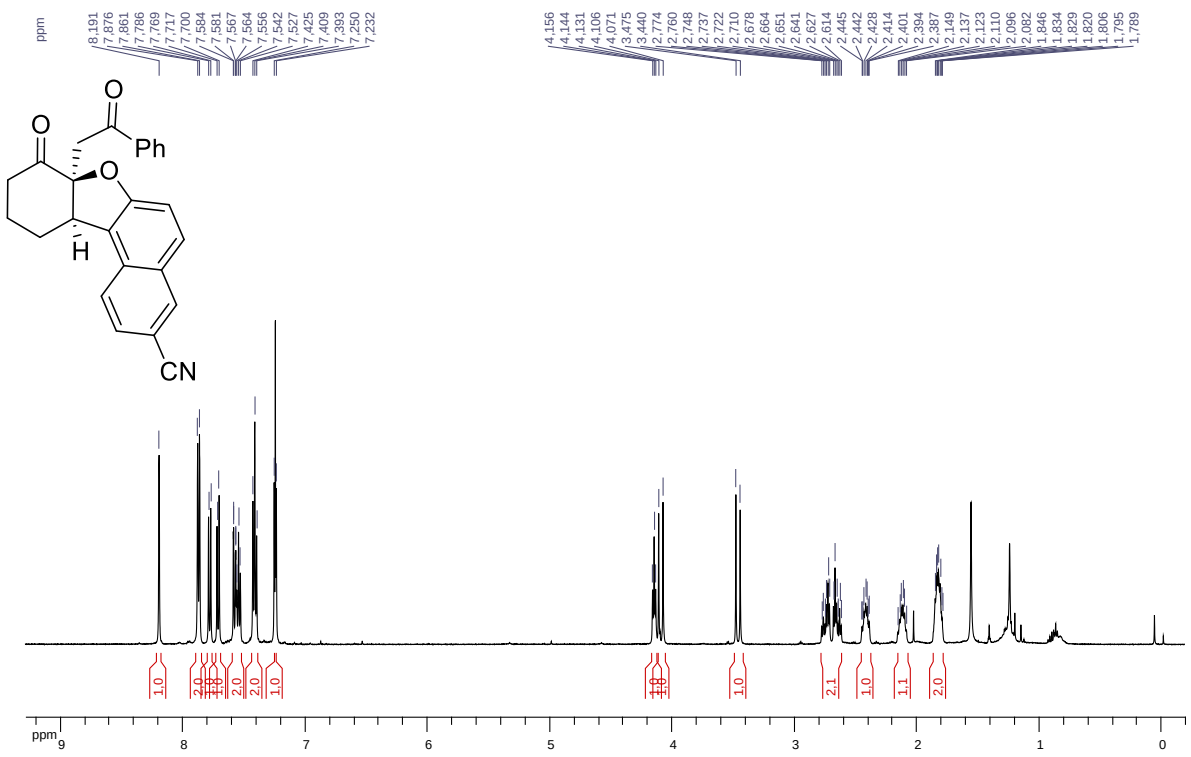

^{13}C NMR ($CDCl_3$, 125 MHz) (**6g**)

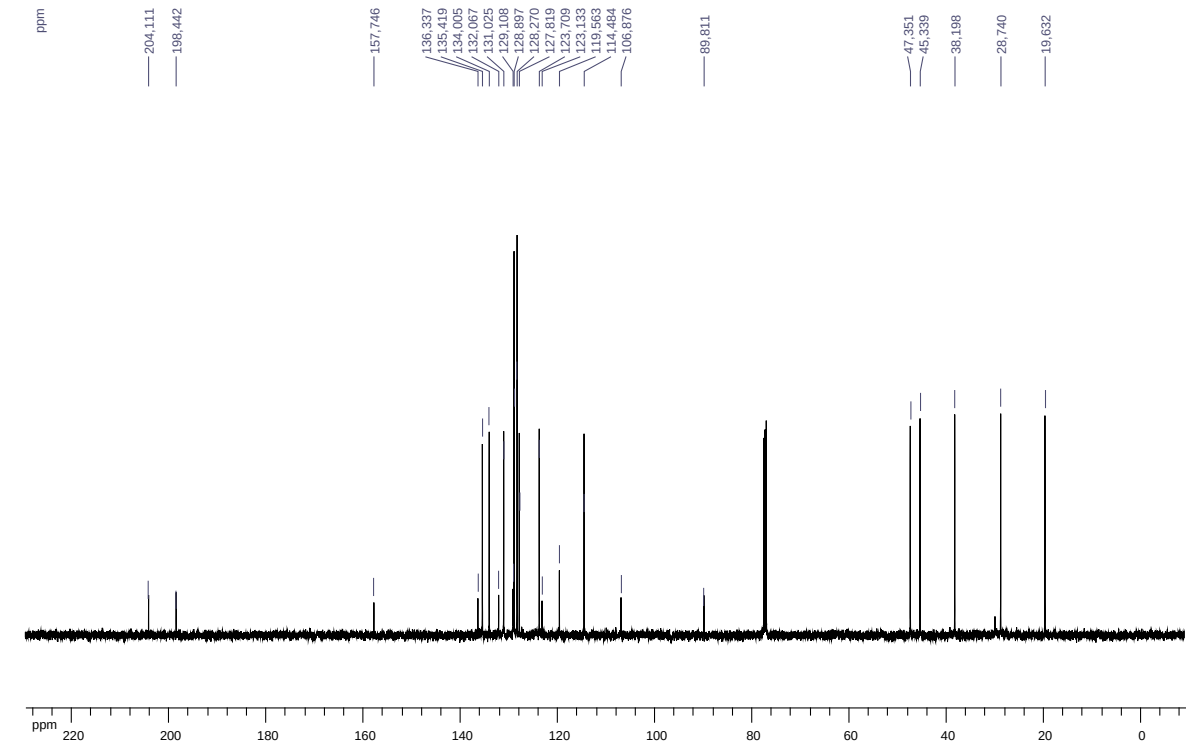

^{1}H NMR ($CDCl_3$, 500 MHz) (**6f**)

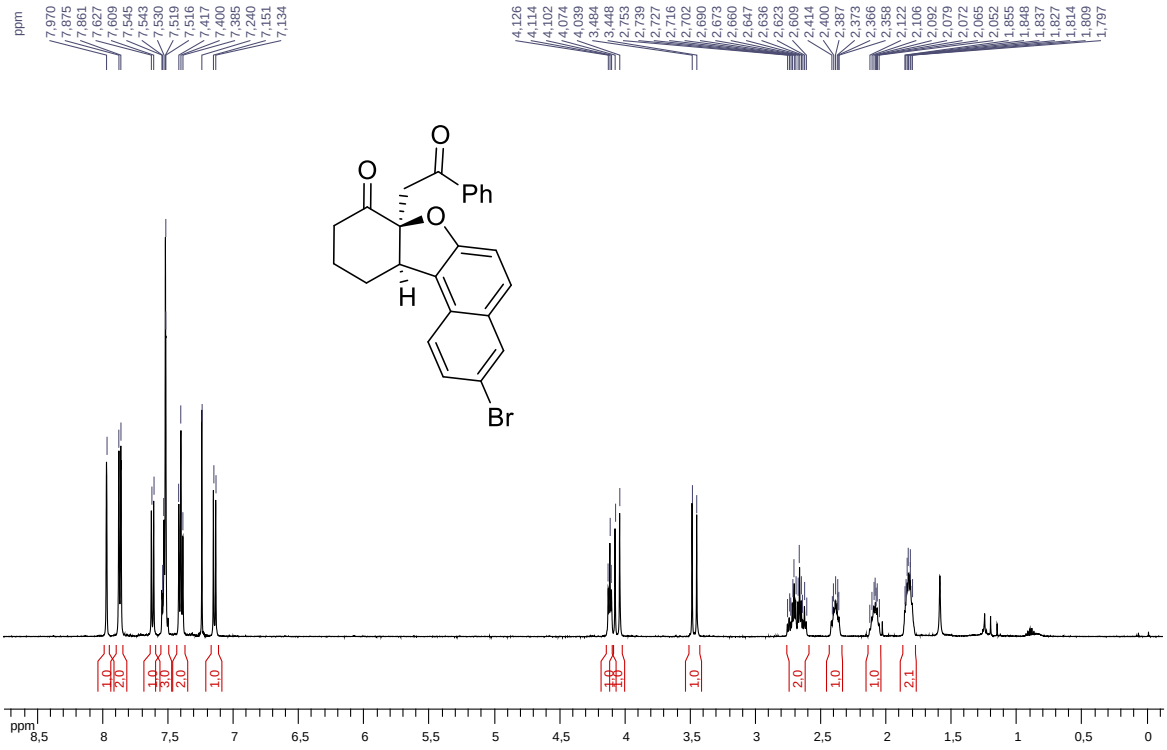

^{13}C NMR ($CDCl_3$, 125 MHz) (**6f**)

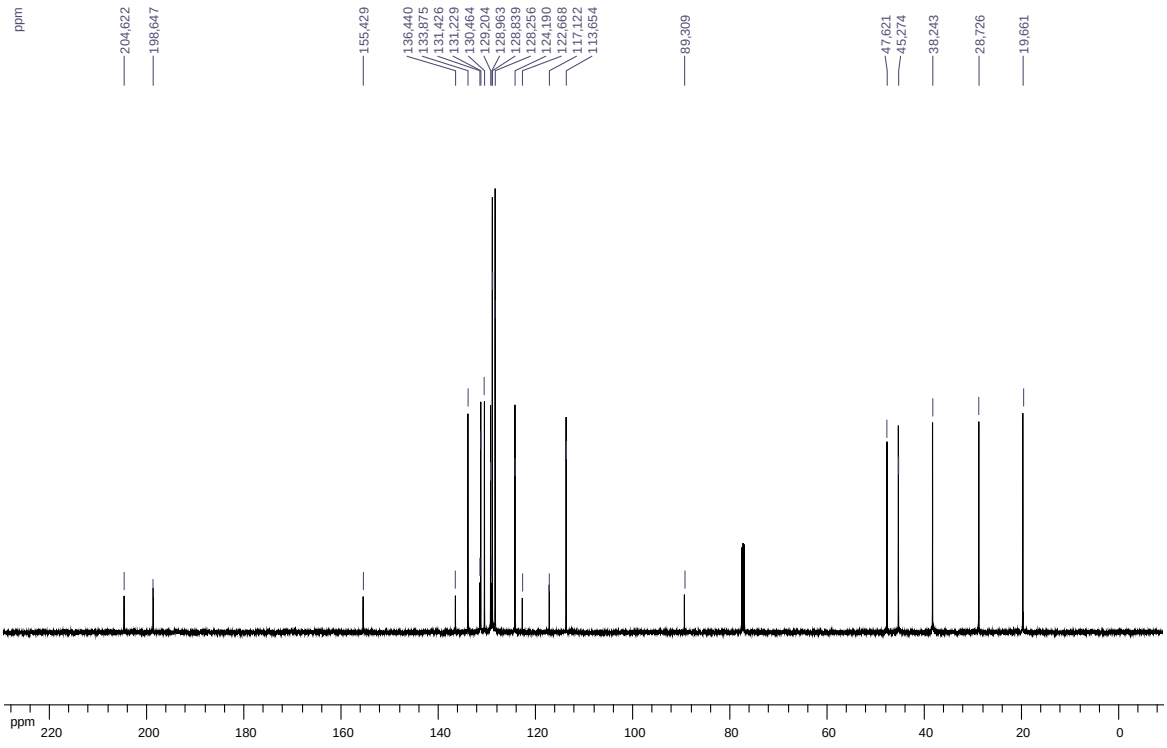

9. HPLC traces

Compound (**4a**)

HPLC Analysis: 85% ee [©Chiralpak IA, 25 °C, 5% iPrOH/n-heptane, 1 mL/min, 264 nm, retention times: 5.3 min (minor) and 6.0 min (major)].

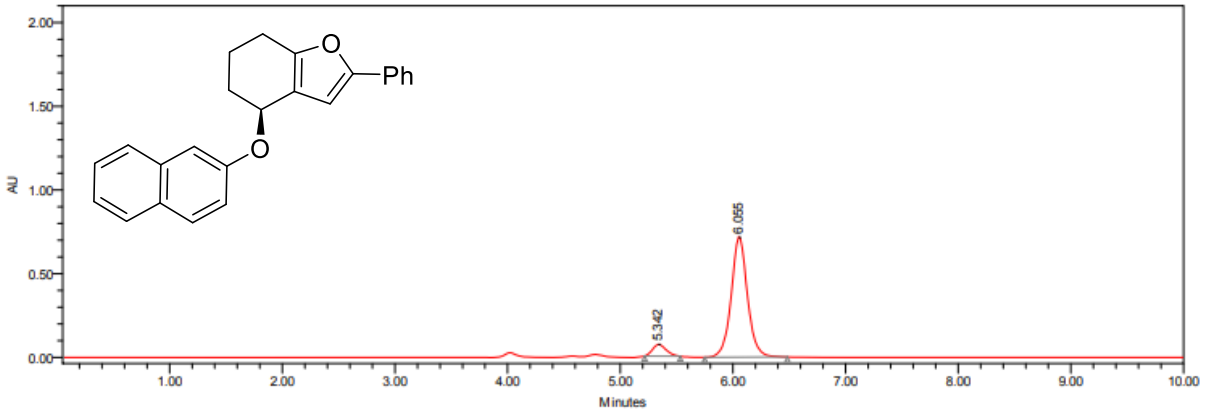

	Channel Description	RT	Area	% Area
1	PDA 200.0 to 400.0 nm at 2.4 nm	5.342	591799	7.60
2	PDA 200.0 to 400.0 nm at 2.4 nm	6.055	7194279	92.40

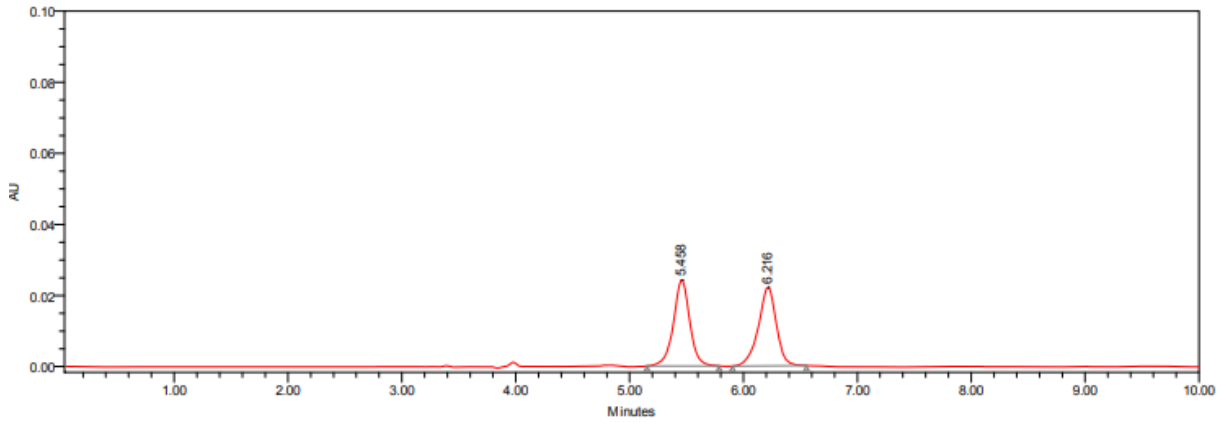

	Channel Description	RT	Area	% Area
1	PDA 200.0 to 400.0 nm at 2.4 nm	5.458	241397	49.96
2	PDA 200.0 to 400.0 nm at 2.4 nm	6.216	241757	50.04

Compound (**4a**)

HPLC Analysis: 87% ee [©Chiralpak IA, 25 °C, 5% iPrOH/n-heptane, 1 mL/min, 264 nm, retention times: 5.4 min (major) and 6.2 min (minor)].

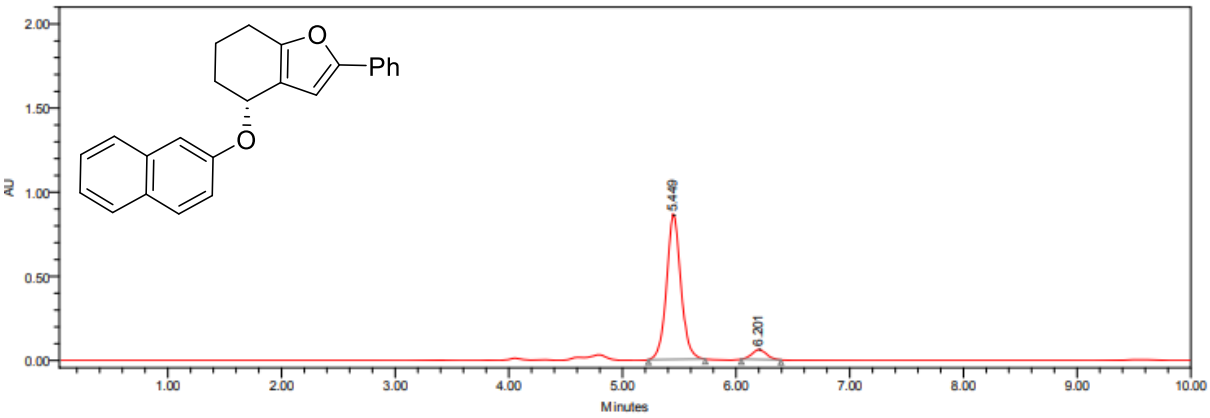

	Channel Description	RT	Area	% Area
1	PDA 200.0 to 400.0 nm at 2.4 nm	5.449	7561988	93.55
2	PDA 200.0 to 400.0 nm at 2.4 nm	6.201	521791	6.45

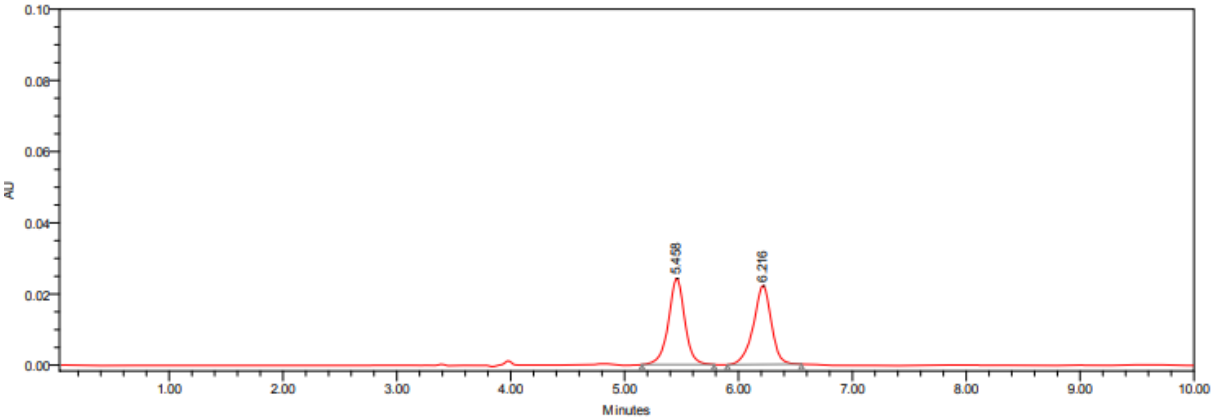

	Channel Description	RT	Area	% Area
1	PDA 200.0 to 400.0 nm at 2.4 nm	5.458	241397	49.96
2	PDA 200.0 to 400.0 nm at 2.4 nm	6.216	241757	50.04

Compound (**4b**)

HPLC Analysis: 75% ee [©Chiralpak IA, 25 °C, 5% iPrOH/n-heptane, 1 mL/min, 260 nm, retention times: 7.7 min (minor) and 8.8 min (major)].

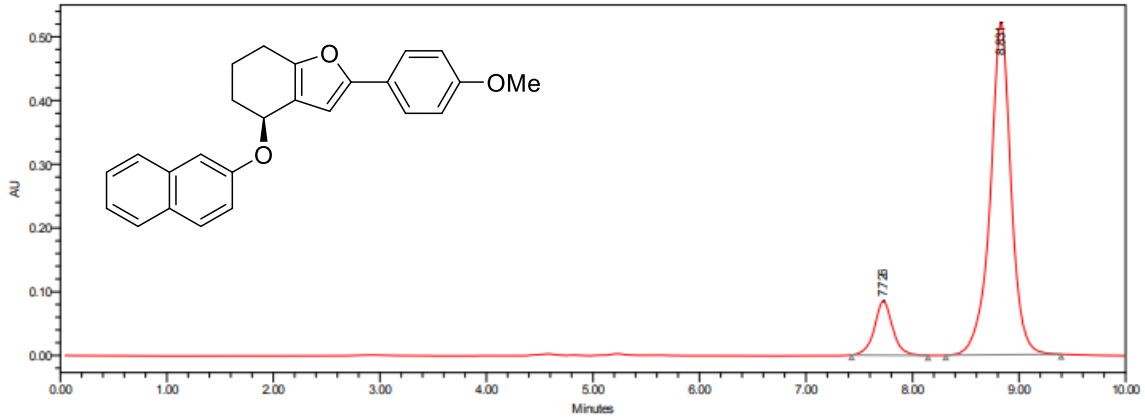

	Channel Description	RT	Area	% Area
1	PDA 200.0 to 400.0 nm at 2.4 nm	7.726	1007061	12.43
2	PDA 200.0 to 400.0 nm at 2.4 nm	8.831	7094374	87.57

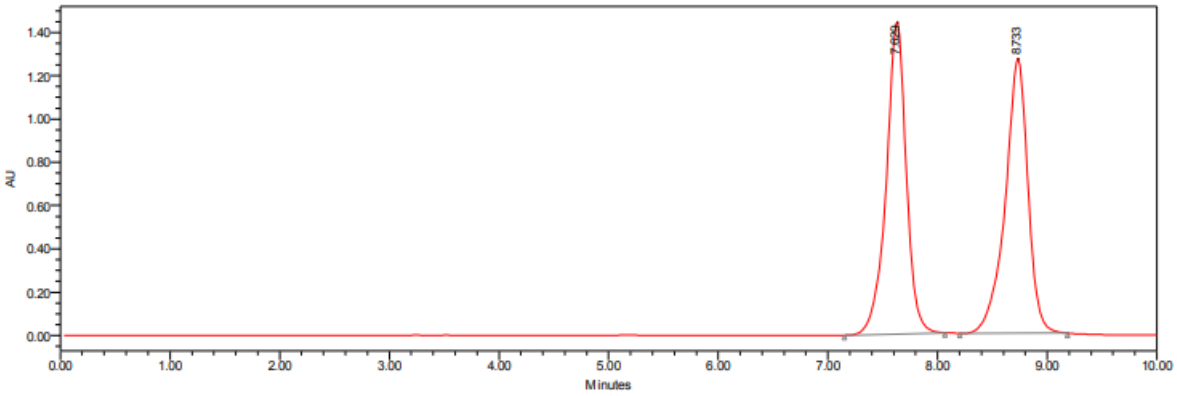

	Channel Description	RT	Area	% Area
1	PDA 200.0 to 400.0 nm at 2.4 nm	7.629	18287867	50.00
2	PDA 200.0 to 400.0 nm at 2.4 nm	8.733	18287261	50.00

Compound (4c)

HPLC Analysis: 64% ee [©Chiralpak IA, 25 °C, 5% *i*PrOH/*n*-heptane, 1 mL/min, 227 nm, retention times: 6.8 min (minor) and 8.7 min (major)].

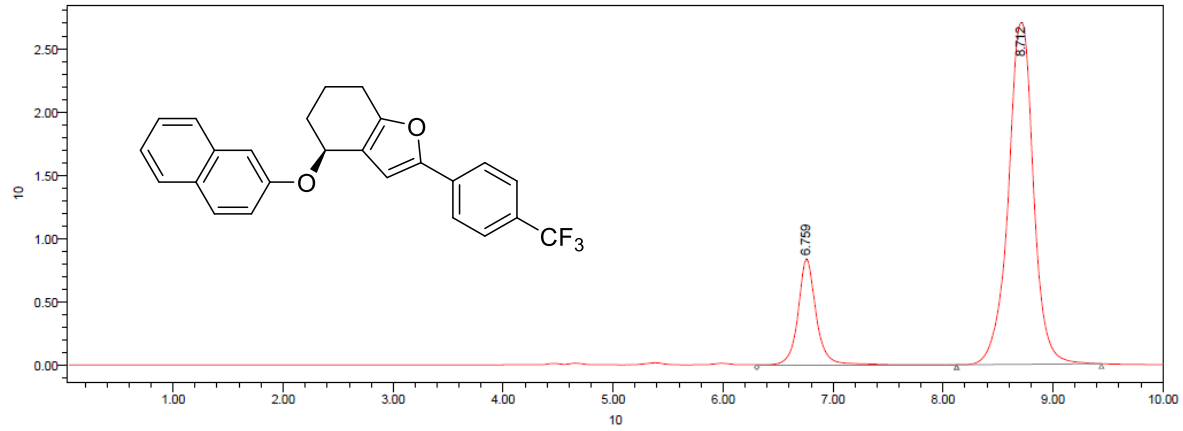

	Channel Description	RT	Area	% Area
1	PDA 200.0 to 400.0 nm at 2.4 nm	6.759	9607515	18.22
2	PDA 200.0 to 400.0 nm at 2.4 nm	8.712	43129065	81.78

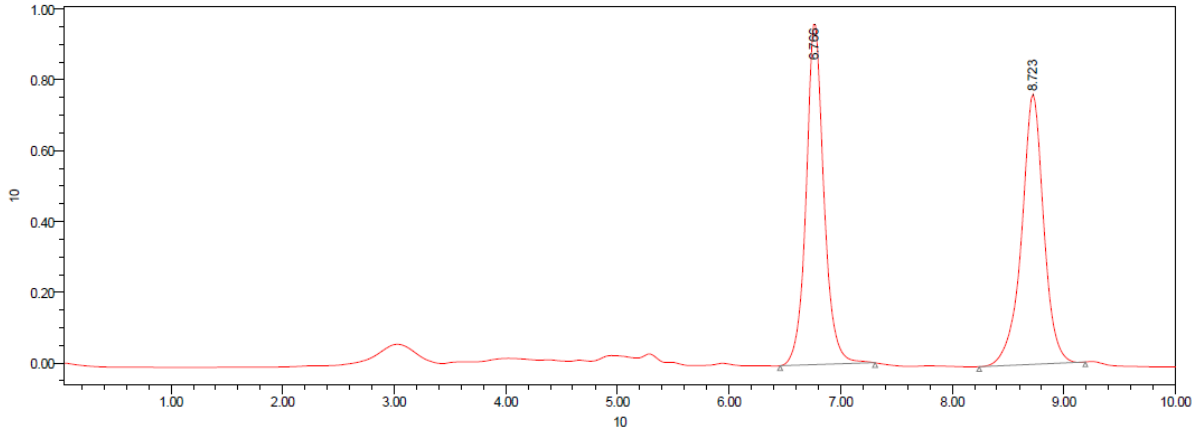

	Channel Description	RT	Area	% Area
1	PDA 200.0 to 400.0 nm at 2.4 nm	6.766	10653033	50.36
2	PDA 200.0 to 400.0 nm at 2.4 nm	8.723	10502123	49.64

Compound (4d).

HPLC Analysis: 84% ee [©Chiralpak IB, 25 °C, 20% iPrOH/n-heptane, 1 mL/min, 285 nm, retention times: 6.4 min (major) and 8.5 min (minor)].

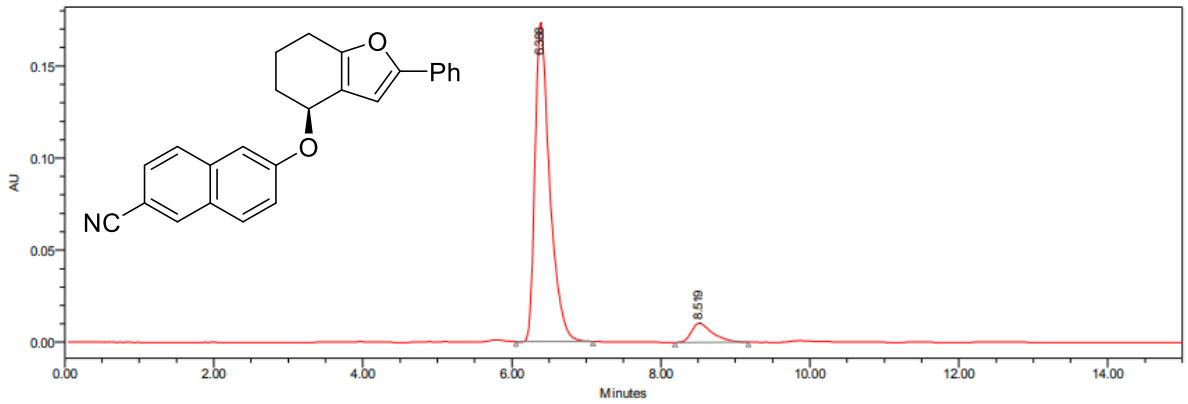

	Channel Description	RT	Area	% Area
1	PDA 200.0 to 400.0 nm at 2.4 nm	6.388	2376654	92.16
2	PDA 200.0 to 400.0 nm at 2.4 nm	8.519	202151	7.84

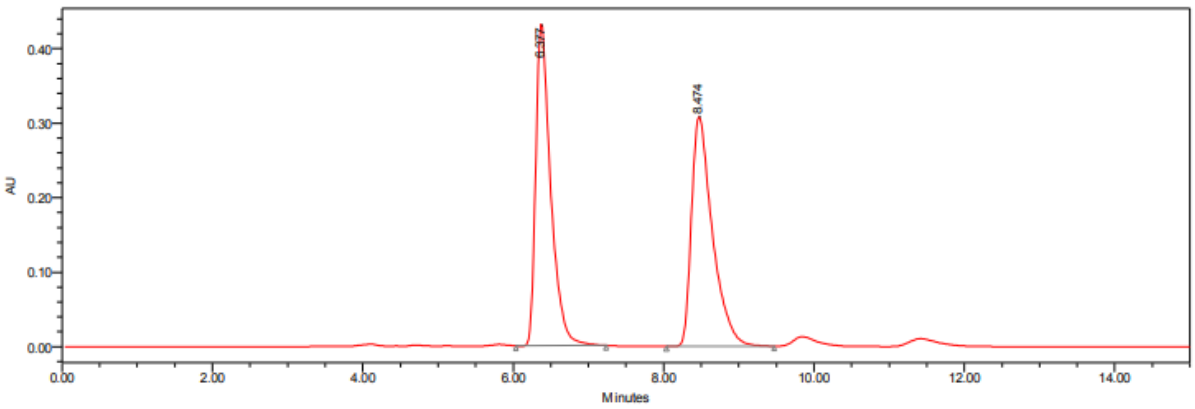

	Channel Description	RT	Area	% Area
1	PDA 200.0 to 400.0 nm at 2.4 nm	6.377	5969137	50.07
2	PDA 200.0 to 400.0 nm at 2.4 nm	8.474	5952384	49.93

Compound (4e)

HPLC Analysis: 79% ee [©Chiralpak IB, 25 °C, 20% iPrOH/n-heptane, 1 mL/min, 312 nm, retention times: 4.5 min (major) and 5.6 min (minor)].

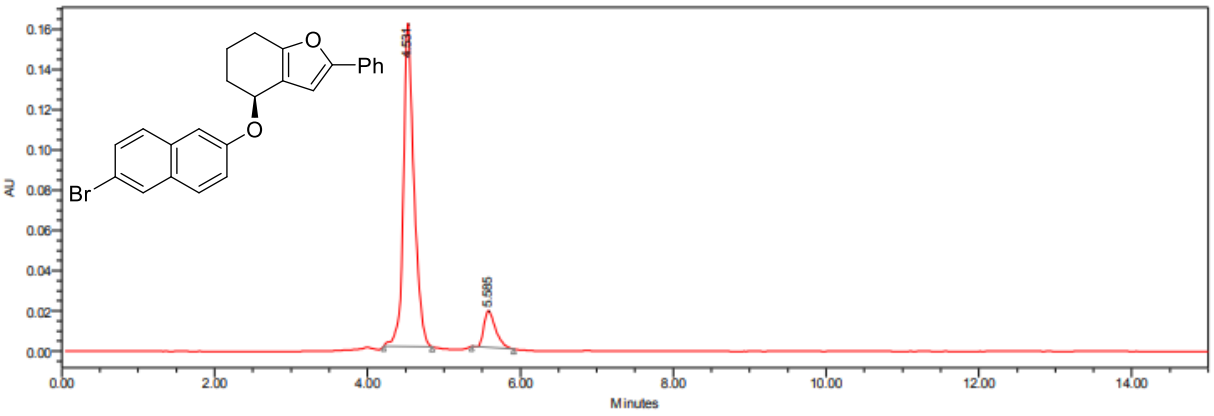

	Channel Description	RT	Area	% Area
1	PDA 200.0 to 400.0 nm at 2.4 nm	4.531	1548172	88.91
2	PDA 200.0 to 400.0 nm at 2.4 nm	5.585	193033	11.09

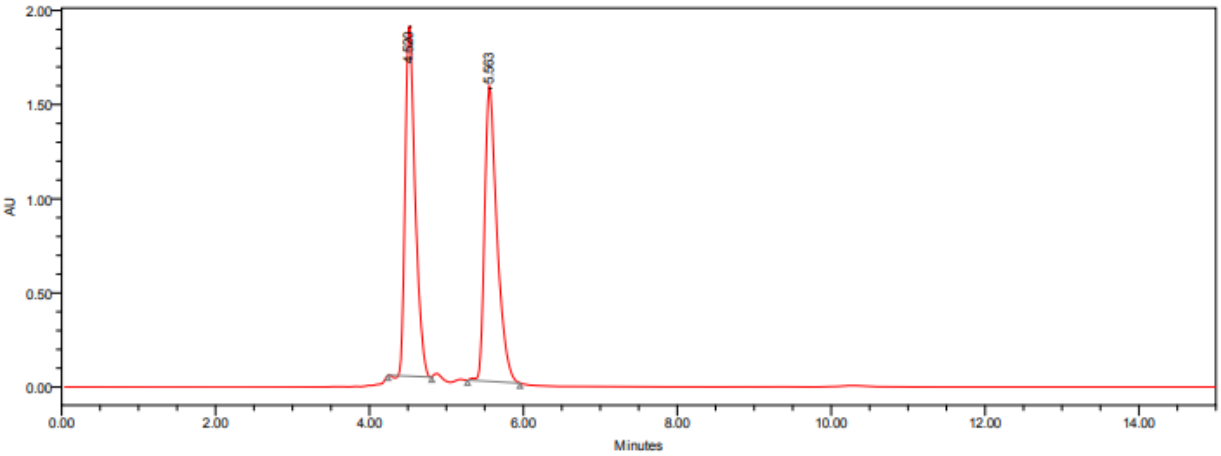

	Channel Description	RT	Area	% Area
1	PDA 200.0 to 400.0 nm at 2.4 nm	4.520	16873901	49.17
2	PDA 200.0 to 400.0 nm at 2.4 nm	5.563	17441131	50.83

Compound **(4e).**

HPLC Analysis: 64% ee [©Chiralpak IB, 25 °C, 20% iPrOH/n-heptane, 1 mL/min, 229 nm, retention times: 4.5 min (minor) and 5.6 min (major)].

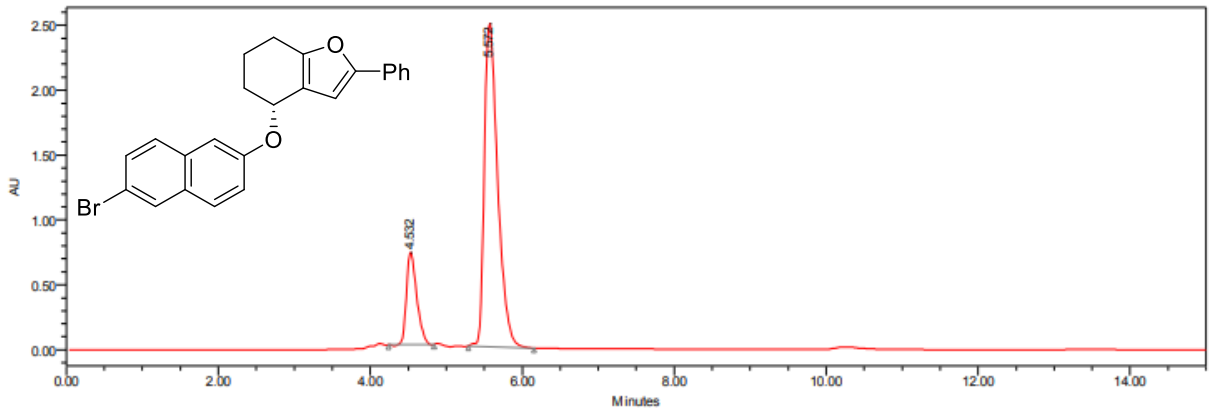

	Channel Description	RT	Area	% Area
1	PDA 200.0 to 400.0 nm at 2.4 nm	4.532	6647968	17.96
2	PDA 200.0 to 400.0 nm at 2.4 nm	5.572	30363551	82.04

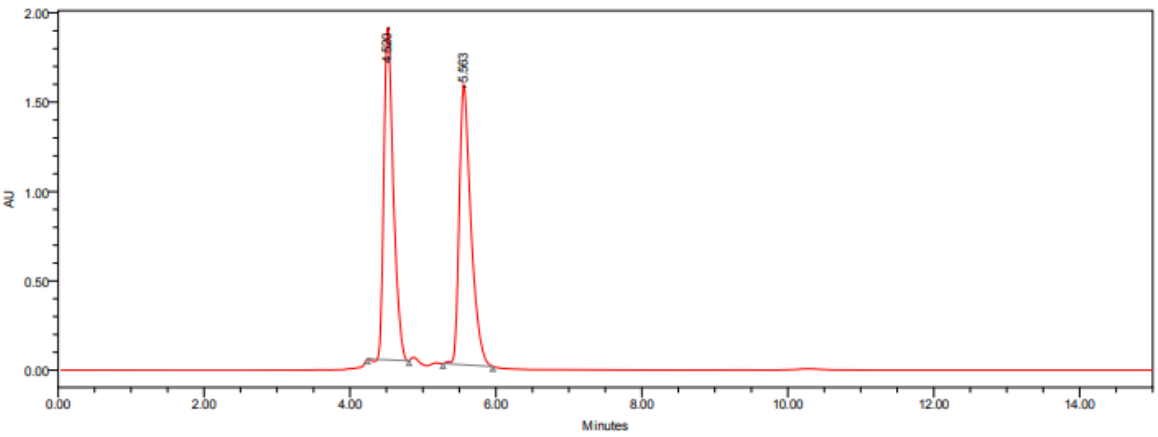

	Channel Description	RT	Area	% Area
1	PDA 200.0 to 400.0 nm at 2.4 nm	4.520	16873901	49.17
2	PDA 200.0 to 400.0 nm at 2.4 nm	5.563	17441131	50.83

Compound (**4f**)

HPLC Analysis: 85% ee [©Chiralpak IF, 25 °C, 2% iPrOH/n-heptane, 1 mL/min, 338 nm, retention times: 5.7 min (minor) and 6.2 min (major)].

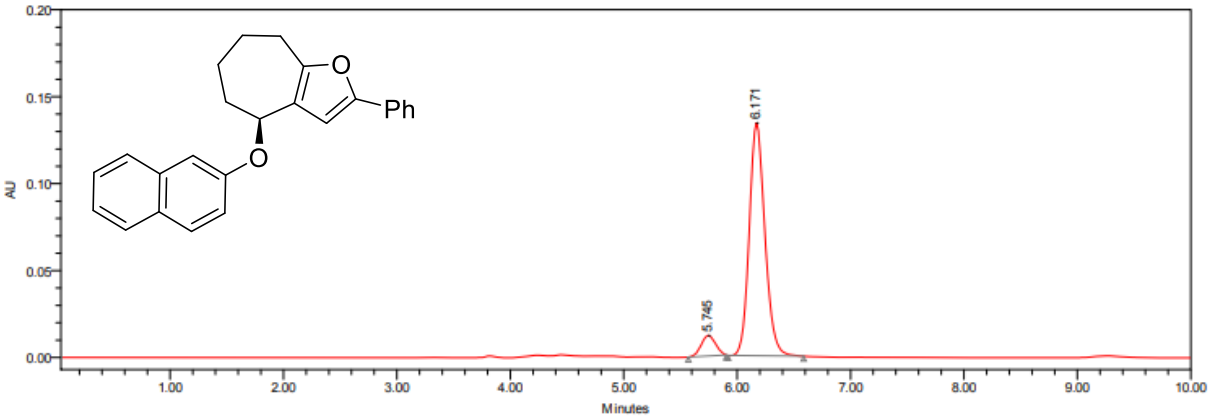

	Channel Description	RT	Area	% Area
1	PDA 200.0 to 400.0 nm at 2.4 nm	5.745	102761	7.40
2	PDA 200.0 to 400.0 nm at 2.4 nm	6.171	1285413	92.60

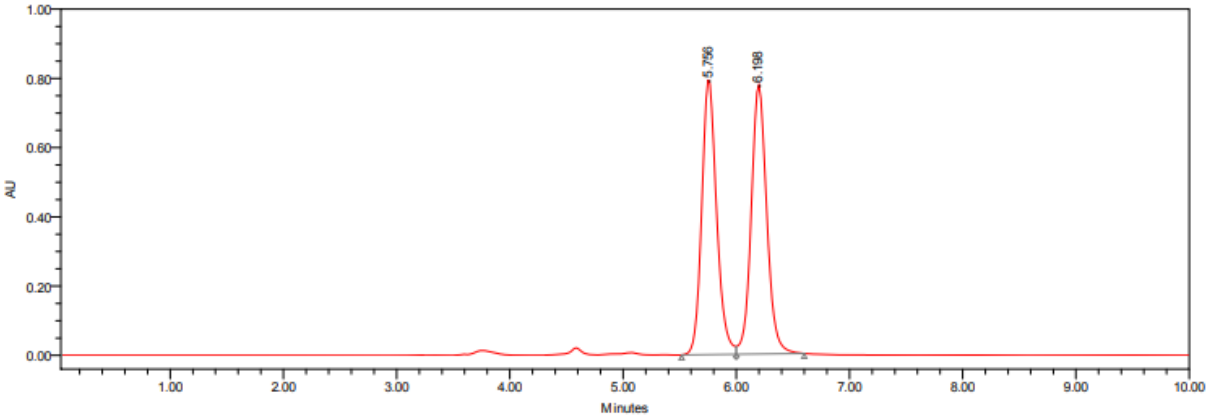

	Channel Description	RT	Area	% Area
1	PDA 200.0 to 400.0 nm at 2.4 nm	5.756	7255897	49.56
2	PDA 200.0 to 400.0 nm at 2.4 nm	6.198	7386163	50.44

Compound (**4a'**)

HPLC Analysis: 88% ee [©Chiralpak IA, 25 °C, 5% iPrOH/n-heptane, 1 mL/min, 212 nm, retention times: 4.5 min (minor) and 5.0 min (major)].

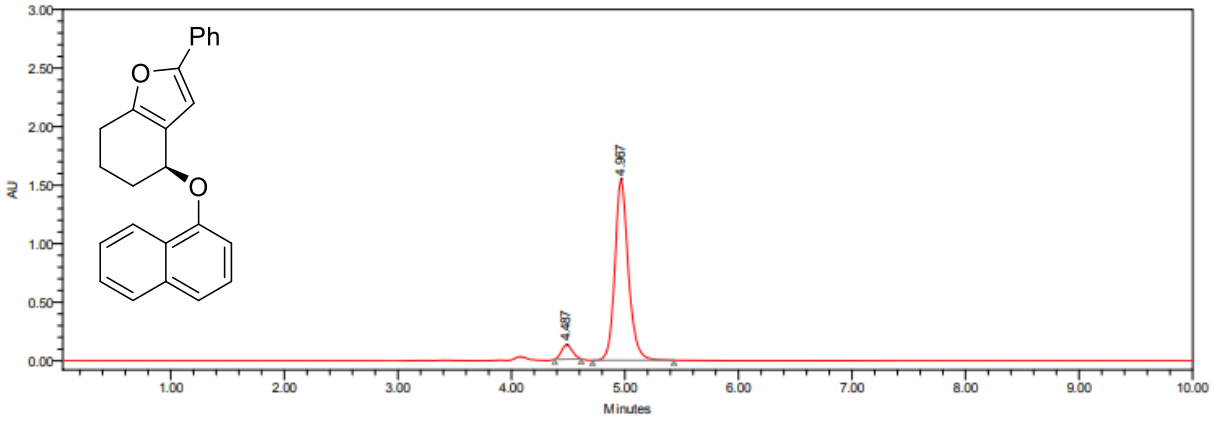

	Channel Description	RT	Area	% Area
1	PDA 200.0 to 400.0 nm at 2.4 nm	4.487	804611	5.96
2	PDA 200.0 to 400.0 nm at 2.4 nm	4.967	12692741	94.04

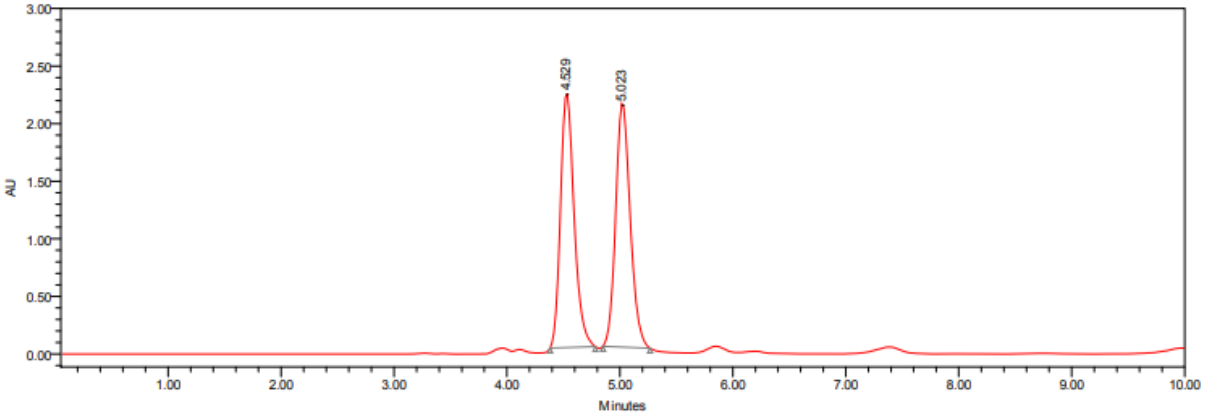

	Channel Description	RT	Area	% Area
1	PDA 200.0 to 400.0 nm at 2.4 nm	4.529	18571244	49.45
2	PDA 200.0 to 400.0 nm at 2.4 nm	5.023	18986237	50.55

Compound (**4a'**)

HPLC Analysis: 50% ee [©Chiralpak IA, 25 °C, 5% iPrOH/n-heptane, 1 mL/min, 212 nm, retention times: 4.5 min (minor) and 5.0 min (major)].

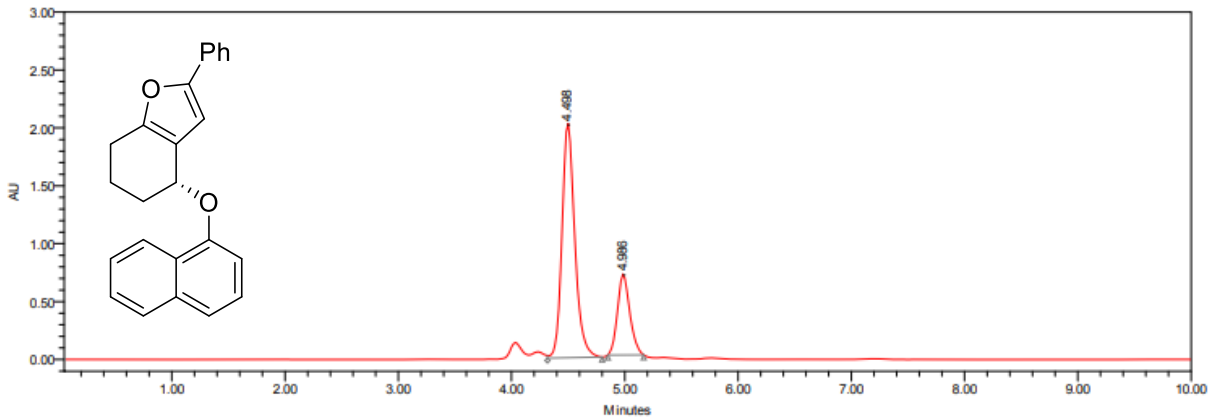

	Channel Description	RT	Area	% Area
1	PDA 200.0 to 400.0 nm at 2.4 nm	4.498	15832600	75.03
2	PDA 200.0 to 400.0 nm at 2.4 nm	4.986	5268513	24.97

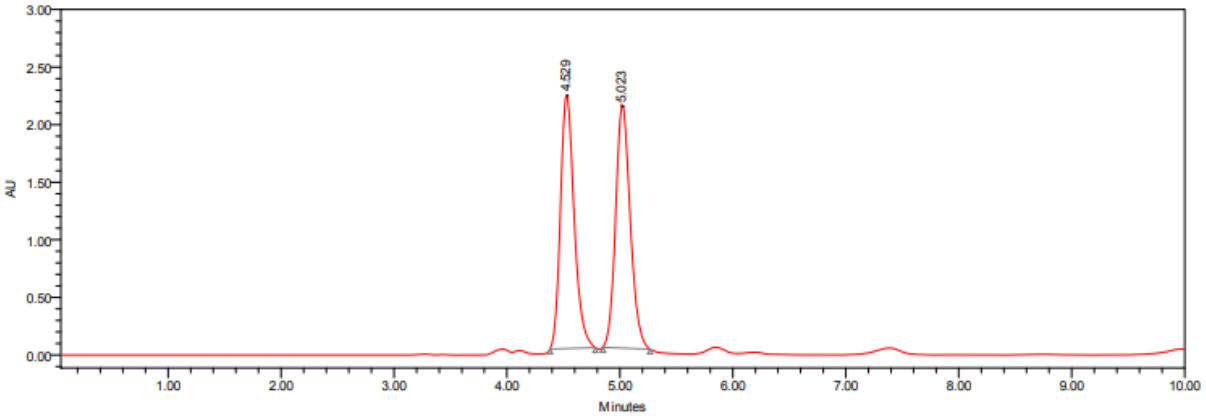

	Channel Description	RT	Area	% Area
1	PDA 200.0 to 400.0 nm at 2.4 nm	4.529	18571244	49.45
2	PDA 200.0 to 400.0 nm at 2.4 nm	5.023	18986237	50.55

Compound (**5a**)

HPLC Analysis: 93% ee [©Chiralpak IA, 25 °C, 5% iPrOH/n-heptane, 1 mL/min, 318 nm, retention times: 9.7 min (minor) and 10.7 min (major)].

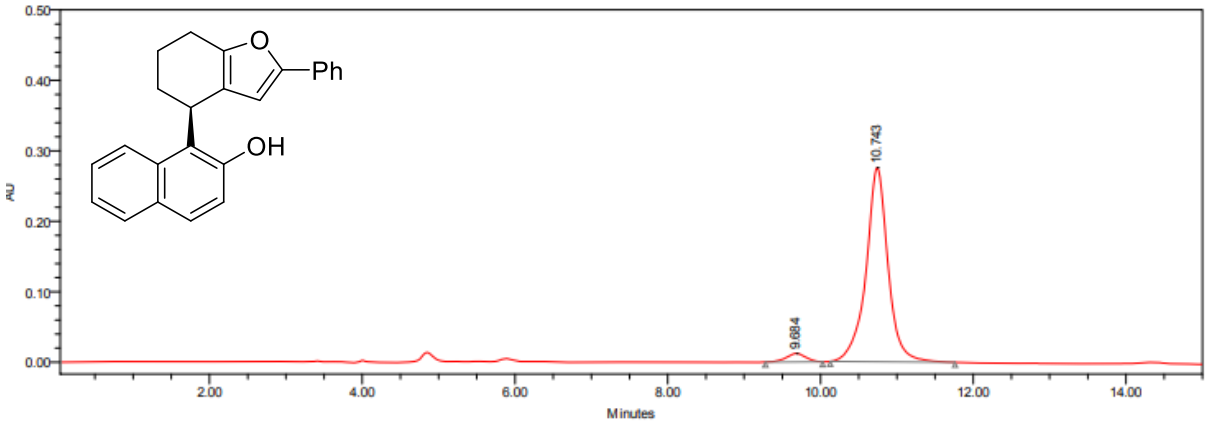

	Channel Description	RT	Area	% Area
1	PDA 200.0 to 400.0 nm at 2.4 nm	9.684	212047	3.69
2	PDA 200.0 to 400.0 nm at 2.4 nm	10.743	5531007	96.31

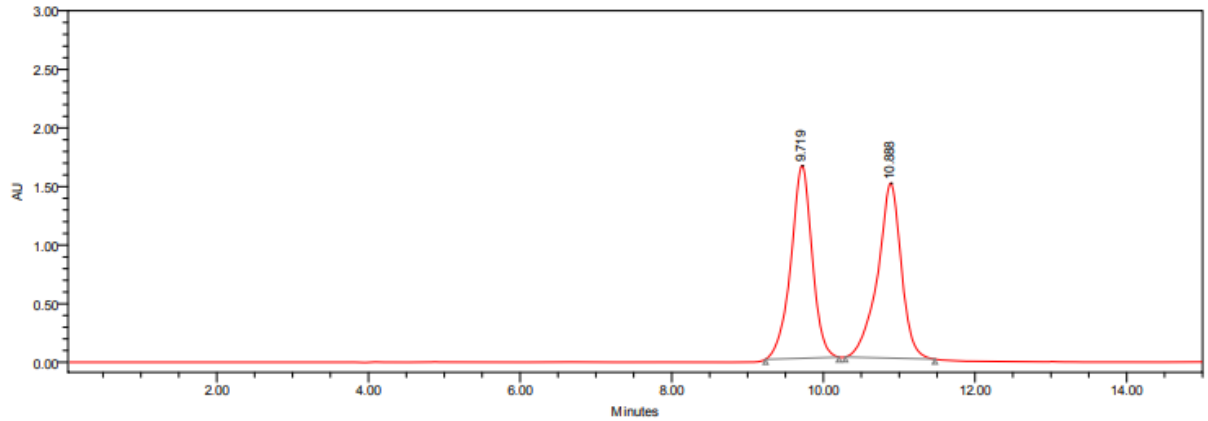

	Channel Description	RT	Area	% Area
1	PDA 200.0 to 400.0 nm at 2.4 nm	9.719	31961945	49.78
2	PDA 200.0 to 400.0 nm at 2.4 nm	10.888	32249831	50.22

Compound (**5b**)

HPLC Analysis: 93% ee [©Chiralpak IA, 25 °C, 5% iPrOH/n-heptane, 1 mL/min, 241 nm, retention times: 6.6 min (minor) and 7.2 min (major)].

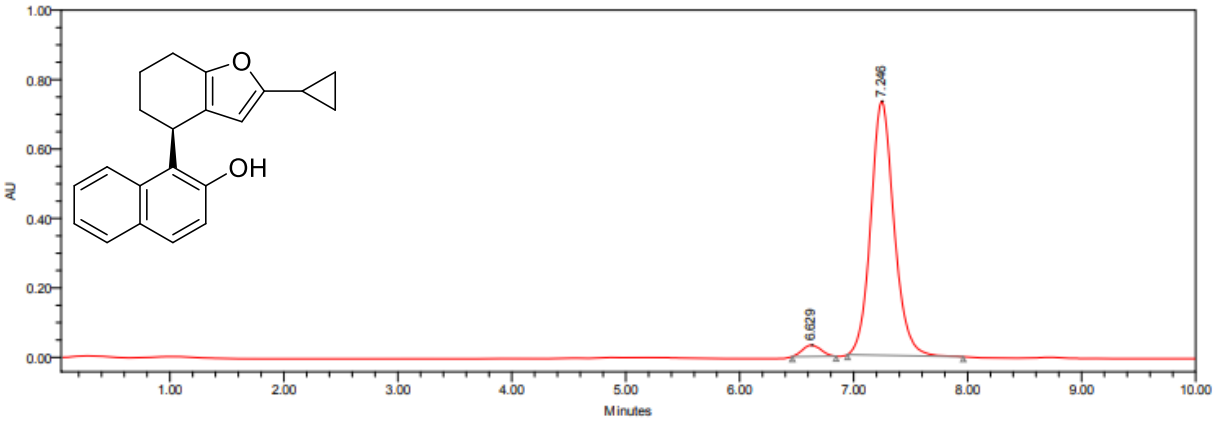

	Channel Description	RT	Area	% Area
1	PDA 200.0 to 400.0 nm at 2.4 nm	6.629	368589	3.43
2	PDA 200.0 to 400.0 nm at 2.4 nm	7.246	10377467	96.57

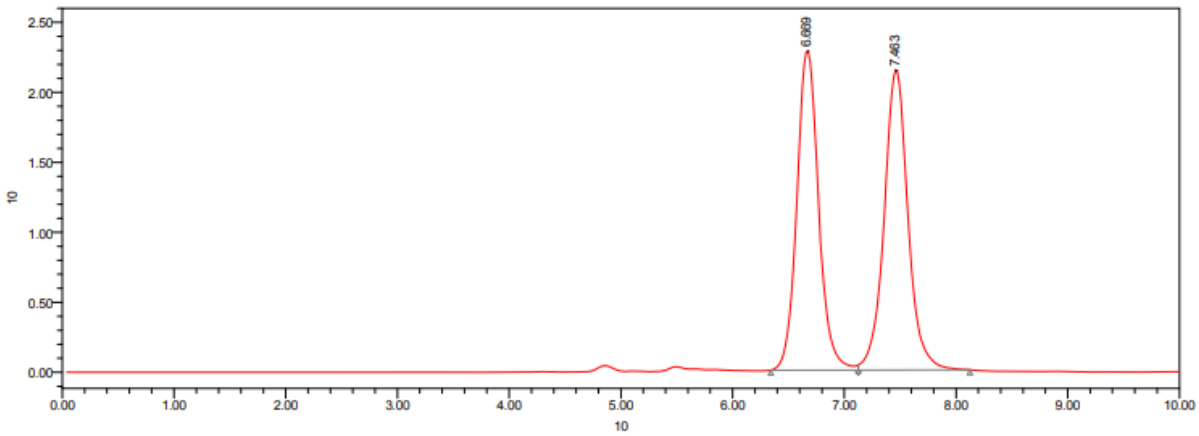

	Channel Description	RT	Area	% Area
1	PDA 200.0 to 400.0 nm at 2.4 nm	6.669	30865828	49.24
2	PDA 200.0 to 400.0 nm at 2.4 nm	7.463	31821241	50.76

Compound (**5c**)

HPLC Analysis: 99% ee [©Chiralpak IA, 25 °C, 2% iPrOH/n-heptane, 1 mL/min, 280 nm, retention times: 7.4 min (minor) and 8.1 min (major)].

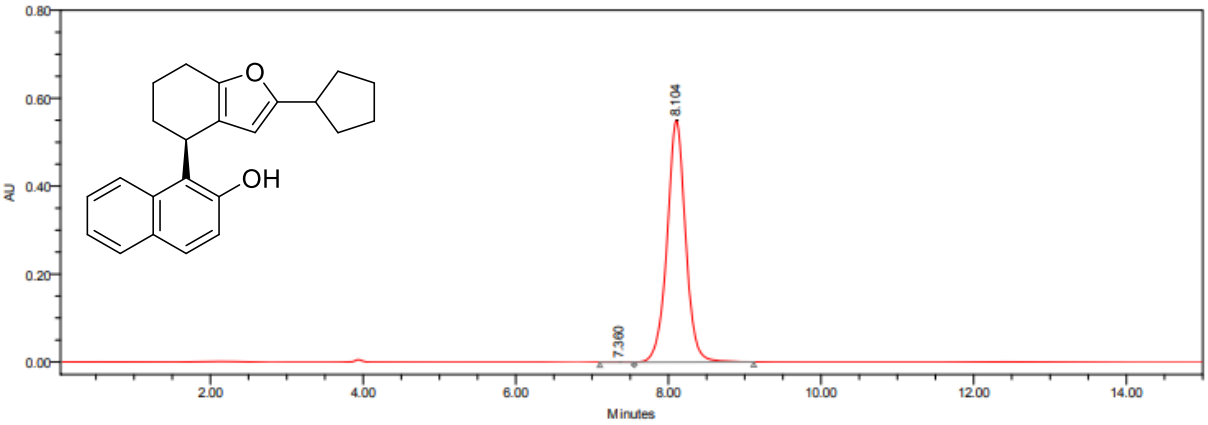

	Channel Description	RT	Area	% Area
1	PDA 200.0 to 400.0 nm at 2.4 nm	7.360	11433	0.12
2	PDA 200.0 to 400.0 nm at 2.4 nm	8.104	9254703	99.88

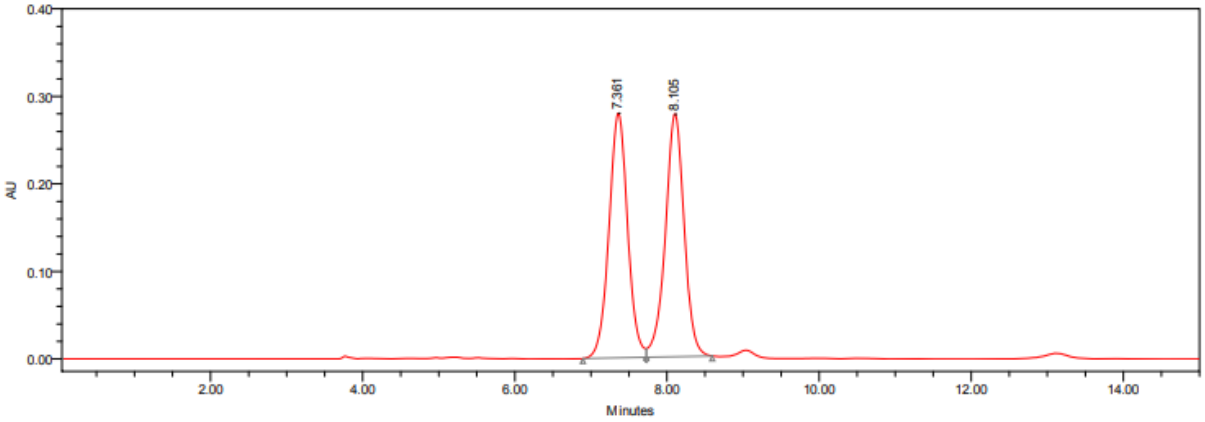

	Channel Description	RT	Area	% Area
1	PDA 200.0 to 400.0 nm at 2.4 nm	7.361	4762242	50.06
2	PDA 200.0 to 400.0 nm at 2.4 nm	8.105	4751621	49.94

Compound (**5a'**)

HPLC Analysis: 98% ee [©Chiralpak IA, 25 °C, 5% iPrOH/n-heptane, 1 mL/min, 280 nm, retention times: 13.4 min (major) and 16.3 min (minor)].

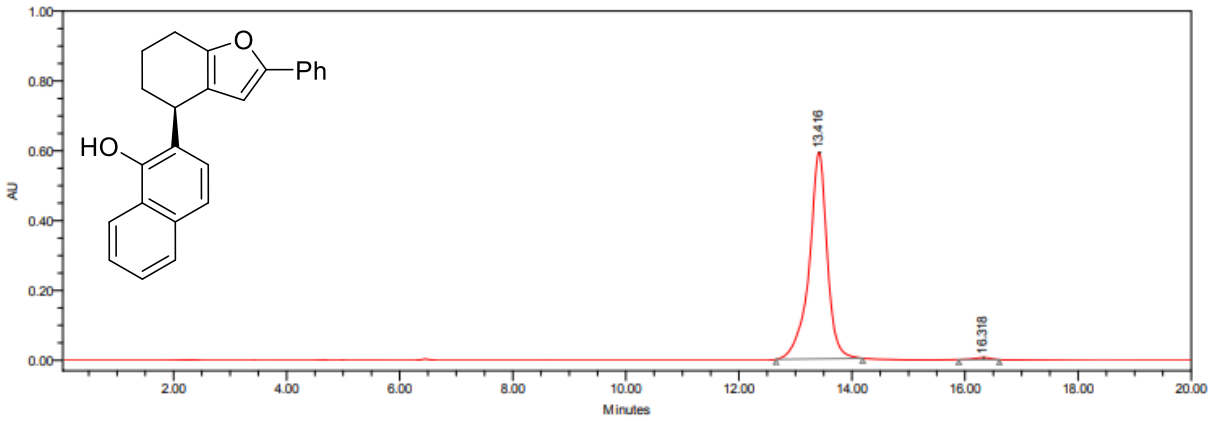

	Channel Description	RT	Area	% Area
1	PDA 200.0 to 400.0 nm at 2.4 nm	13.416	13052049	99.13
2	PDA 200.0 to 400.0 nm at 2.4 nm	16.318	115208	0.87

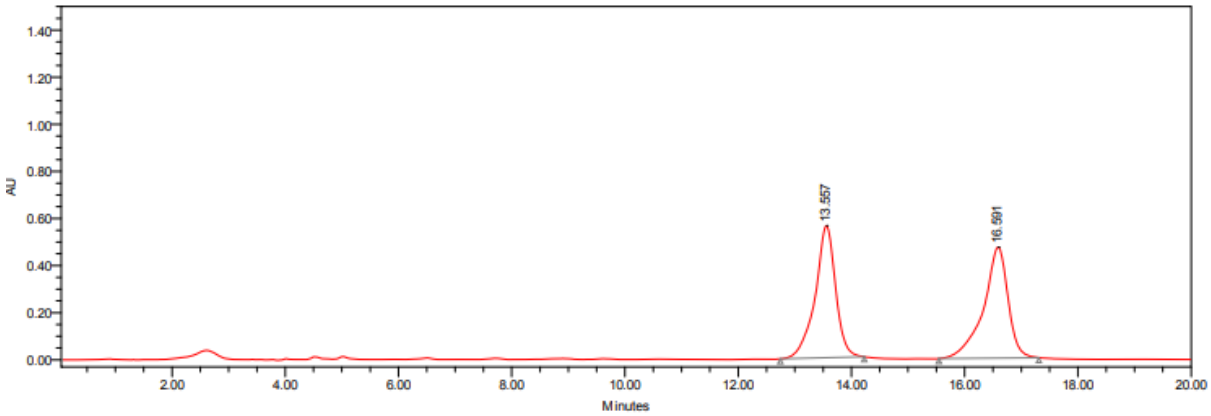

	Channel Description	RT	Area	% Area
1	PDA 200.0 to 400.0 nm at 2.4 nm	13.557	14059357	49.81
2	PDA 200.0 to 400.0 nm at 2.4 nm	16.591	14168380	50.19

Compound (**6a**)

HPLC Analysis: 93% ee [©Chiralpak IA, 25 °C, 20% iPrOH/n-heptane, 1 mL/min, 251 nm, retention times: 7.7 min (minor) and 8.9 min (major)].

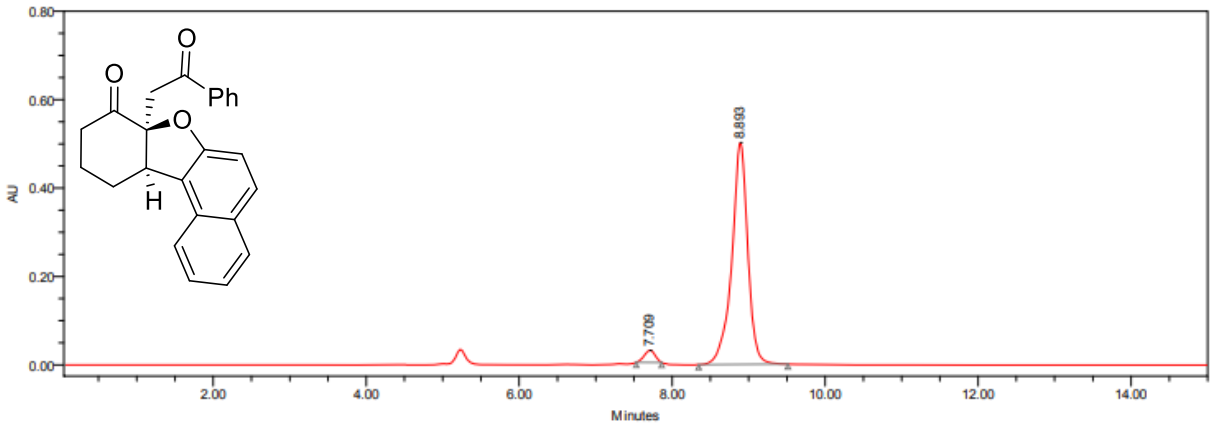

	Channel Description	RT	Area	% Area
1	PDA 200.0 to 400.0 nm at 2.4 nm	7.709	270683	3.59
2	PDA 200.0 to 400.0 nm at 2.4 nm	8.893	7276213	96.41

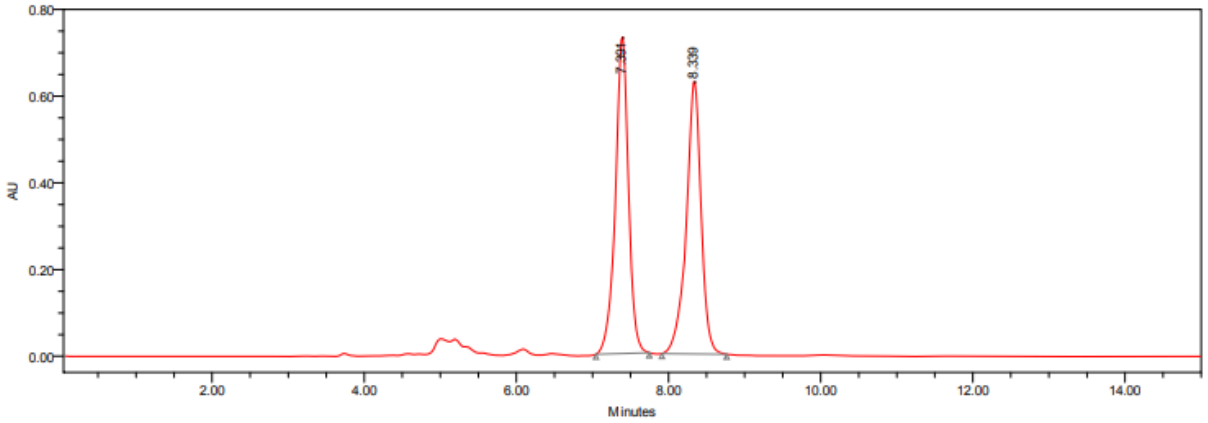

	Channel Description	RT	Area	% Area
1	PDA 200.0 to 400.0 nm at 2.4 nm	7.391	8722958	50.67
2	PDA 200.0 to 400.0 nm at 2.4 nm	8.339	8490754	49.33

Compound (**6g**)

HPLC Analysis: 85% ee [©Chiralpak IA, 25 °C, 20% iPrOH/n-heptane, 1 mL/min, 242 nm, retention times: 16.6 min (minor) and 19.6 min (major)].

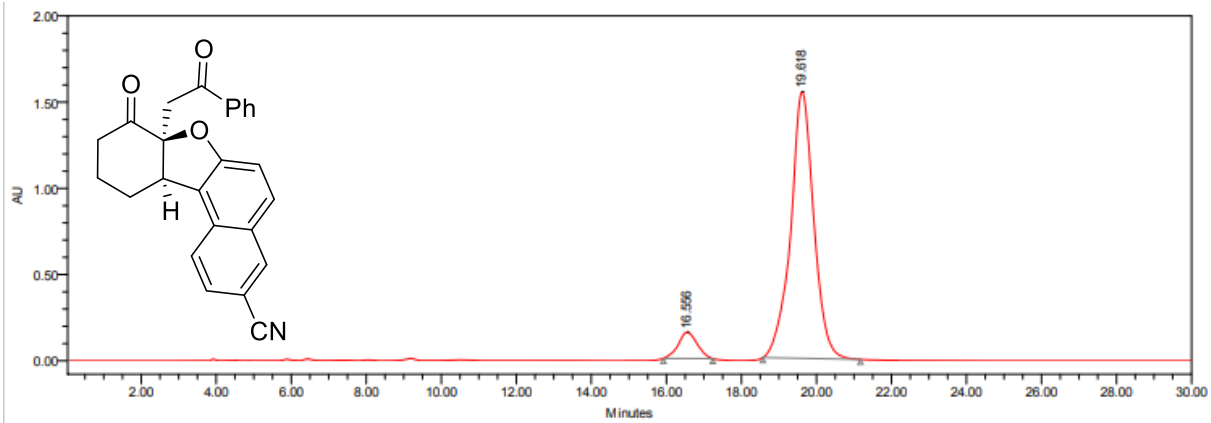

	Channel Description	RT	Area	% Area
1	PDA 200.0 to 400.0 nm at 2.4 nm	16.556	5308716	7.42
2	PDA 200.0 to 400.0 nm at 2.4 nm	19.618	66196392	92.58

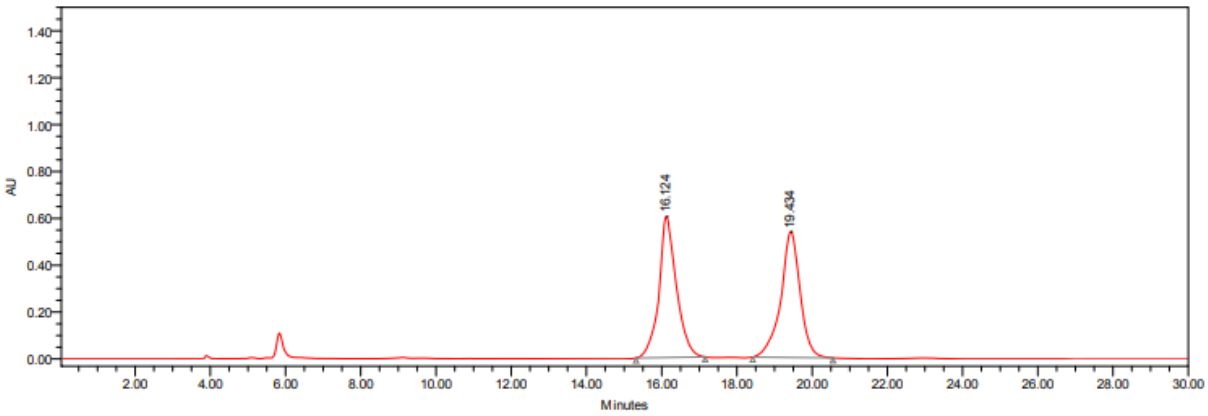

	Channel Description	RT	Area	% Area
1	PDA 200.0 to 400.0 nm at 2.4 nm	16.124	19371797	50.30
2	PDA 200.0 to 400.0 nm at 2.4 nm	19.434	19139551	49.70

Compound (**6b**)

HPLC Analysis: 86% ee [©Chiralpak IA, 25 °C, 10% iPrOH/n-heptane, 1 mL/min, 246 nm, retention times: 12.5 min (minor) and 15.1 min (major)].

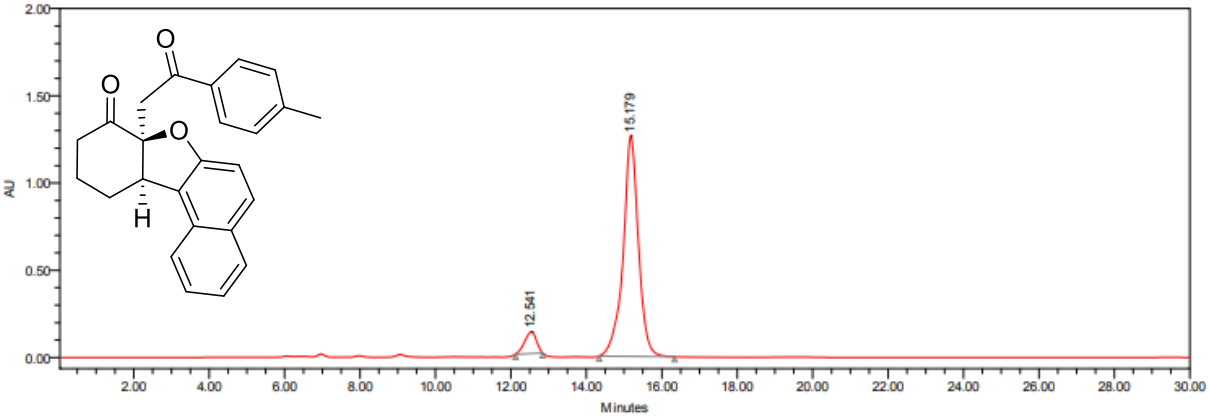

	Channel Description	RT	Area	% Area
1	PDA 200.0 to 400.0 nm at 2.4 nm	12.541	2701097	7.05
2	PDA 200.0 to 400.0 nm at 2.4 nm	15.179	35605599	92.95

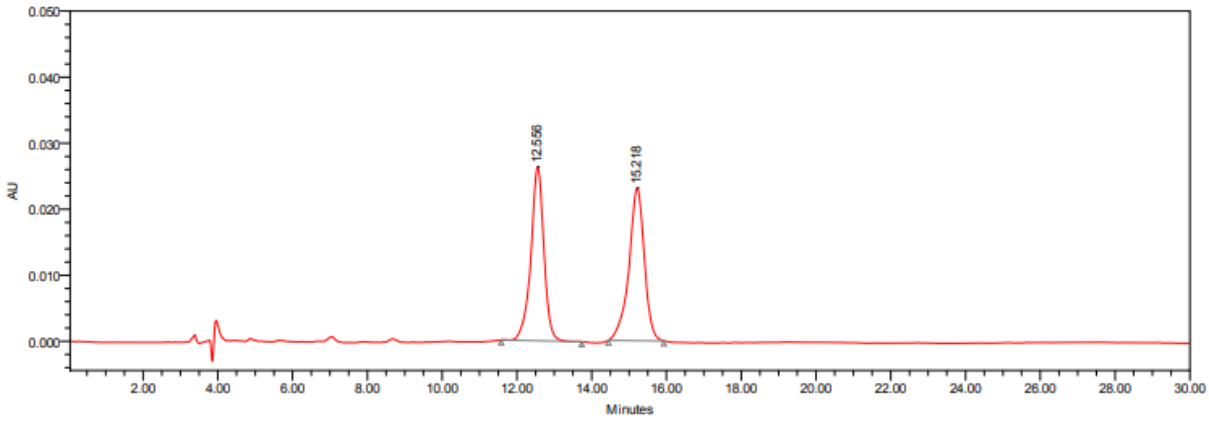

	Channel Description	RT	Area	% Area
1	PDA 200.0 to 400.0 nm at 2.4 nm	12.556	635253	49.03
2	PDA 200.0 to 400.0 nm at 2.4 nm	15.218	660415	50.97

Compound (**6c**)

HPLC Analysis: 91% ee [©Chiralpak IA, 25 °C, 20% *i*PrOH/*n*-heptane, 1 mL/min, 234 nm, retention times: 16.4 min (major) and 13.4 min (minor)].

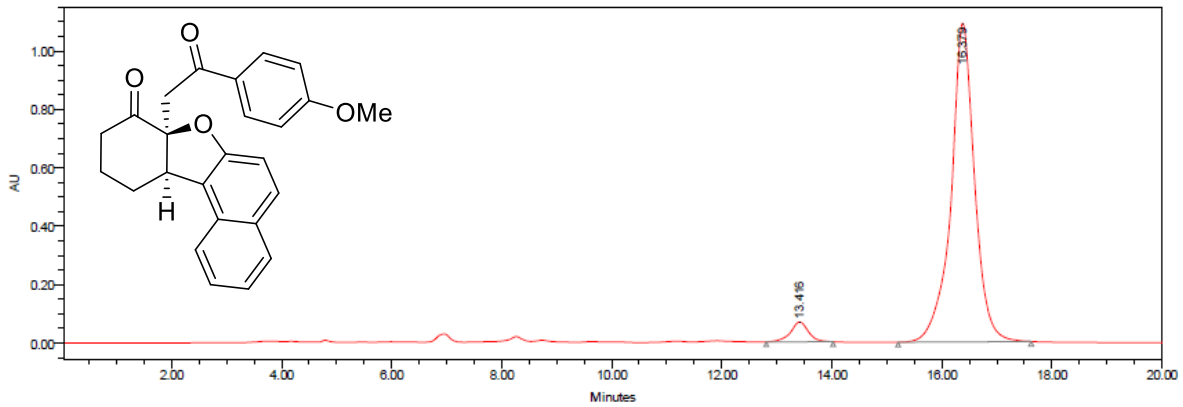

	Processed Channel Descr.	RT
1	996 PDA 240.7 nm (PDA 200.0 to 400.0 nm at 2.4 nm)	13.416
2	996 PDA 240.7 nm (PDA 200.0 to 400.0 nm at 2.4 nm)	16.379

	Area	% Area
1	1534764	4.52
2	32456696	95.48

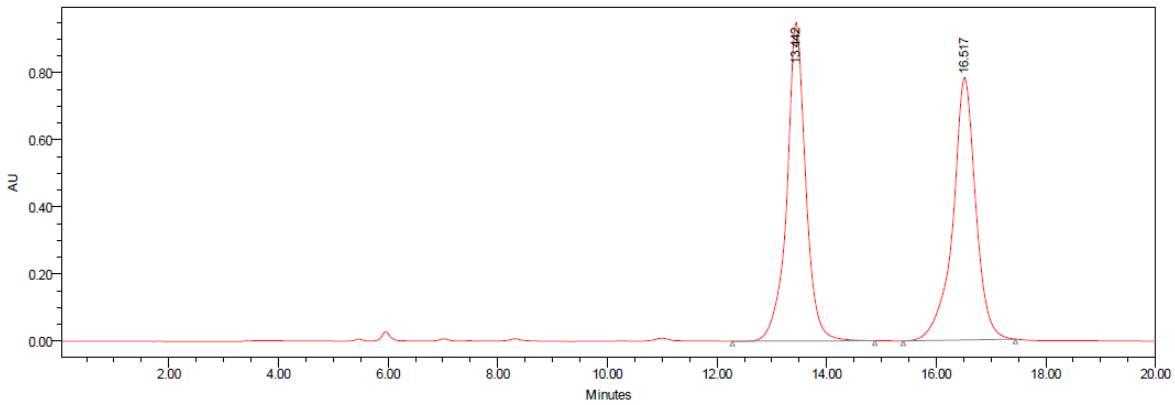

	Processed Channel Descr.	RT
1	996 PDA 268.1 nm (PDA 200.0 to 400.0 nm at 2.4 nm)	13.442
2	996 PDA 268.1 nm (PDA 200.0 to 400.0 nm at 2.4 nm)	16.517

	Area	% Area
1	22685579	50.00
2	22686024	50.00

Compound (**6d**)

HPLC Analysis: 87% ee [©Chiralpak IA, 25 °C, 10% iPrOH/n-heptane, 1 mL/min, 236 nm, retention times: 6.3 min (minor) and 12.3 min (major)].

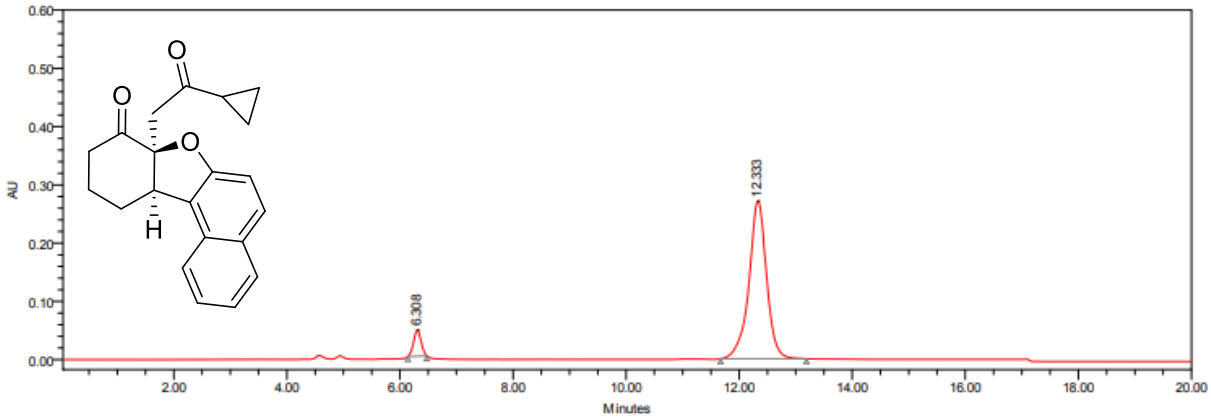

	Channel Description	RT	Area	% Area
1	PDA 200.0 to 400.0 nm at 2.4 nm	6.308	410317	6.53
2	PDA 200.0 to 400.0 nm at 2.4 nm	12.333	5877621	93.47

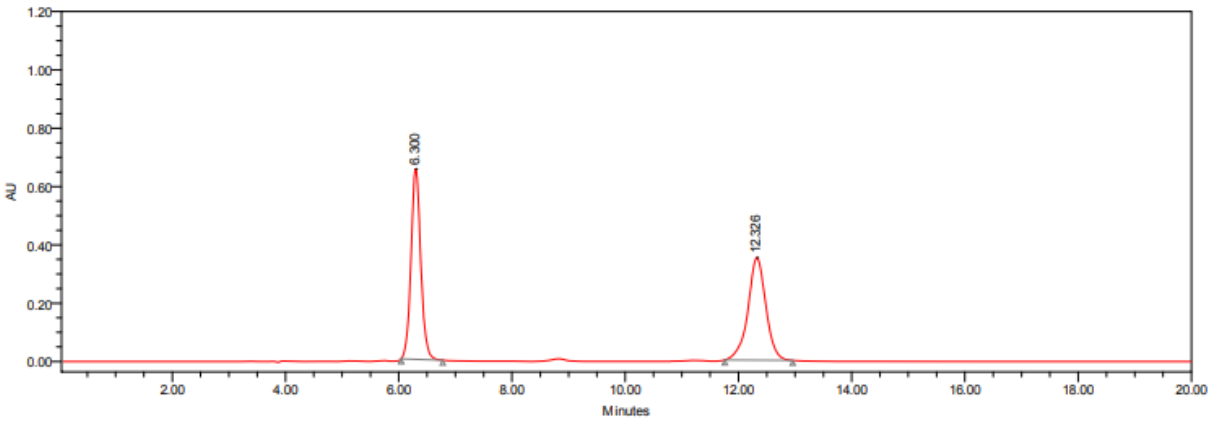

	Channel Description	RT	Area	% Area
1	PDA 200.0 to 400.0 nm at 2.4 nm	6.300	7793869	50.20
2	PDA 200.0 to 400.0 nm at 2.4 nm	12.326	7730308	49.80

Compound (**6e**)

HPLC Analysis: 98% ee [©Chiralpak IA, 25 °C, 2% iPrOH/n-heptane, 1 mL/min, 245 nm, retention times: 8.9 min (minor) and 12.6 min (major)].

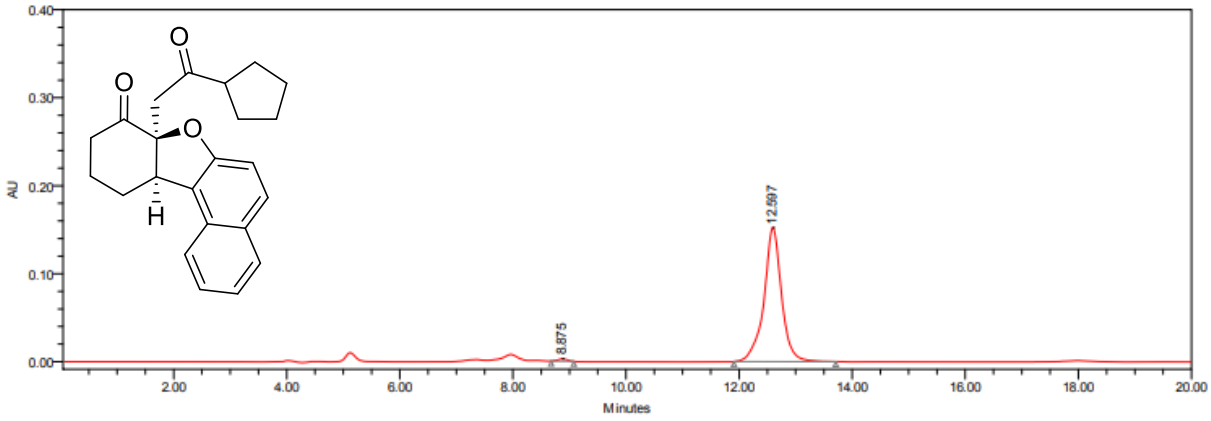

	Channel Description	RT	Area	% Area
1	PDA 200.0 to 400.0 nm at 2.4 nm	8.875	30798	0.93
2	PDA 200.0 to 400.0 nm at 2.4 nm	12.597	3289375	99.07

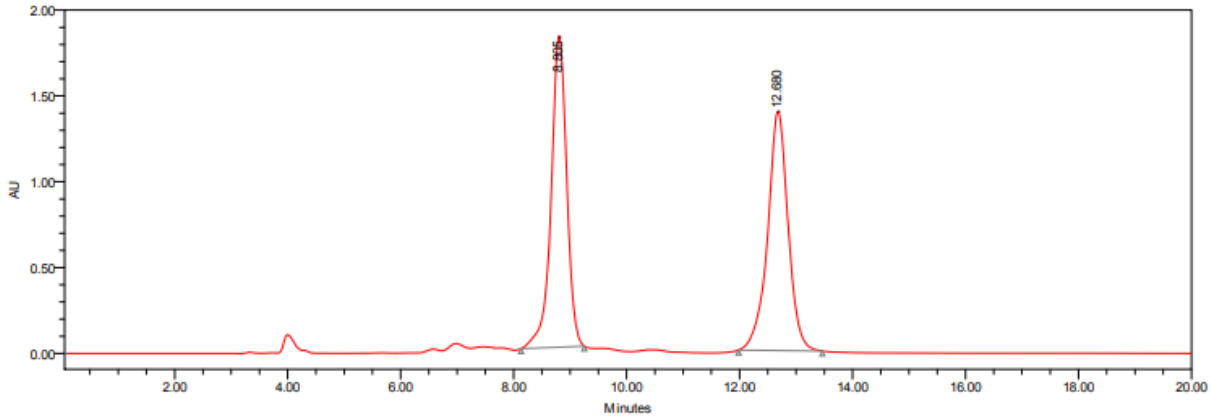

	Channel Description	RT	Area	% Area
1	PDA 200.0 to 400.0 nm at 2.4 nm	8.805	34703084	49.77
2	PDA 200.0 to 400.0 nm at 2.4 nm	12.680	35020278	50.23

Compound (**6f**)

HPLC Analysis: 85% ee [©Chiralpak IA, 25 °C, 20% iPrOH/n-heptane, 1 mL/min, 283 nm, retention times: 11.7 min (minor) and 12.8 min (major)].

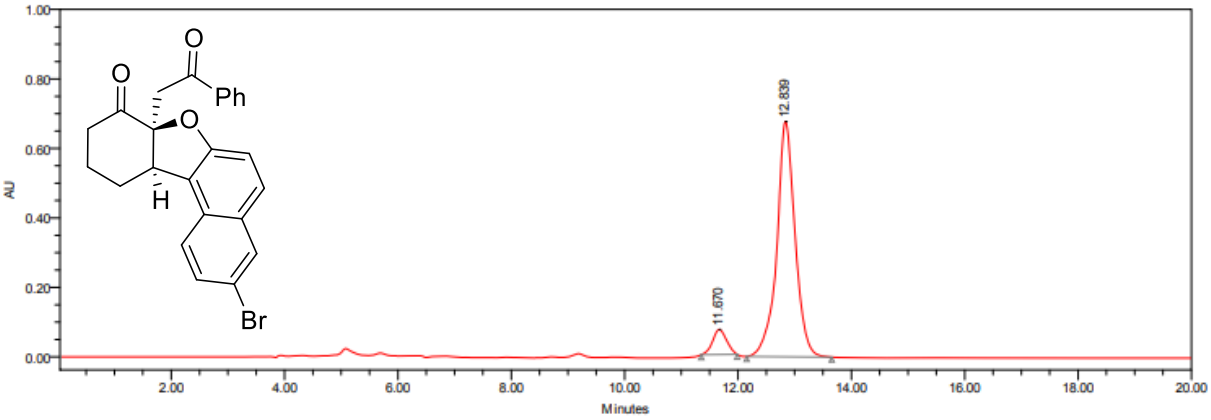

	Channel Description	RT	Area	% Area
1	PDA 200.0 to 400.0 nm at 2.4 nm	11.670	1239046	7.58
2	PDA 200.0 to 400.0 nm at 2.4 nm	12.839	15115011	92.42

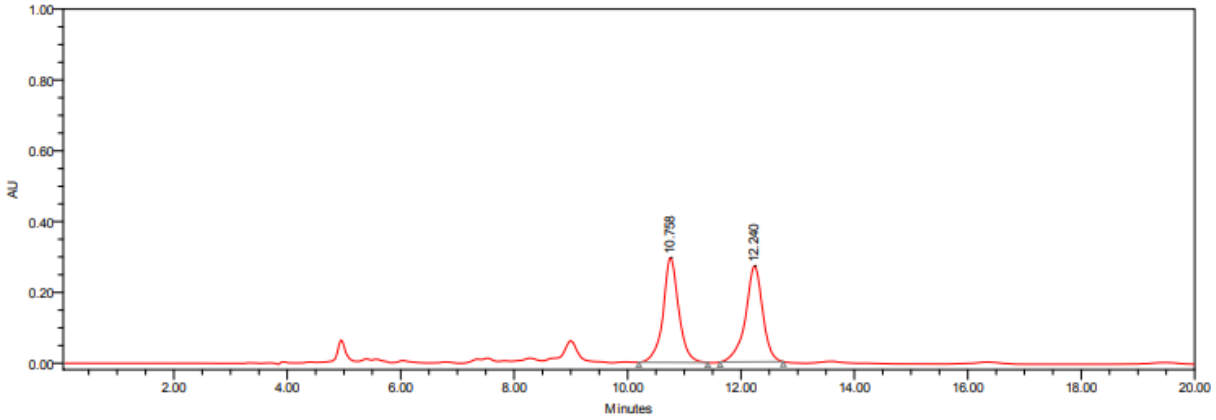

	Channel Description	RT	Area	% Area
1	PDA 200.0 to 400.0 nm at 2.4 nm	10.758	5673659	49.96
2	PDA 200.0 to 400.0 nm at 2.4 nm	12.240	5682911	50.04

10. Computational data

10.1. Technical details

Calculations were carried out with the Gaussian09 package [11] and all structures were fully optimized without any symmetry constraints at the DFT level by means of the M06 functional.[12] The def2-SVP basis set[13] was applied for all atoms and solvent effects are accounted for by continuum solvation method (integral equation formalism version of the polarizable continuum model (IEFPCM) for dichloromethane DCM). Each stationary point has been characterized with frequency analysis and shows the correct number of negative eigenvalues (zero for a local minimum and one for a transition state). All transition states were verified by stepping along the reaction coordinate (intrinsic reaction coordinate calculations) and confirming that they transformed into the corresponding reactants/products. Final energy calculations at the M06 level associated with the def2-TZVPP basis set, including solvation effect, have been achieved on the IEFPCM(DCM)-M06/def2-SVP geometries. To get accurate geometries and energies, the SCF convergence criterion was systematically tightened to 10^{-8} au, and the force minimizations were carried out until the rms force became smaller that (at least) 1 x 10^{-5} au ("tight" optimization keyword in Gaussian 09). The "UltraFine" grid (99 radial shells and 590 angular points per shell) was used throughout the calculations, as recommended when using Gaussian 09. The Gibbs free energies presented in this article are IEFPCM(DCM)-M06/def2-TZVPP//IEFPCM(DCM)-M06/def2-SVP electronic energies (which include solvation-energy corrections from the IEFPCM method) modified with thermal and entropy corrections from IEFPCM(DCM)-M06/def2-SVP calculations. Due to the well-known errors associated with entropy calculations, we apply a scaling factor of 0.5 to the entropic contributions as recommended in the literature.[14] Therefore, the calculated ΔG values reported in this study include the ZPE, enthalpic temperature correction, solvation energy, and half the entropy, as has been done in our previous studies.[15].

A large number of reaction paths are conceivable to explain the experimental observations. Due to the size of the system under study, we did not exhaustively investigate all possible reaction mechanisms, but only the most relevant ones. Thus, we describe here a set of plausible reaction pathways that allow to rationalize the experimental results. In the same way, numerous conformers exist for almost all the obtained stationary points. We have not performed a conformational study for each one. An exhaustive conformational study has nevertheless been performed for the (*S*)-**7a** complex

[11] Frisch, M. J.; Trucks, G. W.; Schlegel, H. B.; Scuseria, G. E.; Robb, M. A.; Cheeseman, J. R.; Scalmani, G.; Barone, V.; Mennucci, B.; Petersson, G. A.; Nakatsuji, H.; Caricato, M.; Li, X.; Hratchian, H. P.; Izmaylov, A. F.; Bloino, J.; Zheng, G.; Sonnenberg, J. L.; Hada, M.; Ehara, M.; Toyota, K.; Fukuda, R.; Hasegawa, J.; Ishida, M.; Nakajima, T.; Honda, Y.; Kitao, O.; Nakai, H.; Vreven, T.; Montgomery, J. A. Jr.; Peralta, J. E.; Ogliaro, F.; Bearpark, M.; Heyd, J. J.; Brothers, E.; Kudin, K. N.; Staroverov, V. N.; Kobayashi, R.; Normand, J.; Raghavachari, K.; Rendell, A.; Burant, J. C.; Iyengar, S. S.; Tomasi, J.; Cossi, M.; Rega, N.; Millam, J. M.; Klene, M.; Knox, J. E.; Cross, J. B.; Bakken, V.; Adamo, C.; Jaramillo, J.; Gomperts, R.; Stratmann, R. E.; Yazyev, O.; Austin, A. J.; Cammi, R.; Pomelli, C.; Ochterski, J. W.; Martin, R. L.; Morokuma, K.; Zakrzewski, V. G.; Voth, G. A.; Salvador, P.; Dannenberg, J. J.; Dapprich, S.; Daniels, A. D.; Farkas, Ö.; Foresman, J. B.; Ortiz, J. V.; Cioslowski, J.; Fox, D. J. Gaussian, Inc., Wallingford CT, Gaussian 09, Revision D.01, **2013**.

[12] Zhao, Y.; Truhlar, D. G. *Theor. Chem. Acc.* **2008**, *120*, 215.

[13] Weigend, F.; Ahlrichs, R. *Phys. Chem. Chem. Phys.* **2005**, *7*, 3297.

[14] (a) Cooper, J.; Ziegler, T. A *Inorg. Chem.* **2002**, *41*, 6614; (b) Lau, J. K. C.; Deudel, D. V. *J. Chem. Theory Comput.* **2006**, *2*, 103; (c) Li, H.; Lu, G.; Jiang, J.; Huang, F.; Wang, Z. X. *Organometallics* **2011**, *30*, 2349; (d) Hua, J.; Krizner, H. E.; De Haan, D. O. *J. Phys. Chem. A* **2011**, *115*, 1667.

[15] (a) Pastor, J.; Rezabal, E.; Voituriez, A.; Betzer, J.-F.; Marinetti, A.; Frison, G. *J. Org. Chem.* **2018**, *83*, 2779; (b) Zhang, Z.; Smal, V.; Retailleau, P.; Voituriez, A.; Frison, G.; Marinetti, A.; Guinchard, X. *J. Am. Chem. Soc.* **2020**, *142*, 3797; (c) Yu, Y.; Zhang, Z.; Voituriez, A.; Rabasso, N.; Frison, G.; Marinetti, A.; Guinchard, X. *Chem. Commun.* **2021**, *57*, 10779.

(*vide infra*), and our entire study was then based on the global energy minimum obtained after this exploration.

Table S4. Absolute electronic energies and thermal corrections for all molecules.

	E (IEFPCM(DCM)-M06/Def2-SVP	Thermal correction to enthalpy	Thermal correction to Gibbs Free Energy	E (IEFPCM(DCM)-M06/Def2-TZVPP)[a]
(*S*)-**2c**	-1410.712594	0.302880	0.237388	-1412.041872
(*S*)-**4a**	-1075.493694	0.395920	0.323954	-1076.657489
(*S*)-**7a**	-2486.234729	0.700665	0.585644	-2488.719377
7a1	-2486.236887	0.701244	0.588773	-2488.721001
7a2	-2486.234537	0.700819	0.587863	-2488.719140
7a3	-2486.231247	0.700992	0.584163	-2488.716963
7a4	-2486.232436	0.701700	0.586641	-2488.717755
7a5	-2486.232102	0.700739	0.586179	-2488.716655
7a6	-2486.234011	0.701171	0.586982	-2488.717260
7a7	-2486.231692	0.701339	0.586784	-2488.716902
7a8	-2486.230664	0.701025	0.584477	-2488.714666
7a9	-2486.228497	0.701031	0.585550	-2488.714686
7a10	-2486.229860	0.701479	0.586665	-2488.714120
7a11	-2486.228272	0.701008	0.586991	-2488.713633
7a12	-2486.227996	0.701491	0.586202	-2488.712491
pro-(*S*)-**TS1a**	-2486.203905	0.697111	0.582973	-2488.691326
pro-(*S*)-**8a**	-2486.205195	0.699464	0.583884	-2488.694440
9a	-615.429620	0.243729	0.192457	-616.101205
10	-1870.730791	0.453192	0.364881	-1872.559222
pro-(*S*)-**11a**	-2486.201193	0.699240	0.584720	-2488.690863
pro-(*S*)-**TS2a**	-2486.199336	0.698830	0.587588	-2488.686802
(*S*)-**12a**	-2486.216833	0.701170	0.590691	-2488.701386
(*S*)-**TS3a**	-2486.194870	0.695553	0.585022	-2488.675544
(*S*)-**13a**	-2486.218613	0.701814	0.590869	-2488.700837
(*S*)-**5a**	-1075.505585	0.396479	0.326015	-1076.667523
pro-(*R*)-**8a**	-2486.204607	0.698282	0.582547	-2488.694523
pro-(*R*)-**TS1a**	-2486.200569	0.694769	0.582898	-2488.686311
(*R*)-**7a**	-2486.232566	0.701336	0.589175	-2488.717766

[a] Energies computed at the IEFPCM(DCM)-M06/Def2-SVP geometries.

10.2. Conformational study of the phosphoric acid – *O*-products 4 complexes.

A large number of conformers can exist for the complex formed by the interaction between the phosphoric acid (*S*)-**2c** and the *O*-product (*S*)-**4a**, starting point of the reaction profile of the epimerization reaction. We have performed a conformational study of this complex. 13 different conformers (**Figure S4**) were obtained in the 0.0-20.0 kJ/mol range relative to the most stable conformer (**7a**) that was used to perform the mechanistic study. The search for transition states for C-

O bond breaking from other conformers shows similar activation barriers to that obtained to reach pro-(*S*)-**TS1a** from (*S*)-**7a** (+65.5 kJ/mol).

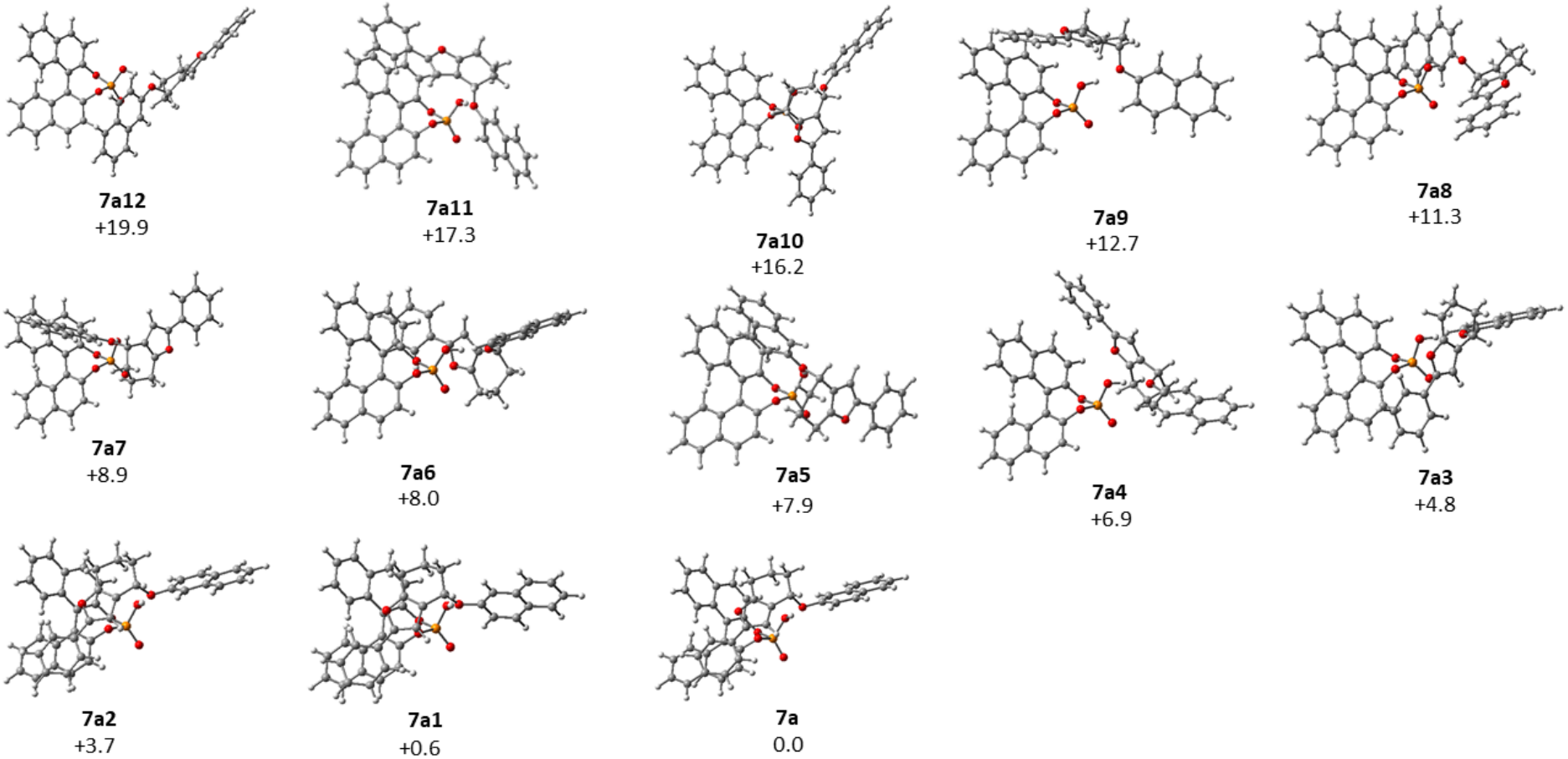

Figure S4. DFT calculated structures, at the IEFPCM(DCM)-M06/def2-TZVPP//IEFPCM(DCM)-M06/def2-SVP level, of various conformers of the (*S*)-**7** type complex between the phosphoric acid (*S*)-**2c** and the *O*-product (S)-**4a**. Relative Gibbs free energy in kJ mol^{-1}.

10.3. Erosion of enantioselectivity and structural instability of *O*-addition products

The erosion of the enantioselectivity and the structural instability of the *O*-addition products **4** have been computationally studied at the DFT level (see 10.1 above for computational details). The calculations started from product (*S*)-**4a** and the BINOL-derived chiral phosphoric acid (*S*)-**2c** (Scheme S2), as a model of the phosphoric acid unit of (*S*)-**2a**. **4a** binds to **2c** through *H*-bonding, forming **7a**. This complex can evolve, via the breaking of a C-O bond and a proton transfer, to form pro-(*S*)-**8a**. This carbocationic intermediate retains the initial stereochemical information, due to the interaction between the naphthol oxygen and the cationic site. This interaction induces a 51.1 kJ/mol stabilization of **8a** with respect to the dissociated ion pair **9a**·**10**.

Although dissociation of **8a** into **9a**·**10** is highly endothermic (112.7 kJ/mol from **7a**, 51.1 kJ/mol from the analogous intermediate **8a**), it is likely to be responsible for the racemization of (*S*)-**4a**, since the stereochemical information is lost in the carbocation and the subsequent *O*-addition of naphthol can take place from both faces (the whole energetic pathways to reach pro-(*R*)-**4a** is shown in Scheme S3). At room temperature, this barrier is difficult to cross while remaining accessible, which explains why this process is slow (see Scheme 2).

Alternatively, intermediate **8a** can also change its geometry. In particular, the naphthol and the cyclic cationic moieties, both approximately planar and located in parallel planes, can shift relative to each other, leading to pro-(*S*)-**11a** where the cationic site interacts preferentially with the electron-rich carbon of the naphthol. **11a** retains the chiral information present in **4a**, **7a** and **8a**. The formation of the C-C bond followed by re-aromatization of the naphthol moiety leads to (*S*)-**5a** in 2 steps from **11a**. Overall, the conversion of **4a** to **5a** is exothermic by 22.9 kJ/mol, which explains the irreversible formation of the *C*-addition product. However, the activation barrier of this process is high (107.6 kJ/mol from **7a**), which explains why the conversion of *O*- to *C*-product is slow. Furthermore, we assume that a similar reaction pathway occurs from pro-(*R*)-**8a** to account for the experimentally observed formation of (*R*)-**5a**, although this has not been calculated.

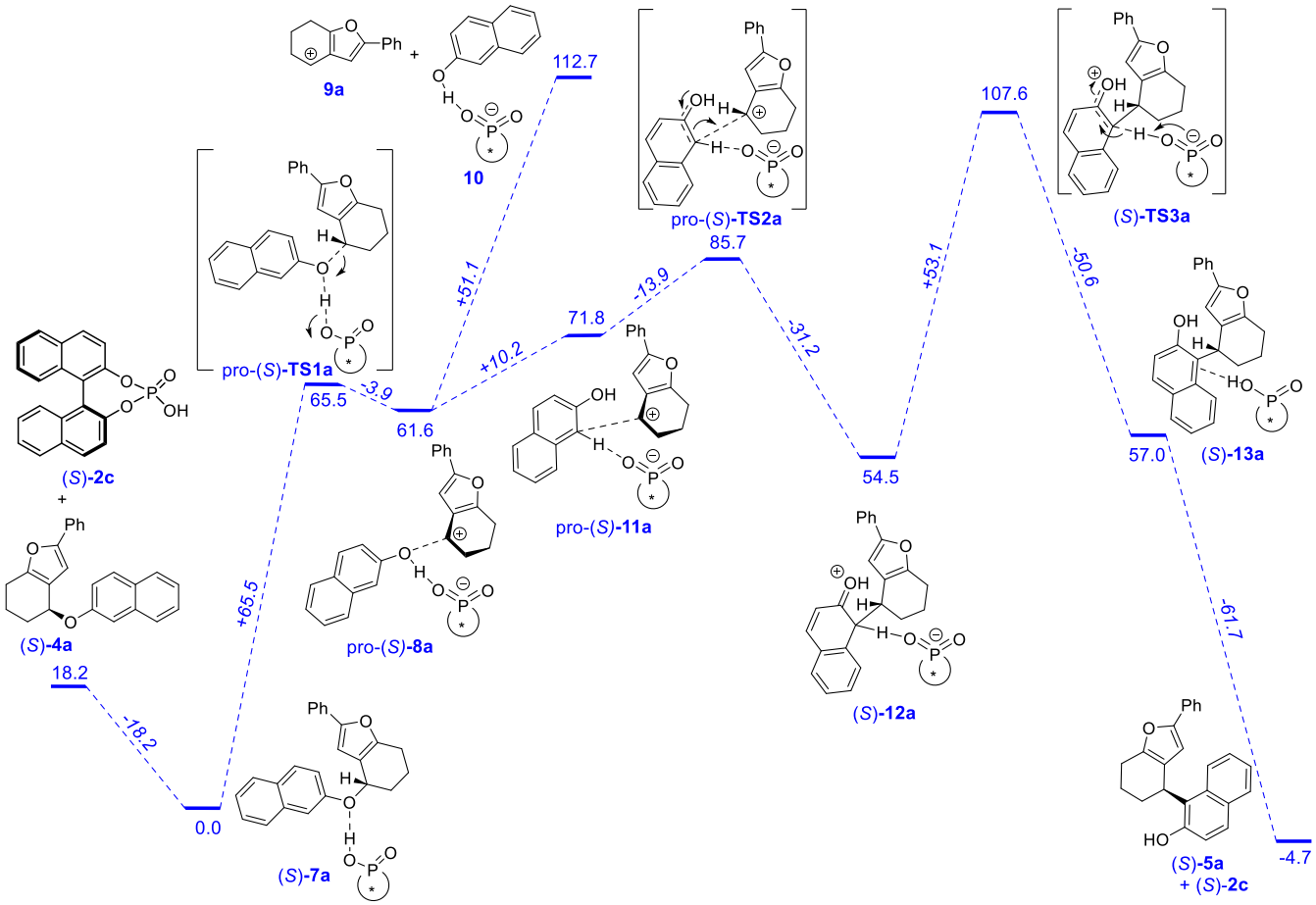

Scheme S2. Schematic potential energy surface (Gibbs free energy in kJ mol^{-1}) for the erosion of the enantioselectivity and the structural instability of the *O*-addition product **4a** obtained at the IEFPCM(DCM)-M06/Def2-TZVPP//IEFPCM(DCM)-M06/Def2-SVP level.

The dissociation of the pro-(*S*)-**8a** complex into **9a** and **10** leads to the loss of all the chiral information initially present in the *O*-addition product (*S*)-**4a**. The re-coordination of the cationic intermediate **9a** to the naphtol-phosphoric acid complex **10** can then take place on either side (**Scheme S3**), leading to both pro-(*S*)-**8a** or pro-(*R*)-**8a** without control of the enantioselectivity. These two intermediates then readily lead to the re-formation of the *O*-addition product **4a** with either (*S*) or (*R*) configuration.

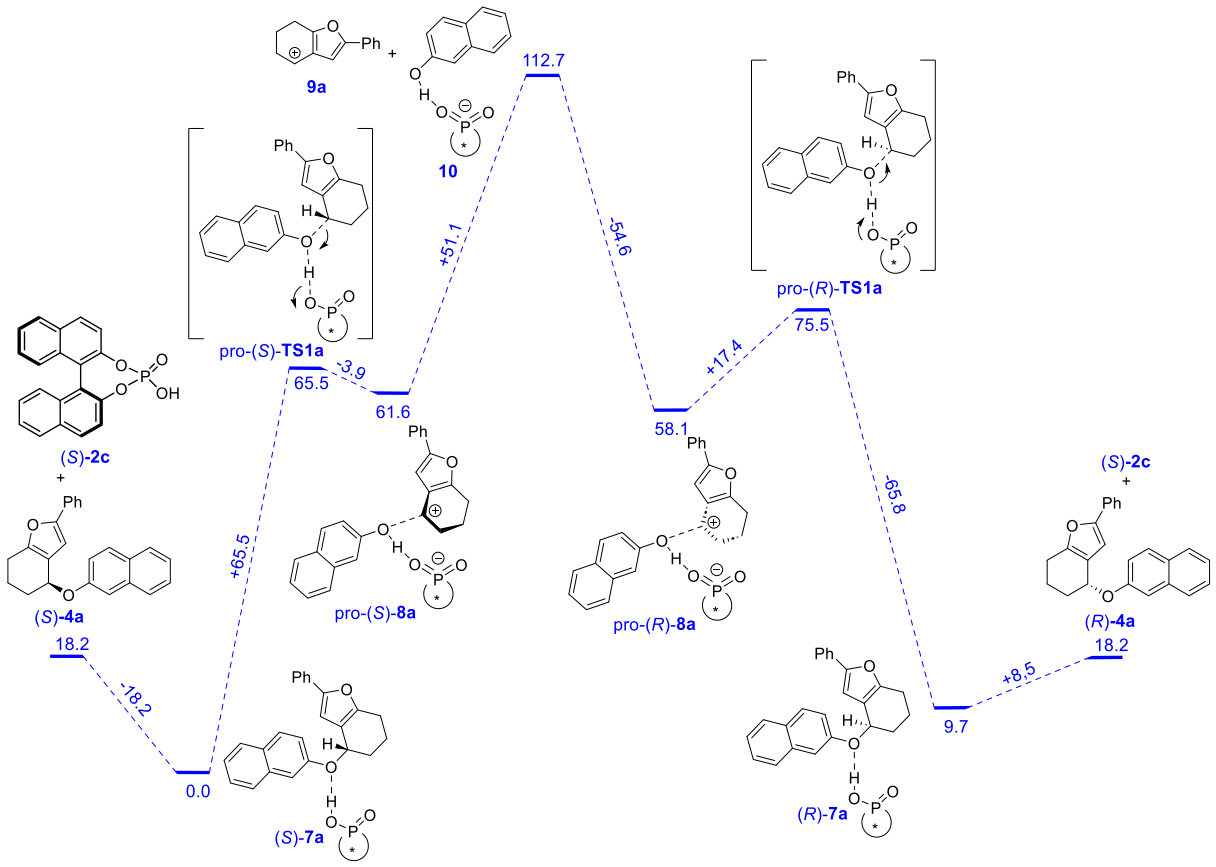

Scheme S3. Schematic potential energy surface (Gibbs free energy in kJ mol^{-1}) for the formation of both (*S*)- and (*R*)-**4a** from the dissociated **9a** and **10** intermediates, computed at the IEFPCM(DCM)-M06/Def2-TZVPP//IEFPCM(DCM)-M06/Def2-SVP level.